A CIRCULAR DICHROISM STUDY OF THE CONFORMATION OF A SYNTHETIC ANALOG OF ALAMETHICIN

BY

RANDY BABIUK

A Thesis Submitted to the Faculty of Graduate Studies
in Partial Fulfillment of the Requirements For the Degree of

MASTER OF SCIENCE

Department of Chemistry
University of Manitoba
Winnipeg, Manitoba

ISBN 0-612-12966-7

Name RANDAL PETER BABIUK

Dissertation Abstracts International is arranged by broad, general subject categories. Please select the one subject which most nearly describes the content of your dissertation. Enter the corresponding four-digit code in the spaces provided.

BIOCHEMISTRY
SUBJECT TERM

0487
SUBJECT CODE

U·M·I

Subject Categories

THE HUMANITIES AND SOCIAL SCIENCES

COMMUNICATIONS AND THE ARTS
Architecture 0729
Art History 0377
Cinema 0900
Dance 0378
Fine Arts 0357
Information Science 0723
Journalism 0391
Library Science 0399
Mass Communications 0708
Music 0413
Speech Communication 0459
Theater 0465

EDUCATION
General 0515
Administration 0514
Adult and Continuing 0516
Agricultural 0517
Art 0273
Bilingual and Multicultural 0282
Business 0688
Community College 0275
Curriculum and Instruction 0727
Early Childhood 0518
Elementary 0524
Finance 0277
Guidance and Counseling 0519
Health 0680
Higher 0745
History of 0520
Home Economics 0278
Industrial 0521
Language and Literature 0279
Mathematics 0280
Music 0522
Philosophy of 0998
Physical 0523

Psychology 0525
Reading 0535
Religious 0527
Sciences 0714
Secondary 0533
Social Sciences 0534
Sociology of 0340
Special 0529
Teacher Training 0530
Technology 0710
Tests and Measurements 0288
Vocational 0747

LANGUAGE, LITERATURE AND LINGUISTICS
Language
- General 0679
- Ancient 0289
- Linguistics 0290
- Modern 0291

Literature
- General 0401
- Classical 0294
- Comparative 0295
- Medieval 0297
- Modern 0298
- African 0316
- American 0591
- Asian 0305
- Canadian (English) 0352
- Canadian (French) 0355
- English 0593
- Germanic 0311
- Latin American 0312
- Middle Eastern 0315
- Romance 0313
- Slavic and East European 0314

PHILOSOPHY, RELIGION AND THEOLOGY
Philosophy 0422
Religion
- General 0318
- Biblical Studies 0321
- Clergy 0319
- History of 0320
- Philosophy of 0322

Theology 0469

SOCIAL SCIENCES
American Studies 0323
Anthropology
- Archaeology 0324
- Cultural 0326
- Physical 0327

Business Administration
- General 0310
- Accounting 0272
- Banking 0770
- Management 0454
- Marketing 0338

Canadian Studies 0385
Economics
- General 0501
- Agricultural 0503
- Commerce-Business 0505
- Finance 0508
- History 0509
- Labor 0510
- Theory 0511

Folklore 0358
Geography 0366
Gerontology 0351
History
- General 0578
- Ancient 0579
- Medieval 0581
- Modern 0582
- Black 0328
- African 0331
- Asia, Australia and Oceania 0332
- Canadian 0334
- European 0335
- Latin American 0336
- Middle Eastern 0333
- United States 0337

History of Science 0585
Law 0398
Political Science
- General 0615
- International Law and Relations 0616
- Public Administration 0617

Recreation 0814
Social Work 0452
Sociology
- General 0626
- Criminology and Penology ... 0627
- Demography 0938
- Ethnic and Racial Studies 0631
- Individual and Family Studies 0628
- Industrial and Labor Relations 0629
- Public and Social Welfare 0630
- Social Structure and Development 0700
- Theory and Methods 0344

Transportation 0709
Urban and Regional Planning 0999
Women's Studies 0453

THE SCIENCES AND ENGINEERING

BIOLOGICAL SCIENCES
Agriculture
- General 0473
- Agronomy 0285
- Animal Culture and Nutrition 0475
- Animal Pathology 0476
- Food Science and Technology 0359
- Forestry and Wildlife 0478
- Plant Culture 0479
- Plant Pathology 0480
- Plant Physiology 0817
- Range Management 0777
- Wood Technology 0746

Biology
- General 0306
- Anatomy 0287
- Biostatistics 0308
- Botany 0309
- Cell 0379
- Ecology 0329
- Entomology 0353
- Genetics 0369
- Limnology 0793
- Microbiology 0410
- Molecular 0307
- Neuroscience 0317
- Oceanography 0416
- Physiology 0433
- Radiation 0821
- Veterinary Science 0778
- Zoology 0472

Biophysics
- General 0786
- Medical 0760

EARTH SCIENCES
Biogeochemistry 0425
Geochemistry 0996
Geodesy 0370
Geology 0372
Geophysics 0373
Hydrology 0388
Mineralogy 0411
Paleobotany 0345
Paleoecology 0426
Paleontology 0418
Paleozoology 0985
Palynology 0427
Physical Geography 0368
Physical Oceanography 0415

HEALTH AND ENVIRONMENTAL SCIENCES
Environmental Sciences 0768
Health Sciences
- General 0566
- Audiology 0300
- Chemotherapy 0992
- Dentistry 0567
- Education 0350
- Hospital Management 0769
- Human Development 0758
- Immunology 0982
- Medicine and Surgery 0564
- Mental Health 0347
- Nursing 0569
- Nutrition 0570
- Obstetrics and Gynecology .. 0380
- Occupational Health and Therapy 0354
- Ophthalmology 0381
- Pathology 0571
- Pharmacology 0419
- Pharmacy 0572
- Physical Therapy 0382
- Public Health 0573
- Radiology 0574
- Recreation 0575
- Speech Pathology 0460
- Toxicology 0383

Home Economics 0386

PHYSICAL SCIENCES
Pure Sciences
Chemistry
- General 0485
- Agricultural 0749
- Analytical 0486
- Biochemistry 0487
- Inorganic 0488
- Nuclear 0738
- Organic 0490
- Pharmaceutical 0491
- Physical 0494
- Polymer 0495
- Radiation 0754

Mathematics 0405
Physics
- General 0605
- Acoustics 0986
- Astronomy and Astrophysics 0606
- Atmospheric Science 0608
- Atomic 0748
- Electronics and Electricity 0607
- Elementary Particles and High Energy 0798
- Fluid and Plasma 0759
- Molecular 0609
- Nuclear 0610
- Optics 0752
- Radiation 0756
- Solid State 0611

Statistics 0463

Applied Sciences
Applied Mechanics 0346
Computer Science 0984

Engineering
- General 0537
- Aerospace 0538
- Agricultural 0539
- Automotive 0540
- Biomedical 0541
- Chemical 0542
- Civil 0543
- Electronics and Electrical 0544
- Heat and Thermodynamics ... 0348
- Hydraulic 0545
- Industrial 0546
- Marine 0547
- Materials Science 0794
- Mechanical 0548
- Metallurgy 0743
- Mining 0551
- Nuclear 0552
- Packaging 0549
- Petroleum 0765
- Sanitary and Municipal 0554
- System Science 0790

Geotechnology 0428
Operations Research 0796
Plastics Technology 0795
Textile Technology 0994

PSYCHOLOGY
General 0621
Behavioral 0384
Clinical 0622
Developmental 0620
Experimental 0623
Industrial 0624
Personality 0625
Physiological 0989
Psychobiology 0349
Psychometrics 0632
Social 0451

A CIRCULAR DICHROISM STUDY OF THE CONFORMATION OF A SYNTHETIC ANALOG OF ALAMETHICIN

BY

RANDY BABIUK

A Thesis submitted to the Faculty of Graduate Studies of the University of Manitoba in partial fulfillment of the requirements of the degree of

MASTER OF SCIENCE

"Never retract,
never retreat.
never apologize,
get the thing done
and let them howl."

Nellie McClung

Table of Contents

Acknowledgements

I would like to thank Dr. Joe O'Neil for all he has done for me during this project. Without his advice and encouragement, this thesis would not exist. I wish to extend my deep gratitude to him for accepting me as his student and sticking with me through all of the trials and tribulations which were a part of the project. His financial support through his research grants and his wonderful supervision made this possible.

Also, I want to thank Dr. Lynda Donald of Chemistry and Dr. Glen Klassen and Dr. Elizabeth Worobec and their students for valuable advice and technical assistance regarding molecular biology in the earlier stages of the research.

Thank you to all the staff and students both current and past who gave me assistance and their friendship during my tenure in the Chemistry. Particularly, Adelinda Yee and Leo Spyracopoulos from the O'Neil Research Group for all their assistance and friendship over the years and Dr. Frank Hruska for reading the thesis, permitting me to use his lab for the writing process and many enlightening conversations must be acknowledged.

I was fortunate to make a lot of friends in Chemistry and other departments. Their comraderie and discussions made it pleasant to go into the University each day. I want to thank Jeremy, Don, Guy, Rob, John, Jo-Anne, Travis, Andrew, Ted Z. and everyone else in Chem and Micro.

Special thanks to my family, especially my mom Joyce, brother Alan, sister-in-law Cindy and aunt Alice for their unfaltering support and

encouragement over the course of the years.

List of Figures

List of Tables

Abbreviations

ala, A : alanine

aib, B : α-aminoisobutyric acid

pro, P : proline

O : phenylalaninol

NMR : nuclear magnetic resonance

Å : angstrom

ΔA : dehydroalanine

CD : circular dichroism

SDS : sodium dodecyl sulfate

TFE : trifluoroethanol

NOE : Nuclear Overhauser Effect

ORD : optical rotatory dispersion

UV : ultraviolet

Vis : visible

ε : molar absorptivity

λ : wavelength

nm : nanometer

θ_{obs} : observed ellipticity

θ_{222} : ellipticity at 222 nm

$\theta_{100\%}$: ellipticity corresponding to a completely helical molecule

$\theta_{0\%}$: ellipticity corresponding to a completely unordered molecule

$[\theta]_{\lambda}$: mean residue ellipticity at the particular wavelength

$[\theta_\lambda]_M$: molar ellipticity

MRW : mean residue weight

MW : molecular weight

T_m : midpoint of helix/coil transition

f_H : helix fraction

Abstract

The peptide RBP-1 is a synthetic analog to the fungal peptaibol alamethicin. RBP-1, however, has alanine residues in place of the α-aminoisobutyric acid (Aib) residues in alamethicin. These two amino acids have very strong helix-forming characteristics sometimes called helix propensities.

Differences are observed in the amount of helical structure found in the synthetic peptide in different solvents as determined by circular dichroism spectroscopy. The percentage of helix attained by RBP-1 at low temperatures in organic alcohols increases considerably as the solvent is changed from methanol (17% helix) to ethanol (37%) to trifluoroethanol (67%). Placing the peptide in sodium dodecyl sulfate (SDS) results in the formation of the largest degree of helicity (87%). In water, RBP-1 has a mainly unordered structure. These differences can be rationalized in terms of the helicogenic traits of the solvents.

Comparison of RBP-1 and alamethicin in methanol and SDS shows significantly higher helix content in alamethicin than in RBP-1 in both solvents (49% to 17% and 100% to 87% in methanol and SDS respectively). This observation indicates that the helix propensity of Aib is much greater than that of its common counterpart alanine.

Measurements of the temperature dependence of the amide proton chemical shifts of the residues of alamethicin show that the majority of the amide protons, except those in the very middle and ends of the peptide are

involved in hydrogen bonds. This suggests that most residues are part of an ordered secondary structure, presumably a helical conformation.

From these findings, it is concluded that helix formation in peptides is determined by both the solvent and the amino acid content.

CHAPTER 1

INTRODUCTION

1.1 Structural Basis of Peptide Structure Preferences

Recently, advances in techniques such as X-ray crystallography and NMR spectroscopy have resulted in an almost exponential increase in the amount of information about the folded conformations of proteins. However, the pathways followed by folding proteins and the underlying reasons why protein sequences fold into particular secondary and tertiary structures are still not well understood.

Experiments have been performed which support the theory that folding is a sequential process (Baldwin and Garel, 1973); i.e. the protein follows a pathway populated by structural intermediates. Hydrogen exchange between backbone amide protons and solvent protons measured during the re-folding process has demonstrated the existence of intermediates in the folding pathways of ribonuclease A (Baldwin and Udgaonkar, 1988) and cytochrome C (Englander et al., 1988). The folding pathway is being elucidated in part by characterization of such structural intermediates.

Although protein folding pathways are being discovered, there still remains the question of what factors govern the folding behaviour. The primary structure of a protein, or the amino acid sequence, is considered to contain all the information necessary for protein folding (Anfinsen et al., 1961). The

manner in which this folding behaviour is encoded in the primary structure is the result of several factors: the propensity of the individual residues to form secondary structures, the sequence of these residues in the protein, and the environmental conditions in which the amino acids, amino acid sequences, and the entire protein find themselves are all likely to be important.

Individual amino acids sometimes have a preference with regard to the secondary structural elements in which they will be found. The helix propensity of an amino acid denotes its predilection for the formation of a helix in a protein or peptide. These propensities initially were measured for the common amino acids by employing a technique called a "host-guest" experiment (Sueki et al., 1984). The amino acid whose propensity is being determined is termed the "guest" residue. It is incorporated into a co-polymer of "host" residues, typically hydroxypropyl- or hydroxybutyl-L-glutamate. In the absence of a guest residue, the host residues will form stable α-helices in aqueous solution. The stability of the α-helix formed when the guest residue is incorporated is measured in terms of the Zimm-Bragg helix-coil initiation parameter σ, the helix nucleation parameter n, and the helix stability constant s (Zimm and Bragg, 1959). The Zimm-Bragg theory describes cooperative helix-coil transitions. The transition is cooperative because the formation of the first turn of an α-helix is difficult, whereas further turns are added to the helix relatively easily. The first turn acts as a nucleus for helix formation. The two parameters, the initiation (σ) and stability (s) constants, are calculated from a partition function. These two

constants can be thought of as follows: σ is the contribution to the partition function of a peptide unit at the beginning of an uninterrupted sequence of helical states; s is a factor contributing to the partition function by a peptide unit at the interior of an uninterrupted sequence of helical states. The constant s can also be considered to be an equilibrium constant for the bonding of the peptide unit to a portion of the peptide chain already in a helical state.

However, results from "host-guest" experiments for α-helix formation in water for the common amino acids (Sueki et al., 1984) have shown that the helix propagation constants σ and n show only small differences (except for Pro) and exhibit an average value of ~1. These results suggest that helix-formation in small peptides is nearly independent of amino acid content and that helix formation in water by short peptides (<20 residues) is unlikely.

The use of the Zimm-Bragg model does not take into account factors like sequence- and position-dependent side chain interactions (Marquesee et al., 1989). In addition, the copolymer residues in the host-guest experiments are not any of the 20 naturally-occurring amino acids. Thus, host-guest studies do not mimic natural conditions of residues in real proteins. A new method, developed for measuring helix propensities, gives different results. The new technique involves residue substitution into small, monomeric helix-forming alanine-based peptides and measurement of the stabilities of the substituted peptides (Padmanabhan et al., 1990). Natural peptides and small, helix-forming protein fragments, as well as short synthetic peptides composed of the 20

common amino acids have been used in such substitution trials (Marquesee and Baldwin, 1987). This technique provides a more natural environment for the guest residue, resulting in more realistic helix propensities than use of the copolymers in host-guest experiments. This substitution experiment is in actuality a "host-guest" technique, but different in that the host environment is a much more natural context for the guest residue to be placed in. (For clarity, the methods for determining propensities will be referred to as "host-guest" when referring to studies using other than natural amino acids as host residues, and "substitution" experiments when a more natural host is used, respectively.)

Substitutions of 1-3 non-polar residues (Ala, Ile, Val, Leu, Phe) were made into seventeen-residue alanine-based peptides at various positions in the sequence and helix formation was measured by CD (Padmanabhan et al., 1990). From these measurements, the helix propagation parameter s was extracted. The results of these experiments differ significantly from those found by the host-guest method, in magnitudes of propensities and the order of helix-forming strength of the amino acids. Comparison of helix propensities from these substitution experiments with helical preference, P_α, is interesting. P_α, determined from X-ray data, is found by taking the frequency of the amino acid found in helical regions of proteins relative to the frequency of occurrence of an amino acid in the protein as a whole. The substitution-derived propensities agree with the P_α values in some cases. For instance, Ala has a high P_α and a large s value (Padmanabhan et al., 1990). Phenylalanine has the third

highest P_α value among the amino acids, and yet, it is found to be helix-destabilizing through substitution experiments. This indicates that other factors in addition to the helix propagation constant are important in determining P_α for an amino acid.

In order to understand these discrepancies, it is necessary to examine the helix propensities of the individual amino acids in more detail. Substitution experiments yield a wide range of helix propensities for the amino acids. To make sense of this, it would be helpful if one could understand the range of propensities in terms of the structures of the individual amino acids. The basic structure of all amino acids, except proline, is the same:

$$^{+}H_3N\text{-}CHR\text{-}COOH$$

The unique property of each is the R-group. Each R-group of the common residues is different, suggesting that there is a structural basis for amino acid α-helix propensity.

There have been numerous studies which have demonstrated a structural basis for α-helix propensity. The substitution experiment discussed previously (Padmanabhan et al., 1990) illustrated a point not seen in host-guest results. Substitution with Phe, Ile, and Val yielded significantly larger decreases in the s values with respect to those for Ala and Leu. This contrasts with earlier data that designated Ile as a better helix former than both Ala and Leu. These results are also in agreement with theoretical studies of α-helix versus β-sheet formation which indicate that β-branching in an amino acid causes the residue

to be helix-destabilizing (Padmanabhan and Baldwin, 1991). Host-guest studies did not detect any effect of β-branching. The destabilizing effect of β-branched amino acids and bulky side-chain substituents (Phe) has been interpreted to mean that the conformational freedom of the side-chain available to a residue is energetically important to the helix propensity of the amino acid. Larger side-chains, as well as polar side chains tend to reduce the stability of an α-helix and, correspondingly, the helix propensity of the amino acids.

Further experiments have been done regarding the role of the side-chains of non-polar amino acids in determining helix propensity (Lyu et al., 1991). In these, helical peptides were synthesized containing unnatural side-chains consisting of two to four carbons with the purpose of examining some potential factors in helix stabilization. A number of definite conclusions can be drawn from the results. It was seen that linear side-chains of up to 4 carbons displayed the same degree of helix-stabilization as the alanine methyl side-chain. A linear side-chain was a stronger helix stabilizer than a non-polar branched side-chain such as that of isoleucine, valine, or t-leucine. The results also showed significant differences in helix propensity among the natural amino acids with alkyl side-chains. The order of helix forming character is Ala>Leu>Ile>Val (Lyu et al., 1991). Thus, non-polar amino acids with unbranched side chains preferentially stabilize α-helices, whereas β-branched R-groups destabilize helices. This was explained by the restriction in the conformational freedom of the side-chain that results from helix-formation.

Another study has shown that glycine (-H) has a smaller helix propensity than alanine ($-CH_3$) (Chakrabartty et al., 1991). If branching reduces the conformational freedom of the side-chain and therefore the ability to stabilize the helix, the lack of a side-chain in glycine might be expected to enhance helix-formation. Gly has virtually unrestricted conformational freedom due to the absence of a β-carbon. However, this probably favours the random coil, not the α-helix, because of the missing favourable enthalpic interactions between the helical backbone and the β-carbon (Chakrabartty et al., 1991).

According to Lyu (1991), the length of the side-chain does not exert any real influence on helix formation in amino acids with linear alkyl side-chains. This is in contrast to other reported results. A study of homologous polymers with increasing aliphatic side-chain length was performed in aqueous solution (Berger et al., 1966), 25 years previous to the work of Lyu et al., 1991. The findings of these early tests provided evidence that an increase in helix stability does occur with increasing chain length, likely due to formation of hydrophobic interactions between the side-chains. This conclusion was supported by the absence of this effect in organic solvents. Studies similar to the more recent ones discussed above (Padmanabhan and Baldwin, 1991) indicate that some increase in helix stabilization with increased linear side-chain length does indeed occur. There is thought to be a small stabilizing hydrophobic interaction occurring with longer side chains.

The results for straight and branched-chain alkyl R-groups are well-

documented. But this only covers less than one-third of the 20 natural amino acids. The remaining polar/charged side-chains must also have effects on helix propensities and stabilities. Host-guest and substitution experiments have been carried out on the remaining amino acids. In substitution experiments, substitutions were made at interior sites within blocks of glutamic acid and lysine. This synthetic peptide is highly soluble and displays partial helix formation at low temperature in aqueous solution. Near neutral pH, the alternate oppositely charged blocks of amino acids allow ion pairing between positions i and i+4 of the chain. Substitutions were made into the peptide succinyl-EEEEKKKKXXXEEEEKKKK-NH_2 at the positions designated X. Both the amidation of the carboxy terminus and the succinyl group at the opposite end promote helicity (Shoemaker et al., 1985). CD studies were used to measure the helicity. The results agree to some degree with the previous studies of non-polar side-chains. Ala exhibits high helix propensity and Gly shows little propensity. The order of stabilizing strength of the 10 residues studied by Kim and Baldwin (1984) is A>L>M>Q>I>V>S>T>N>G. These findings disagree with the host-guest stabilities of Sueki et al., 1984, and statistical helical preference values, P_α (Chou and Fasman, 1973), but do conform to results for residues with non-polar side-chains (Padmanabhan et al., 1990) and with the observations of O'Neill and DeGrado (1990). One slight difference is the finding that Ser is even more strongly helix-destabilizing than Ile and Val. It is believed that having three Ser residues in sequence causes a

destabilizing effect on the helical structure (Kim and Baldwin, 1984).

Another study used multiple substitution of all 20 amino acids at two sites in the helical regions of T4 lysozyme (Blaber et al.,1993). Each remaining one of the 19 alternate amino acids was substituted at site forty-four. The resulting mutant proteins were purified and in 13 cases, crystallized and studied by X-ray diffraction. The stabilities of the substituted proteins were determined by temperature titrations by CD. The differences in free energy between each mutant and a reference T4 molecule with Gly at site forty-four were found to agree very well with propensities determined by substitution experiments (Padmananbhan and Baldwin, 1990) and P_α values as determined from X-ray data.

The results of these experiments are interpreted in terms of side-chain structure. In an α-helix, the backbone or side-chain atoms of a residue can be in contact with the side-chain atoms of a residue in the next turn of the helix. Such contact denies contact of these atoms with the solvent. This is further support for the idea that helix propensity is a function of side-chain hydrophobic effects. Observed free energy differences (see above) were plotted against the side-chain hydrophobic surface area which becomes buried when the site of the substitutions is part of an α-helix. A number of the amino acids fall on a straight line which has a slope of 19 kcal mol^{-1} $A°^{-2}$. This value is in agreement with the energy of 20-30 kcal mol^{-1} $A°^{-2}$ that is accepted as the hydrophobic stabilization energy. The lack of agreement for amino acids including Ala, Pro,

Gly, Arg, Trp, and Phe has a structural basis. Pro does not exhibit the same hydrophobic stabilization and possesses a low helix propensity because its structure introduces considerable strain energy to the peptide chain in an α-helix. Proline causes the helix axis to bend when it occurs in the interior of a helix. Gly has a low helix propensity because of its backbone conformational flexibility and inability to participate in hydrophobic stabilization (no β-carbon). Arg has a long side-chain which adopts an extended conformation and can participate in hydrogen bonds. The lower propensities of Trp and Phe are likely due to the bulkiness of their side-chains. The close agreement between helix propensity determined this way and studies of helical peptides seems to be linked strongly to the buried hydrophobic surface variations of the amino acids.

Charged groups have a strong influence on helix stability and residue helix propensity. This "charged group" effect on stability has been investigated using analogues of the C peptide of ribonuclease A (Shoemaker et al., 1985) in which charged residues involved in the pH-dependent stability are replaced with uncharged residues. Using this technique, charged residues needed for helix stability and formation have been identified. The positioning of charged residues is a factor in helix stability. It has been observed that positively and negatively charged residues occur at opposite ends of helices with acidic residues near the N-terminus and basic ones near the C-terminus (Anfinsen, 1961). This occurrence has been discussed in terms of a helix dipole model which connects the distribution of charged residues in a helix with their helix-

stabilizing tendency. The occurrence of oppositely charged residues at the opposite ends of helices has the effect of neutralizing the helix macro dipole and is a helix-stabilizing factor. Charged side-chains can play another direct role in the stabilization of a helix. When amino acids having oppositely charged side-chains are positioned three positions apart along a polypeptide chain, upon helix-formation they will face each other on the helix surface and potentially have the opportunity to form ion pairs (Lyu et al., 1990). Charged residues have been shown to stabilize the helix formed in the C peptide. pH titration data of this peptide have shown that a salt bridge stabilizes the C peptide helix in that both the Glu-9$^-$ residue and His-12$^+$ residue are required if a stable helix is to be formed by the peptide. The salt bridge between these residues stabilizes one turn of the helix which acts as a nucleation point.

It has been shown that protein conformations are strongly influenced by short-range interactions (Scheraga, 1974). By "short-range" we mean an interaction between the side-chain of an amino acid residue and the peptide backbone of that same residue. Using conformational energy calculations, Scheraga demonstrated that the energy of interaction of side-chains with the backbone (the lowest energy conformations) correlates with the helix propensities determined empirically from the host-guest experiments. Thus, it would appear that helical propensities may be a function of the short-range interactions of the side-chain. If this is so, it seems that the conformational preferences of the amino acids are independent of the nature of the

neighbouring residues. Scheraga's results indicate that Ala and Leu have high helical propensity, and Gly is a helix breaker. This can be rationalized in that the conformational entropy of an amino acid in the random coil state has to be overcome by favourable energy terms to become helix forming. These favourable terms are the result of short-range interactions between the side-chain and the backbone of the residue. Since Gly has no side-chain, it possesses no factors which can contribute to helix-forming properties. When there is a methyl or other β substituent present, non-bonded short-range interactions will favour helix formation. In some cases, the interaction of the side-chain is unfavourable and makes a residue helix-destabilizing. Asn has a polar side chain, and helix-destabilizing electrostatic interactions between the side chain and the amide group of the backbone occur.

In addition to the observations above, other research has demonstrated that there is a definite sequence-dependent contribution to the formation of helical regions in a protein. Studies have shown that there is a significant contribution to helix formation by the context in which the amino acid is located (Padmanabhan et al., 1990). The results indicate that the helix propensities of different amino acids strongly contribute to the formation of a helix within a specific sequence, but are not solely responsible for the secondary structure which develops.

According to Kabsch and Sander (1984), the helical propensity of single residues does not dictate what secondary structure a stretch of amino acids will

adopt nor can it override sequence effects. Proteins of known sequence and structure were searched for stretches of homologous sequence. Sixty-two proteins were examined and the longest stretch of homologous sequence between any of the proteins was 5 residues. Twenty-five of these five-residue homologies were found. Six of the twenty-five homologous sequences were located in different types of secondary structure. For example, a pentapeptide in hemoglobin (horse) existed in an alpha-helix. The identical five residue sequence in alcohol dehydrogenase is located in a beta strand region of the protein. This demonstrates that local sequence is insufficient to determine secondary structure formation.

The environment can also be a determining factor in the secondary structure preference of amino acid sequences. Three sequences have been found that, on the basis of the helix propensities only, are predicted to be helical. However, X-ray diffraction has shown them to be primarily beta-strand in the proteins where they are found (Johnson and Zhong,1992). Under different solvent conditions, the sequences display the predicted α-helical structure. In a number of organic solvents and at high concentrations of SDS, the α-helical conformation is attained and can be measured by CD. Conversely, solvent systems which mimic the hydrophobic interiors of proteins result in the sequences showing significant β-character. Another study examined α-helix stability in some alanine-based peptides as influenced by the amino acid sequences of the peptides and sequence-dependent short-range

interactions (Padmanabhan et al., 1990). The results showed that the helix propensities of the residues in a segment of a protein contribute strongly to the determination of helix-formation within a segment of a polypeptide chain (local sequence effect).

Recently, a number of studies have been published on β-sheet propensities. The thermodynamics of β-sheet propensities have been measured in a substitution experiment using a zinc-finger peptide as the host peptide (Kim and Berg, 1993). Substitutions into a solvent-exposed site of the peptide with the 20 common amino acids were assayed by a metal ion binding experiment to obtain the folding energy differences that resulted from the substitutions. The peptides are in an unfolded conformation in the absence of metal ions but attain a folded state when a metal ion such as cobalt is present. Thus, the metal-ion binding energy is believed to be representative of the peptide-folding energy. Since the β-sheet is the normal folded conformation of the zinc-finger peptide, the relative free energy of folding initiated by metal binding to the unsubstituted peptide can be used as a standard value for β-sheet formation. Deviations from this standard value when different amino acids are substituted into the guest site can be used to quantify the β-sheet propensities of the residues. The differences in energy determined for the different substitutions correlate well with the statistical β-sheet preferences, P_{β}, (Chou and Fasman, 1989) of the amino acids determined using the same procedure as for the determination of helical preference, P_{α}. The agreement

between the two sets of data is much greater than a similar correlation of helical preferences. Unlike helix propensities, β-sheet propensities are not significantly affected by side chain conformations. Helix propensities can be discussed in terms of decreases in side-chain entropy, but theoretical calculations based on side-chain conformations in secondary structures indicate that such considerations are of less importance for β-sheet propensities.

Another study of β-sheet propensities suggests that context is a strong factor in determining the propensities (Minor Jr. and Kim, 1994). Context refers to tertiary interactions or interactions among specific secondary structural units. There are two such contexts in which sheet-forming residues can exist. A residue can be in a central strand of a β-sheet, bounded on each side by other β-sheet residues, or it can be in an edge strand which has another β-strand on only one side and is exposed to the solvent on the other side. In this work, the twenty amino acids were substituted at position forty-four in an edge strand of the protein G(GB1). The replacements were made by site-directed mutagenesis in a modified protein in which neighbouring residues to site forty-four had been replaced by alanine residues to minimize local (short-range) interactions involving the replacement amino acid. The resulting stabilities of the mutants were determined by following the thermal unfolding of the proteins by circular dichroism. Energy differences were referenced to the host protein with alanine at site forty-four. Differences in each mutant protein's stability with respect to the reference protein were taken to be representative of the residue's ability to

maintain the β conformation and thus be a measure of its β-sheet propensity. Energy differences among residues substituted at the edge position are smaller than those for central strand substitutions. The overall magnitudes of the β-sheet formation energies for replacements at the edge and central positions are similar and the significant differences between them correlate with the accessible hydrophobic surface areas of the side-chains. This finding, along with the statistically-determined β-sheet preferences, suggests that the ability of the residues to interact with the surrounding β-sheet structure plays a large role in determination of the β-sheet propensities.

In a related study, β-sheet propensities have been shown to be dependent on the side-chains of residues (Bai and Englander, 1994). Using hydrogen exchange in dipeptides, Bai and Englander demonstrated that the rate of exchange of backbone amide protons in the model were dependent on the nature of the residue side-chains. The side-chains exerted a blocking effect on both acid- and base-catalyzed exchange. The reason for the effect on β-sheet propensities by this mechanism is that the blocking effect strengthens the peptide group hydrogen bond by inhibiting a hydrogen bond that might form between the peptide group and the solvent. In examination of non-polar R-groups, the blocking effect was measured relative to Ala. The non-polar side-chains exhibited retardation of the exchange rates of acid and base-catalyzed exchange to the same extent.

Polar side chains enhanced the base-catalyzed exchange rate through an

inductive effect, and thereby decreased the acid-catalyzed exchange rate. A high correlation was observed between the β-sheet propensities and the solvent activation energy, which supported the theory that side-chain blocking effects are almost wholly responsible for observed β-sheet propensities in proteins and peptides. Only cysteine and phenylalanine showed any significant deviation from the pattern, but no suitable explanation for this observation was given.

An attempt by Bai and Englander to rationalize α-helix propensities in terms of side-chain blocking effects was not as definitive. Theoretical contributions of the blocking effect and the helix propensities measured using the host-guest technique (Sueki et al., 1984) agreed well, but, as the propensities measured by the host-guest method and those determined from substitution experiments differ widely, interactions between the guest residue side-chain and neighbouring residue side-chains in each experimental system studied could be significant.

1.2 Properties of Aib Residues

Most proteins and peptides which occur naturally have compositions that consist of the twenty common amino acids. However, a number of molecules, mainly small peptides, do exist in nature having amino acids different from the normal twenty. Peptides which have sequences containing an uncommon amino acid, α-aminoisobutyric acid (Aib), are classed as peptaibols. An amino

alcohol is usually found at the C-terminus in these molecules. The peptides in this category are small peptides produced by fungal sources, and often possess anti-bacterial properties.

The peptaibol most thoroughly studied to this time is alamethicin. Alamethicin is a twenty-residue peptide synthesized by the fungus *Trichoderma viride*. It has eight Aib residues in its sequence and has phenylalaninol at the C-terminus. (see Figure 1). Alamethicin has an anti-microbial activity that arises from its ability to insert into bacterial membranes. Bundles of alamethicin peptides can form amphipathic transmembrane helices surrounding a central pore. This channel formation alters the membrane permeability to ions and small molecules eventually leading to swelling of the cell and its lysis. The ability of alamethicin to insert into cell membranes is a function of its hydrophobicity.

Ac-B-P-B-A-B-A-Q-B-V-B-G-L-B-P-V-B-B-Q-Q-O

Figure 1: The amino acid sequence of alamethicin

Pore forming properties make these peptides very interesting. The molecular structures of alamethicin and related peptaibols have been studied and characterized primarily by X-ray crystallography (Fox and Richards, 1982; Karle et al., 1987). These studies have indicated that molecules in this class are predominantly α-helical, and often possess a 3_{10} hydrogen bond at the C-terminus and sometimes, even in the interior of the molecule. Peptaibols commonly have a proline residue at position 14 and are often kinked in the

middle to accommodate the ring of the proline in the helical backbone.

This α-helical preference is a common characteristic of Aib-containing molecules, as shown by the primarily helical conformation of alamethicin, as well as other membrane-traversing peptides from *T. viride* (Mayr et al., 1979) and more than sixty Aib-containing peptides (Marshall et al., 1990; Karle and Balaram, 1990). It has been suggested that such a predilection for the helical conformation could be a result of the unique structure of the Aib residue. The α-aminoisobutyric acid residue has an achiral C^{α} with two methyl substituents. This structure has significant influence on the possible conformations that the amino acid can adopt. The structure of Aib is analogous to the structure of alanine, except the lone alpha proton of Ala is replaced with a second methyl group. (Figure 2)

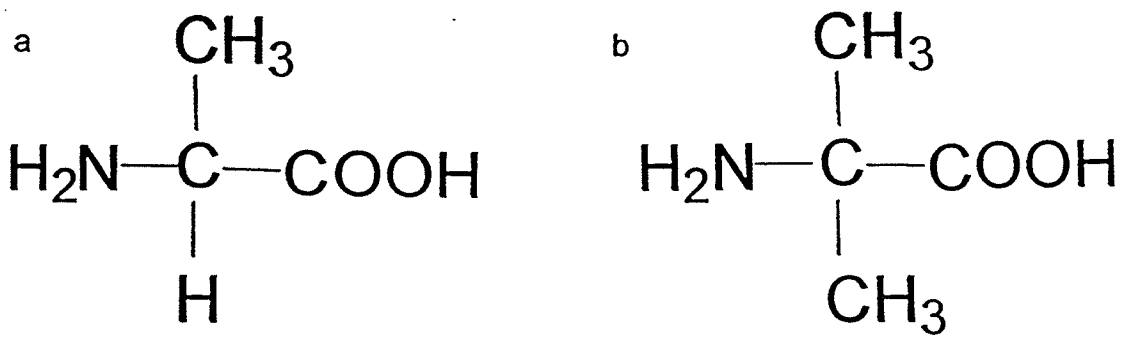

Figure 2: (a) Alanine and (b) α-aminoisobutyric acid

This second methyl substituent at the C^{α} severely hinders the rotational freedom about the N-C^{α} and C^{α}-C' bonds in the residue and restricts the

backbone conformations of polypeptides containing Aib. Only a small range of torsional angles, ϕ and φ, respectively, about the previously mentioned bonds are allowable. Ramachandran plots published by Marshall and Bosshard (1972) show that the addition of another alkyl substituent on the C^{α} reduces allowable torsional angles for Aib in comparison to normal amino acids (Marshall et al.,1990). Values for the ϕ and φ angles available to Aib residues are confined to two major areas near -57°, -47° and 57°, 47°. These two areas correspond to right-handed (3_{10}- or α-) and left-handed (3_{10}- or α-) helices, respectively. Note that there is no chirality at the α-carbon in an Aib residue. However, helices containing Aib residues have their handedness fixed by the configurations of the other residues in the sequence (Karle and Balaram, 1990). Examination of the crystal structures of numerous Aib-containing peptides supports the implications of the calculations of the Aib Ramachandran plots. With only a few exceptions, Aib residues in peptides are found in mainly α-helical segments or 3_{10}-helices (Karle and Balaram, 1990).

The preference of the Aib residue in a peptide for a particular helical state is dependent on several factors, including the Aib content and placement, peptide length, and solvent (Otada et al., 1993). Polypeptides containing only Aib form 3_{10} helices (Toniolo et al., 1991). Thus, polypeptides composed of Ala and Aib have been used to study the transition from a 3_{10}-helix to an α-helix (Otada et al., 1993). The critical chain length required for the $3_{10}/\alpha$ transition is seven. That is, Aib-containing peptides of less than seven residues usually are

in the 3_{10} conformation, but if there are seven or more residues, the peptide will convert to the α-helical conformation (Karle and Balaram, 1990). The Aib content is another factor in this transition. If the Aib content is 50% or greater, the peptide will have the 3_{10} conformation, but if the Aib content is less than 35%, the peptide will take the α-helical state. Solvent polarity also plays a role in the $3_{10}/\alpha$ transition. The α-helical state is preferred in polar solvents, while in less polar media, the 3_{10} conformation is preferentially adopted. A factor which has been determined to be as significant in determination of the preferred helical conformation is the sequence of the molecule (Basu et al., 1991). If monosubstituted residues like alanines are contiguously positioned in the peptide, the α-helical conformation is formed preferentially.

This restriction to helical conformations for Aib imposed by the disubstitution at the α-carbon has generated interest in the potential usage of Aib residues in the area of protein design. It is interesting to compare the helical propensities of Aib and the monosubstituted form Ala. If the disubstituted Aib has a greater propensity than the similar monosubstituted Ala, this very strong tendency could be used to positive effect in synthesis of artificial sequences designed to fill specific roles. For example, a sequence designed to mimic a receptor protein may require a segment of the molecule to be helical. Incorporation of Aib residues into the synthetic sequence in place of Ala could expedite the formation of a helical segment in the molecule.

The abilities of Aib, Ala, and dehydroalanine to stabilize helical

conformations have been investigated in a quantum mechanical study (Alemán, 1994). Semi-empirical calculations were performed for oligomers of 1- 6 residues (Aib, Ala or dehydroalanine). The results showed that the residues modified at the C^{α} position were more successful at forming helices than Ala. This result for Aib is not surprising, because, as previously discussed, X-ray structures of more than 60 Aib-containing peptides show a pronounced preference for the α-helical conformation. Dehydroalanine (ΔAla) is an α,β-unsaturated amino acid that is commonly found in bacterially-produced antibiotics. The side-chain of this residue contains a double bond which results in defined conformational behaviour and is predicted to favour the extended conformation in a small peptide with a low number of dehydroalanine residues, which is supported by X-ray and NMR data. However, Alemán (1994) recently has predicted that the 3_{10}-helix is the conformation of greatest stability in polypeptides containing a high degree of dehydroalanine residues since quantum mechanical calculations suggest that helical conformations are stabilized in comparison to the extended conformation when more than six dehydroalanine residues are present in the sequence. The calculated tendency of the Aib and ΔAla is to stabilize helical conformations.

1.3 Solvent Effects on Peptide Conformations

Conformational and functional investigations of biological molecules such as proteins have traditionally been performed using samples prepared in

aqueous solution. This seems intuitively to be an obvious solvent system to employ for proteins, since a protein's normal environment is highly aqueous in character, as biological fluids are water-based. Understanding the behaviour of proteins in solvents similar to the natural protein environment is critical to understanding the roles and functions of proteins in living organisms.

However, the examination of protein properties in non-aqueous solvent systems, particularly the function and conformation, is of increasing interest. Although the findings in non-aqueous systems do not have direct applications in medical research (for example), important information can be gained about the basic properties of proteins, which can be used to understand the properties of proteins in biological systems.

Experiments done under non-aqueous conditions have several advantages over those carried out in water-based media (Singer, 1962). A number of interesting physical and chemical properties of solvents are accessible if non-aqueous solvents are used to dissolve the solute. A wide range of solvent dielectric constants becomes available for studying solubility properties of biological molecules. Solvents with viscosities different from water may be used to examine viscosity effects on protein function or form. Non-aqueous solvents such as organic liquids may be used to study proteins in solution at much lower temperatures that can be reached using aqueous systems. This property of non-aqueous media is very helpful for studies on temperature effects on protein conformations. Another property of

solvents other than water is a different capacity for hydrogen bonding. Different solvents possess varying abilities to donate or accept protons for hydrogen bonds, and therefore the solvent-solute bonding pattern in non-aqueous solvents may be substantially different than in water. These different bonding interactions could have a definite effect on the folded structures of biological molecules.

A property that non-aqueous solvents used for studying proteins must possess is chemical inertness. The solvent cannot react with the chemical groups or bonds in the protein. For example, it must not be an oxidizing, reducing, or alkylating agent. No new covalent bonds can be formed within the protein as a result of the solvent. Similarly, no pre-existing covalent bonds must be broken. A non-aqueous solvent must also be stable under a variety of conditions. This means that exposure to oxygen, water vapour or temperature variations should not alter solvent properties such that the solvent's inertness is compromised.

The most commonly used non-aqueous solvents employed in protein structural studies are alcohols. These organic solvents meet the criteria that are necessary for protein studies. A very interesting characteristic of many alcohols is that when proteins or polypeptides are dissolved in such solvents, they appear to display enhanced structural order, particularly helix content, in comparison to their structure in aqueous solution. Organic solvents such as methanol and other alcohols are referred to as helicogenic when used as

primary solvents or as cosolvents for proteins (Arakawa and Goddette, 1985).

The effects that organic solvents such as methanol, ethanol and halogenated alcohols have on a folded protein or polypeptide is sometimes described as "denaturing". However, this denaturation is different from that produced by heat or agents such as urea or guanidine hydrochloride. Whereas treatment with these agents results in a disorganization and partial randomization of secondary and tertiary structures, numerous organic solvents cause formation of an apparently more highly ordered conformation of the protein (S.J. Singer, 1962).

Although simple alcohols such as methanol produce some degree of increased helicity in peptides and proteins, many of the more recent studies have focused on studies of protein structure in solutions having halogenated alcohols as the solvent or cosolvent. This class of compound has been observed to be a very good solvent for proteins (Carver and Collins, 1990). In particular, trifluoroethanol (TFE) has found wide usage as a solvent for peptides and proteins. This solvent has been observed to strongly stabilize helical structures in proteins and increase the helical content of some proteins. TFE will enhance existing ordered (helical) structure in small peptides such as the S-peptide (Nelson and Kallenbach, 1986) and it can induce formation of stable structure in peptides which otherwise are unstructured in aqueous solution (Yamamoto et al., 1990). There is still some question as to whether the ability of TFE to induce helix formation is a property that is a function entirely of the

alcohol or if the primary sequence of the peptide is paramount.

TFE was used in a study to determine if the solvent could induce helicity greater than the theoretical value arrived at using predictive methods. Evidence to answer this question was provided by a study of the bovine growth hormone (bGH) (Lehrman et al., 1990). In this work, a series of peptides which encompassed the complete sequence of this protein were examined by CD for helix formation as a function of TFE content of the solvent. The α-helicity of each peptide was predicted using the Chou-Fasman method and compared to the amount of helix formation determined from CD spectroscopy.

The amount of α-helicity developed by the peptides reached maximum values at 10 mol% TFE. These values were compared to the predicted values and showed a correlation for 8 of the 11 peptides; i.e. the predicted and observed values agreed to within 20%.

The fact that increasing TFE concentration above 10 mol% showed no increase in helix formation suggests that a peptide of a given sequence has a maximal potential for α-helix formation that is not dependent on the solvent composition. It was concluded that TFE-enhanced helicity in peptides is a good indication of α-helical propensity. It was observed that two of the three peptides which did not correlate with the predicted helicity were much more hydrophobic than the other nine peptides. This is thought to be a reason for the lower correlation between observed structure formation and that predicted for the sequence. The authors believe that the relationship between TFE-

enhanced and predicted helicity does not apply to very hydrophobic peptides. Conversely, one peptide is in an α-helical region of the protein but has a low predicted helical content and does not form a high degree of helix in TFE solution. Only three of the peptides that were observed to form helical structures in the presence of TFE were found in helical segments of the intact protein.

These results suggest that formation of an α-helix is influenced by long-range interactions within the protein. Potential to enter into a helical conformation in a peptide may be aided by or reduced by tertiary interactions within a protein.

Another study using a synthetic peptide corresponding to a segment of a protein was carried out by Sönnischen et al. (1992) to further study the effect of TFE on sequences to see if the solvent can cause them to form ordered structures. A 28-residue peptide with the same sequence as the 28 N-terminal residues of actin was studied using NMR and CD in solutions with increasing TFE content. The structure measured experimentally was compared to the predicted structure of the peptide and the corresponding structure seen in the crystal structure of actin. The degree of ordered structure in the peptide increases as the concentration of TFE increases. The distribution of ordered structure in the actin peptide was investigated using two additional peptides, one having the sequence of residues 1-20 and the second corresponding to residues 18-28 of the N-terminus. The structure of these two peptides was

studied, again using NMR and CD spectroscopy. From circular dichroism, the first peptide was induced to form a helical structure to a maximum amount of 48%. the smaller of the two peptides did not exhibit any helical or other structure under the same conditions. NOE information produced very similar results. The CD spectra of the peptides 1-28 and 1-20 are essentially the same, both showing strong helical character. As the concentration of TFE is increased, both sets of spectra display significant increases in negative ellipticity at 222 nm. The spectrum of peptide 18-28 was not influenced by higher TFE content. In aqueous solution, none of the peptides had a high degree of helicity based upon the ellipticity at 222 nm. The helicities of the two longer peptides showed a four- to five-fold increase in helical content at a saturating concentration of 80% TFE v/v. This high TFE concentration required to achieve maximal helicity in the peptide suggests that the helical propensities of the actin peptides here are relatively small, as peptides with fairly high helical propensities attain the largest helical content at considerably lower TFE concentrations. Using chemical shift measurements and nOe connectivities found by NMR spectroscopy, the helices in the peptides span residues 4-13 and 16-20 respectively (Sönnischen et al., 1992). Residues 21-28 do not exhibit any helicity. These findings agree quite well with the structure predicted for the peptides as determined by several methods. The residues 5-10 are predicted to exist in a helical conformation by three predictive methods as do residues 16-20. This substantial correlation between predicted structure and

experimentally observed structure indicates that predictive methods such as the Chou-Fasman algorithm may be used to accurately determine some residue- or sequence-specific helical propensities.

This idea that TFE acts to strengthen inherent structural preferences but does not induce new structure in peptides is supported by results with the S-peptide of ribonuclease A. Much work has been done using the S-peptide of ribonuclease A using TFE as a structure-inducing cosolvent since the initial discovery of TFE's helicogenic capacity. This is a short peptide composed of residues 1-20 of the ribonuclease A protein. The peptide is known to form a very stable α-helix in aqueous solution. Both CD and NMR data were collected to measure the effect of TFE on structure (helicity) in the S-peptide. It has been observed that the S-peptide forms a helix consisting of residues 3-12 in aqueous solution at low temperature, but the presence of a "stop-signal" which terminates the helix at position 12 has been proposed, based on the failure of the remaining residues of the peptide to become helical. Nelson and Kallenbach (1989) used NMR spectroscopy to assign which residues become helical in the presence of TFE and to determine whether the solvent can cause the remaining residues of the peptide to become helical or if the stop-signal remains active. Chemical shifts of C^{α}, C^{β}, and C^{γ} protons of the peptide residues at 0° were used to monitor helix-formation as the TFE concentration was increased. Protons of residues 3-13 showed significant upfield changes in their chemical shifts consistent with helix formation. The shifts of the last eight

residues do not indicate such a structural change, suggesting that the stop signal persists even at high TFE concentrations.

The reasons for this ability of TFE to stabilize and enhance the secondary structure of peptides are still subject to some debate. The stability of the S-peptide (in aqueous solution) has been shown by NMR studies on C-peptide analogs (residues 1-13) of ribonuclease A (Kim and Baldwin, 1984) to be the result of a charged-group effect resulting from charges on the amino acid side-chains and the helix termini. Initially, one explanation for the effect of alcohols such as TFE on protein structure was that addition of these organic solvents enhanced such electrostatic interactions and stabilized helix content. The dielectric constant of an alcohol is less than that of water, so larger electrostatic interactions would be expected. However, Nelson and Kallenbach (1986) showed that the magnitude of this charged group effect was negligibly increased even when TFE concentration in peptide solutions was raised to 40% v/v. This was determined by pH titrations of side chains in the peptide. No decrease in the stability of the helix was observed when the pH was decreased below pH 3.8. Thus another mechanism must account for the enhanced helicity seen in the S-peptide and others.

A plausible explanation for the observed effects of TFE is based on hydrogen bonding within a protein versus hydrogen bonding between a protein and the solvent. A solvent acidity or basicity difference such as that which exists between TFE and water can cause a change in the stability of hydrogen

bonds involving the protein or peptide. NMR investigations of the proton donor and acceptor capabilities of TFE have been carried out (Llinás and Klein, 1975) and the results indicate that TFE has weaker basicity than water. This means that it is a slightly weaker proton acceptor and a stronger proton donor. The peptide backbone in a protein or polypeptide has both amide donors and carbonyl acceptors. In aqueous solution, the water protons compete strongly with the amide protons for the hydrogen bonding sites of the backbone. When TFE is added, its lower affinity for protons in comparison to pure water lowers the solvent's ability to compete with the carbonyl acceptor sites (Thomas and Dill, 1993). Thus intramolecular hydrogen bonds between the amide protons of the residues in the protein and the carbonyl oxygens of other residues should be favoured in solutions containing TFE. As a helical conformation possesses such bonds along the polypeptide backbone, this structure should be favoured when TFE is added. This mechanism might also explain the greater stability of helical structures that are observed in proteins in other non-aqueous solvents.

The large degree of stabilization conferred upon peptides and proteins by a solvent like trifluoroethanol is a characteristic that has been used to good effect in studies of structural intermediates (partially re/unfolded states) of proteins. Egg white lysozyme was studied in the native and various denatured states in TFE by circular dichroism spectroscopy and ^{1}H-NMR by Buck et al.(1993). Structural analyses using CD spectra, chemical shift and hydrogen exchange data and NOE measurements of the forms of lysozyme

denatured by TFE, urea, and heat were done to assess the secondary structure in the intermediates. It was determined from the CD spectra that there was apparently a significant reorganization of lysozyme structure into an ordered conformation at TFE concentrations above 15% v/v. This interpretation was made from the examination of the ellipticity at 222 nm which became substantially more negative in the presence of TFE. Data obtained from hydrogen exchange of the amide protons showed a decrease in the rate of exchange in TFE solutions compared to the native aqueous solutions of lysozyme. The slow rate of exchange implies a conformation involving amide H-bonding which would make exchange slow. In contrast with the result of adding TFE, addition of urea to the lysozyme solution changed the ellipticity by decreasing the intensity observed at 222 nm, which suggested a major decrease in helical structure.

Other bodies of research suggest that alcohols such as TFE do not only enhance inherent helix-forming properties, but may in fact enforce helical conformations on peptides and proteins. Jackson and Mantsch (1992) studied the helicogenic capacities of five halogenated alcohols to test for short peptides' intrinsic abilities to form transmembrane helices. When used as pure solvents, each halogenated alcohol induced the conversion of a β-sheet structure to an α-helical one, as detected by Fourier transform infrared spectroscopy. The protein concanavalin A is primarily β-sheet, but can be induced to form a helical structure under certain solvent conditions. Findings of this type tend to suggest

that the halogenated alcohols' high dipole moments and low dielectric constants respectively disrupt the hydrogen bonding network in the β-structure and result in a refolding of the protein into a mainly helical conformation. The usefulness of halogenated alcohols for the study of helical propensities of peptides or as membrane mimetic agents is cast into doubt by the previously described results. If the alcohols' properties can force the peptides to form "unnatural" conformations (radically different from the native form), the results may not reflect the intrinsic tendency of a molecule to form helices, but, rather, reflect the conformation-altering properties of the solvent. Sönnischen et al. (1992) found in their study on an actin peptide that two regions showing helix formation in TFE in the small peptides correspond to β-strands in the protein. This can be explained in part due to the fact that important tertiary interactions (other neighbouring β-strands) necessary to β-sheet formation are missing in the peptides.

Halogenated alcohols contain a strong hydrogen donor which could likely disrupt the normal hydrogen bonding pattern of peptides. Neither the dielectric constant nor the dipole moment of a halogenated alcohol alone is enough to explain the effects that Jackson and Mantsch observe for concanavilin A. Evidence of this is provided by demonstration of different effects on the structure of the protein resulting from dissolution of protein in ethanol and chloroethanol for example, even though the two alcohols have very similar dielectric constants and dipole moments (ε=25, μ=1.69 debeyes for ethanol;

ε=25.8, μ=1.78 debeyes for chloroethanol). The proposed explanation for the difference in the effects of the different alcohols is that both types of solvent "denature" the protein by reducing the sequestering of hydrophobic residues in the protein interior, but the dipole moment of a halogenated alcohol only is sufficient to disrupt the hydrogen bonding scheme of the peptide backbone. A refolding process into a helical conformation is then promoted by the low dielectric constant of the solvent. The helix is energetically the most stable conformation in such environments with low dielectric constants. The solvent reduces hydrophobic interactions which are involved in stabilizing other types of structure such as β-strands. This can explain why β-structures can convert to helices in TFE solution.

Another class of compounds that are widely used to solubilize proteins,especially for conformational studies are detergents or surfactants. The most frequently-used detergents for this type of investigation are anionic detergents like different sulfate derivatives. Sodium dodecyl sulfate [CH_3-$(CH_2)_{11}$-SO_4^- Na^+] is the usual choice. These detergents are conformation-altering agents, usually classified as denaturants even at relatively low concentrations. All polypeptides appear to have similar, elongated shapes when SDS is bound to the protein. The hydrodynamic properties of SDS-protein complexes have been interpreted to indicate ordered, rod-like conformations. The CD properties of such complexes appear to indicate significant increases in helical content (Igou et al., 1974). This binding of an

anionic surfactant like SDS could be the result of different factors. One possibility that comes to mind immediately is that some sort of electrostatic interaction is taking place between the detergent and positively charged sites on the protein or polypeptide. Another possible explanation of the effect of the detergent on the protein is that there are interactions between the non-polar side chains of the residues and the long hydrocarbon tails of the detergent molecules.

A study was performed using poly(L-lysine) and poly(L-ornithine) (Satake and Yang, 1973). It was observed that in SDS, poly(L-lysine) (PLL) underwent a coil/β transition, while a coil/α transition occurred in poly(L-ornithine). In studies with poly(L-glutamic acid) in SDS (Fasman et al., 1964), only small effects were seen with the charged peptide. These results support the existence of an electrostatic contribution to the detergent/protein interaction, but whether placement of the emphasis should be on the attractive electrostatic interaction occurring between dodecyl sulfate and PLL or PLO or the repulsive interaction with poly(L-glutamic acid) is not completely clear. Also the type of transition that PLL undergoes is dependent on the chain length of the surfactant used. In solutions of dodecyl sulfate, the polypeptide shows a coil to β transition, but in octyl sulfate, it undergoes a coil to helix transition. It may be inferred that attractive forces between the detergent hydrocarbon tails and the polypeptide are much more important than electrostatic interactions in determining the conformation proteins exhibit in detergent solutions. Igou et al.,

(1974) studied the effects of dodecyl sulfate on uncharged polypeptides. No major effect was observed with these nonionic peptides. These were homopolypeptides with R groups not ionized at neutral pH, such as poly(N^5-ω-hydroxyethyl- and hydroxypropyl-L-glutamine). As the side chains did not have charged groups, electrostatic interactions did not have any effect. With these polypeptides, both the α-helix and β-structure were sterically possible so no bias existed as to the conformation that could be attained.

In ionic peptides, charge interactions are important but with uncharged peptides, perhaps hydrophobic interactions among the detergent side chains are influential in stabilizing the helical conformation.

There are numerous examples in the literature of the helicogenic properties of SDS on peptides. Bairaktari et al. (1990) studied two hepta-decapeptides, bombolitin I and bombolitin III in a CD and NMR study of the interaction of anionic detergent with peptide sequences. Both peptides are biologically active and believed to interact with cell membranes. Peptides such as these can form amphiphilic α-helices which may be an important determinant of their biological activities. The study was made to determine what conditions are necessary for the formation of the amphiphilic helical conformation and to investigate the interaction of the peptides with membranes and the resulting conformational changes. SDS was used as a mimetic for membranes to provide for the peptides an environment similar to their biological one. CD studies of the bombolitins in aqueous solution showed that the peptides did not

have defined secondary structure, but were not completely random. As SDS was added to the solution, the CD spectra indicated that the degree of secondary structure increased. At concentrations of detergent lower than the critical micelle concentration (cmc), the CD spectra of bombilitin III showed β-structural characteristics, but above the cmc, the peptide appeared to fold into an α-helix. Bombolitin I displayed similar behaviour in SDS solution. Both peptides formed a high degree of ordered (α-helix) structure in SDS, up to 60% for bombolitin III and about 70% for bombolitin I as estimated from the negative ellipticity of the CD band at 222 nm. NMR experiments gave very similar results to the CD data.

This study was extended by Tessari et al., (1993), examining the conformations of two fragments of uteroglobin using CD and NMR. In solution in the absence of SDS, the conformations of the peptides are almost completely random, but CD experiments indicated that at SDS concentrations below the cmc, the two peptides formed β aggregates. At the cmc and above, they fold into an α-helical conformation, with a helical content of close to 40% determined from the 222 nm CD band.

1.4 CD Spectroscopy for Structural Determination

Knowledge of the conformations of proteins is crucial to the understanding of the functions of these molecules. Currently, there are some powerful techniques for determination of the conformations of biological

molecules. X-ray crystallography has been employed for decades for this purpose, with more and more crystal structures of peptides and proteins being published every year. NMR spectroscopy is also used to obtain detailed structural information about molecules like proteins. This technique has a distinct advantage over crystallographic methods: NMR can be used to determine the solution structures of molecules. NMR may also be used to follow structural or conformational changes induced by altering conditions (van Stokkum et al., 1990). Information gained from such changes can provide vital data about protein folding/unfolding.

In a number of instances, use of either X-ray crystallography or NMR spectroscopy is difficult or impossible. In addition to the time and complex equipment required, and the difficulties of interpretation of the data generated by these techniques, there are problems associated with preparation of suitable samples for these methods. A protein may prove to be extremely difficult to crystallize for X-ray crystallographic study or it may not dissolve to a sufficient extent in a suitable solvent for NMR spectroscopy (van Stokkum et al., 1990).

When such a situation arises, it becomes necessary to use techniques which yield less detailed, but still very useful, information about the conformation of biological molecules. Perhaps the most useful "simple" methods that provide structural details are optical spectroscopic means. These spectroscopic procedures measure the interactions of light with chromophores present in biological molecules. Valuable knowledge can be derived this way

since the absorption spectrum of a biological molecule is extremely sensitive to the conformation of the chromophoric groups (Myer, 1985).

The optical activity of macromolecules is a result of their asymmetries. In a polypeptide chain, the amide linkage is a symmetric structure with a plane of symmetry that renders it optically inactive. However, each common amino acid (with the exception of glycine) has an asymmetric C^{α} which does induce optical activity in the amide transitions. Each individual amino acid has only a weak band in the optical activity spectrum. Thus, it is the asymmetric arrangement of the peptide units in space in a polypeptide chain (i.e. the conformation) that results in a distinct optical activity spectrum for a protein (Adler et al., 1973).

Two manifestations of the optical activity of proteins are optical rotatory dispersion spectra (ORD) and circular dichroism spectra (CD). Both of these have been used to obtain conformational information about proteins, but at present, CD spectroscopy is much more widely practiced.

CD differs from ORD in that it measures the wavelength dependence of the difference in the ability of the chromophore to *absorb* right- and left-handed *circularly* polarized light. Unlike ORD, each electronic transition produces only one CD band so a CD band can have only a positive or negative component. The width of the band in a CD spectrum is limited and contains no contributions from outside the spectral range being studied, differing from ORD in this respect (Adler et al., 1973).

Thus, CD spectroscopy has supplanted ORD spectroscopy for studying macromelecular conformation for three major reasons: (1) only a single band of a single sign is produced by each electronic transition,
(2) these bands are more easily located and assigned and (3) each band has only a certain width (range of wavelength) with no contributions from chromophoric transitions outside the region of study, whereas ORD has a finite value over the entire spectral range.

These differences stem from the natures of the two phenomena. ORD is a dispersive technique, meaning that it is displayed at wavelengths both near and far from wavelengths at which the electronic transition(s) occur; CD is an absorptive technique (Beychok, 1966) which can be observed only at wavelength intervals where absorption takes place.
The polypeptide backbone absorbs light at wavelengths lower than 240 nm. The absorption spectra of proteins are dominated in this far-UV region by two specific electronic transitions. The peptide linkage possesses the $\pi \rightarrow \pi^*$ transition. This is found at a wavelength of 190 nm. The second important transition is the $n \rightarrow \pi^*$ amide transition found around 220 nm. These give rise to the two major bands observed in CD spectra in the far-UV region. Other chromophores in proteins such as aromatic residues contribute only slightly to far-UV spectra (Cantor and Schimmel, 1980).

The arrangement of the peptide units with respect to one another determines the shapes and intensities of bands observed in protein CD spectra.

This arrangement is dependent on the conformation of the protein. In polypeptides, there are a limited number of organized structures such as the α- and other helices, the β-sheet, and β turns, as well as the random coil. Each organized structure places the peptide units of the backbone in different orientations and therefore each has a distinct CD spectrum (Johnson, 1988). Spectra of the major pure forms of secondary structure found in proteins are shown in Figure 3 (Yang et al, 1986; Chang et al., 1991).

The α-helix possesses two negative extrema, one around 222 nm and the second centred around 208 nm with a prominent notch or point of separation at 215 nm (Holzwarth and Doty, 1965). A strong positive band around 191-193 nm which is important in characterizing the α-helix was later recognized as a characteristic absorption band for the helical conformation (Greenfield and Fasman, 1969). Its spectrum is distinct from that of the β-form which is characterized by different wavelengths for the bands. The CD spectrum of the β-form, using $(Lys)_n$ at low pH, was first measured in 1966 by Sarkar and Doty (1966). This structure shows a negative band around 216-218 nm and a positive one at 195-200 nm (Yang et al., 1986). There are a variety of β-structures including β-strand and several types of turns which have slightly different CD spectra. Another important type of arrangement occurring in proteins is the random, unordered, or irregular form. The CD spectrum of this form is distinct from the α- or β-forms. It displays an intense, negative band near 200 nm and a much weaker band near 220 nm. This second weak band

can be either positive, or it may be a small negative shoulder to the much larger negative band (Yang et al., 1986).

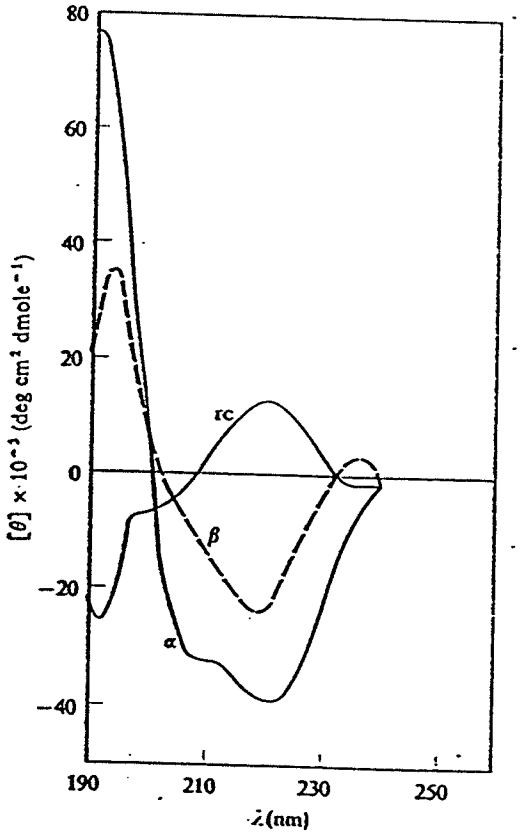

Figure 3: CD spectra of pure component secondary structures which can be present in a protein CD spectrum (Cantor and Schimmel, 1980).

Although each form of secondary structure has a distinct CD spectrum, it is highly unusual for a protein's conformation to consist of only a single type of structure. Thus, a CD spectrum of a protein may be considered to be a linear combination of the different structural elements.

A protein's CD spectrum is very sensitive to changes in the protein conformation. Therefore, it is possible to detect small changes in conformation. Hence, since each peptide chromophore has only a small amount of optical activity individually, there must be a change involving several groups of the polypeptide chain for a detectable difference to be observed in the spectrum. This permits CD spectroscopy to be used to monitor structural variations occurring with changing experimental conditions.

Although the CD bands in a protein spectrum may be the result of several types of secondary structure, it is difficult to determine accurately how much of each conformational type is present. The CD spectrum is an indicator of the secondary structure of a protein in a qualitative sense. It can provide one with an idea of what type of structure may predominate, but quantitatively, it is not a simple matter to get the true values from the spectrum. A number of methods have been devised to extract quantitative information from CD spectra.

For CD spectra of biological molecules to be analyzed and interpreted, there must be some form of reference to use. Different methods of analysis utilize different sets of reference data. In the initial stages of conformational

determination from CD spectra, researchers used homopolymers of amino acids synthesized such that the resulting polypeptide exhibited only a single type of regular structure like α-helix or β-sheet or showed a completely disordered structure when studied under specific conditions of pH and solvent composition. For example, the pure spectrum of an α-helix was determined using a homopolymer of poly-L-alanine. Poly-L-lysine (PLL) was a commonly used homopolymer because it could interconvert between different structural states depending on the pH of a solution of PLL (Dearborn and Wetlaufer, 1970). At a pH of 11.4, the conformation of this polypeptide is α-helical, but at low pH and low ionic strength, the structure becomes "unordered" or "random". The CD of these synthetic polypeptides was measured and compared to proteins of unknown structure in order to estimate the content of α-helix, β-sheet and "other" structure in the protein. For years this was the method of choice used to analyze the CD spectra of proteins. However, the question of the validity of this method was raised when researchers noticed significant differences between the CD of the presumably "unordered" structure of a polylysine homopolymer and the CD spectra of denatured protein solutions (Tiffany and Krimm, 1968). Similarly, film studies of polypeptides in the β-conformation showed that these models could give rise to two different types of spectra, indicating two different forms of β-structure (Fasman et al., 1970). It was suggested that the CD properties of poly-α-amino acids in solution could differ from proteins because of solvent effects which might affect the homopolymers,

but might be absent in the interior of a folded protein (Fasman et al., 1970), the effects of neighbouring groups, and possibly light-scattering (Urry and Ji, 1968).

As the number of protein secondary structures determined by X-ray crystallography increased, measured CD spectra of proteins of known secondary structural content were used to derive reference spectra of the pure secondary structures. In order to get good information about secondary structural types present in experimentally measured CD spectra from deconvolution approaches, it is important to consider the wavelength range used to collect the spectra is very important. Early on, when the fractions of secondary structure determined from CD spectra were compared with the values extracted from crystallographic data, the agreement between the two methods was not strong. Siegel at al., (1981) showed statistically that the CD for proteins over the range of 210-240 nm only correlated well with α-helical content. Hennessey and Johnson (1981) have determined that in order to calculate the amounts of secondary structures from protein CD spectra, measurements must be made from 260 nm to 178 nm. There is information present in CD spectra in the vacuum U.V. region at low wavelengths critical to determining types of β-structure. They suggest that unless the CD spectrum is measured below 190 nm, only the fraction of α-helix in a protein may be determined with any confidence.

1.5 NMR Used for Conformational Studies

NMR has become one of the most valuable techniques for the study of protein conformation. There is a plethora of NMR experiments that can be used to elucidate the conformation of a biological molecule. The temperature dependence of the chemical shifts of amide protons can be used as a marker for the existence of secondary structure (Wishart et al., 1991). In secondary structures such as the α-helix or β-sheet, the amide proton of an amino acid residue in the polypeptide chain is involved in a hydrogen bond with the carbonyl of another residue along the polypeptide chain. Participation in a hydrogen bond by an amide proton reduces the temperature coefficient of the chemical shift of the amide proton resonance. Thus, the magnitude of the temperature coefficient of the amide protons in a peptide can be taken as an indication of the presence or absence of some form of secondary structure. Conversely, in water, if the coefficient is greater than 7 parts per million per degree Kelvin, it can be assumed that the NH proton is exposed to the solvent and therefore is not hydrogen-bonded. If the value is less than 5 ppb/K, the proton is involved in a hydrogen bond such as in a helix or other secondary structure. Negative coefficients may also be taken to indicate that there is hydrogen bonding (Sönnischen et al., 1992). Different values for the coefficients between 0 and 5 ppm/K can be used to infer the strength of the hydrogen bonds. Values of 5-7 ppm/K are vague in their indication, suggesting either weak H-bonding or no such bonding. Measurement of the chemical shift

coefficients can be used to confirm the presence of secondary structure as determined by CD spectroscopy and has the advantage of pinpointing on a residue-specific basis the location of secondary structure detected by CD.

1.6 Goals and Proposed Experiments

As discussed in the introduction, Aib has some interesting properties in terms of preferred conformations. The Aib residue could have important applications in the field of protein design. This project is aimed at obtaining an idea of how strongly the Aib residue can influence peptide conformation with respect to its more common counterpart alanine by studying peptide conformation under different conditions of temperature and solvent. Both types of residue will be examined in analogous sequence contexts under similar experimental conditions using the technique of CD spectroscopy.

Temperature titrations of the peptide conformations will be done using CD to record the data. The CD data will be analyzed by several methods to get quantitative measures of the secondary structural content found in the Aib- and Ala-containing peptides as functions of temperature in the same solvents. This information will give an indication of how influential the Aib residue is in determining formation of ordered structure in an amino acid sequence and to what degree structure is formed and maintained under denaturing condititons.

CHAPTER 2

MATERIALS AND METHODS

2.1 Materials

A synthetic 20 amino acid peptide (RBP-1) was synthesized using the solid-phase method and purified by reverse-phase HPLC by Chiron Mimotypes Pty. Ltd., Australia. The sequence of the peptide was analogous to the published sequence of the fungal peptaibol alamethicin (Yee and O'Neil, 1992), except that alanine residues replace the Aib residues and phenylalanine amide replaces the C-terminal phenylalaninol (see sequence, pg. 19 of **Introduction**). The peptide was received as two lyophilized samples, 6.3 mg of greater than 83% purity and 4.3 mg of greater than 68% purity as determined from reverse-phase HPLC. Chromatograms of the two fractions are shown in Figure 4. The major impurity in the samples is expected to be other peptides differing from the target peptide by only 1 amino acid. These contaminants result from incomplete coupling reactions during the solid-phase synthesis process. In peptide synthesis, each coupling cycle is susceptible to some problems such as incomplete deprotection of the amino group of the peptide and incomplete coupling of the next amino acid to the lengthening sequence. Either occurrence results in peptides produced which are shorter by at least one amino acid. For example, if 19 couplings are carried out at 99% efficiency, then $.99^{19}$ or 82.6% of the product will be the 20 amino acid target peptide and the rest will consist

of 1% each of the 19 residue deletion peptides.

HPLC-grade methanol and ethanol were from Mallinkrodt, Missouri, USA. Trifluoroethanol was from Aldrich Chemical Co., Wisconsin, USA. Other solvents were from Fisher Scientific Co. USA. Water was deionized and distilled. Sodium dodecyl sulfate was from Sigma Chemical Co., and was of the the highest quality avaiable.

Figure 4: Chromatograms from the purification of RBP-1 by analytical reverse-phase HPLC. Absorbance was measured at 214 nm. (a) The chromatogram for fraction A (>83% purity) (b) Chromatogram of fraction B (>68% purity)

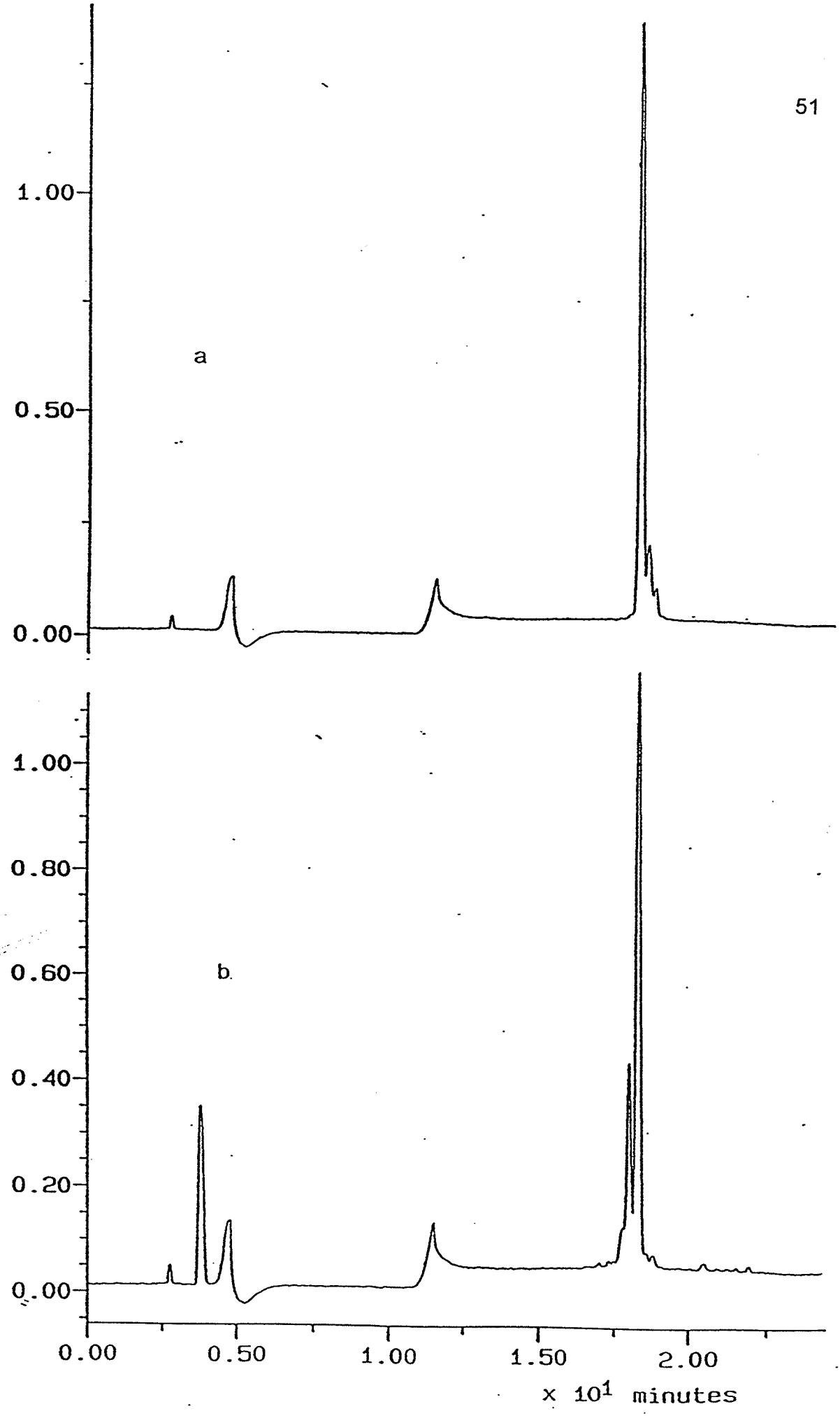
1.00
0.50
0.00
a
1.00
0.80
0.60
0.40
0.20
0.00
b
0.00
0.50
1.00
1.50
2.00
x 10¹ minutes

Methods

2. 2 RBP-1-1 Peptide Study

2.2.1 VERIFICATION OF PEPTIDE IDENTITY

The molecular weight and sequence of the peptide RIB-1 were determined by time-of-flight mass spectrometry by N. Poppe-Schreimer in the Physics Department of the University of Manitoba . A small quantity of peptide (~100 μg) was provided for the analysis.

2.2.2 SOLUBILITY STUDY OF RIB-1

Initially, my intention was to study the conformation of the peptide in solution by NMR spectroscopy. However, this method requires the preparation of samples at concentrations not less than 1 mM. As the peptide was not soluble enough in water or methanol for NMR, study of the solubility of the peptide in various solvents was made in an effort to circumvent this problem. The ability of solvents to solubilize the peptide was measured by acquiring UV absorption spectra of ten different solvent-RIB-1 mixtures. The results of the solubility study are presented in Table 1 in **Results**.

2.2.3 PREPARATION OF PEPTIDE SOLUTIONS FOR CD STUDIES

A weighed mass of peptide (~1-2 mg) was placed in a microcentrifuge tube containing 1.0 mL of solvent (CH_3OH, CH_3CH_2OH, TFE, H_2O, or a solution containing 50 mM SDS, 10 mM phosphate, pH 7.0). Typically, the tube was

repeatedly vortexed in an effort to achieve dissolution of the solid material, which did not reach completion. The tube containing the sample was warmed and cooled to determine if the solubility of the sample was temperature-dependent. The solubility did not appear to be enhanced by warming the sample tube, nor by use of lower temperatures in any of the solvents. In each case, the sample tube was allowed to remain undisturbed for periods ranging from 2 hours to 2 days at ambient, higher, or lower temperatures to permit slow solubilization to take place. Then the tube was vigorously vortexed again, placed in a microfuge (Beckmann Instruments), and centrifuged at top speed for 1-2 minutes to pellet the remaining undissolved material. The supernatant was removed to a new tube, while residual solvent was allowed to evaporate from the solid sediment which was then stored for future use. The resulting particle-free solution was used for UV absorbance measurements prior to CD spectropolarimetry studies.

2.2.4 CONCENTRATION DETERMINATION BY UV SPECTROPHOTOMETRY

Determination of peptide concentration was not straightforward due to sample solubility problems, sample availability, and low extinction in the near U.V. Limitations in the mass of peptide on hand was an important consideration in deciding how to determine the concentration. A method such as the Coomassie Blue Dye Binding Protein Quantization Method could not be

used because the sample could not be recovered for further use. Thus, a non-destructive spectroscopic method was chosen.

Another method used for protein concentration determination is measuring the near ultraviolet absorbance at 260 or 290 nm. This is the region at which aromatic side chains absorb. The concentration can be estimated using the absorbance value at this wavelength. The single Phe residue absorbs too weakly at 260 nm to be used in this manner.

In order to estimate the concentration of peptide based on far UV absorbance, a calculation of a molar extinction coefficient, ε, was done. This calculation was based on the residue extinction coefficients for peptide bonds at 207nm in ethanol (Rosenheck and Doty, *PNAS*, 41, 196, 1968). Two values for ε for the peptide were calculated to be 50950 and 44950 $M^{-1} \bullet cm^{-1}$. The lower value does not include the absorption of the three glutamine side chains. The concentrations of all the peptide solutions were determined using the former value.

The UV absorption spectrum of each solution prepared for CD spectroscopy was obtained for the purpose of determining the peptide concentration. The spectra were recorded on a double-beam Shimadzu UV-2101PC UV-VIS Scanning Spectrophotometer (Shimadzu, Japan). Quartz cuvettes having path length of 1 cm were used. Initially, two cells containing only pure solvent were placed in the instrument and a spectrum of the baseline was recorded over a spectral range of 300-195 nm, using a

slow scanning speed (less than 4 nm/min), slit width 0.2 nm, and a data interval of 0.5 nm•second^{-1}. The baseline was stored in the computer memory. After baseline collection, the cuvette in the sample cell holder was replaced with one containing 1 mL of peptide solution. The spectrum of this solution was collected in exactly the same manner with baseline subtraction being automatically performed. The sample spectrum was plotted on a Hewett-Packard plotter. Only solutions with values of ≤1 (absorbance unit) were used for concentration calculations. Samples with absorbances beyond this range were diluted with pure solvent.

The calculated extinction coefficient and the absorbance of the major peak in the spectrum were used to calculate the concentration of the solution. The position of the maximum for each solution was between 195 nm and 208 nm. A concentration value was calculated using Beer's Law:

$$A=\epsilon cl \qquad (1)$$

where A is the absorbance, ε is the molar extinction coefficient, c is the molar concentration of the solution, and l is the cuvette path length in cm.

Water-jacketed sample cell holders were used to maintain constant sample temperatures. To determine if there was any significant variation in absorbance values or peak position at different temperatures, the spectra of a sample of RBP-1 in methanol were collected at at three different temperatures and analyzed.

2.2.5 CIRCULAR DICHROISM

The same solutions were used for both UV and CD measurements. Circular dichroism studies were performed on a JASCO J-500A Spectropolarimeter (Japan Spectroscopic Co.) equipped with a chart recorder. Temperature titrations were performed over a range of temperatures which varied with the solvent used. These temperature studies were done using a water-jacketed quartz sample cell, path length 0.5 cm . The temperature was controlled using a circulating HAAKE water bath, containing a 90:10 v/v water:ethylene glycol mixture. The bath temperature was set with the temperature control, but the actual water temperature was recorded from the auxiliary thermometer of the bath. Upon stabilization of the temperature, the cell containing the peptide solution was allowed to equilibrate for 5-10 minutes at each temperature. Spectra for each solvent system were recorded over a wavelength range from 250 or 260 nm down to 200 nm. Baseline spectra of each solvent were recorded similarly over the same wavelength range at several temperatures to assess temperature-dependence, and were later used for baseline correction during data analysis. The spectra were collected starting form the low end of the temperature range studied and in some cases reversibility was examined by returning the sample to lower temperatures again.

Parameters used for the temperature titrations were: time constant: 4 seconds; λ expansion: 5 m°/cm; chart speed: 1 cm/minute. The sensitivity

varied from 1 $m^{\circ} \circ cm^{-1}$ to 2$m^{\circ} \circ cm^{-1}$.

2.2.6 ANALYSIS OF CD SPECTRA

After collection of the CD data, the spectra were analyzed. First, a baseline correction was performed to compensate for the spectrum of solvent. The solvent baseline was sketched on the sample spectrum (see Figure 5). The net ellipticity (Θ_{obs}) of the sample spectrum was determined by measurement with a ruler. The measured Θ_{obs} values were used to calculate molar ellipticities and mean residue ellipticities at 222 nm using the equations:

$$[\Theta_{\lambda}]_{MW} = \frac{\Theta_{obs} \, x \, MW}{10dc} \qquad (2)$$

$$[\Theta_{\lambda}] = \frac{\Theta_{obs} \times MRW}{10dc} \qquad (3)$$

where $[\Theta_{\lambda}]_M$ is the molar ellipticity, $[\Theta_{\lambda}]$ is the mean residue ellipticity at the indicated wavelength, Θ_{obs} is the observed ellipticity in degrees, MW is the molecular weight of the peptide, MRW is the mean residue weight of the peptide, d is the cell pathlength in cm and c is the concentration in grams per mL. For each sample, ellipticities at 222 nm were plotted against temperature to obtain a temperature titration profile of the peptide in each solvent. A calculation of the helical content (f_H), determined from Θ_{222} values was done

Figure 5: Experimental CD spectrum of RBP-1 in TFE at 0°C. The baseline of the spectrum was collected over the same wavelength range and the spectra were superimposed.

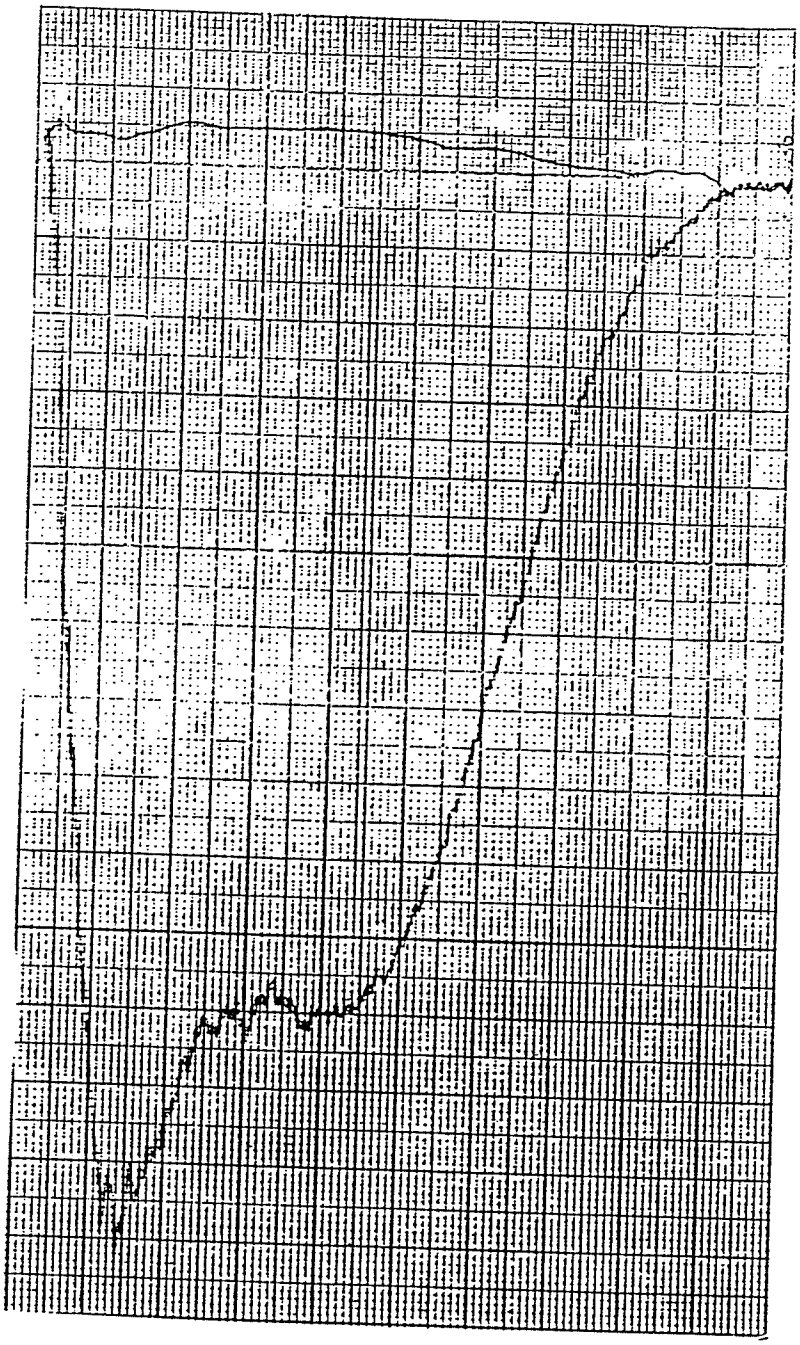

for each temperature using the equation:

$$f_H = \frac{[\Theta_{222}] + 2340}{-30300} \times 100 \qquad (4)$$

A second analysis of the secondary structure content of the peptides was carried out using Equation 5, derived for small peptides (Scholtz et al., 1991):

$$f_H = \frac{\Theta_{obs}}{\Theta_{100\%} - \Theta_{0\%}} \times 100 \qquad (5)$$

where $\theta_{100\%}$ and $\theta_{0\%}$ are the ellipticities for a twenty amino acid peptide in the 100% and 0% helical conformations, respectively. The values for 100% and 0% were calculated from equations 3 and 4 in Scholtz et al., 1991.

A third analysis of the secondary structure content of the peptides was done using the program CCA (Fasman et al.,1991). This employs an algorithm to deconvolute the spectra into their component parts, providing an estimate of the contributions to the total spectra from a number of secondary structure types. The experimental spectra were manually digitized by measuring Θ_{obs} at 1 nm intervals from 240 nm to 200 nm, or as low as could be determined as described above. These values were entered into a data file in the CCA program. Each spectrum was deconvoluted into 2,3,4, or 5 pure components (see **Introduction**). The output generated by the deconvolution algorithm was the conformational weight which could be used

to generate a corresponding spectrum for each pure secondary structure. The sum of the conformational weights of the component curves were plotted to obtain a calculated spectrum which could be plotted against the experimentally observed spectrum to test the fit of the computation.

2.3 Alamethicin Analysis

2.3.1 CD STUDY OF ALAMETHICIN

CD temperature titrations of alamethicin in methanol and in SDS (15mM SDS, 10mM Na_2HPO_4, 10mM NaH_2PO_4) were performed by A.Yee as described above for RBP-1. I analyzed her spectra using the same methods described in the previous section.

2.3.2 CHEMICAL SHIFT TEMPERATURE DEPENDENCE DETERMINATION

The temperature-dependencies of the chemical shifts of the backbone and glutamine side-chain amides of alamethicin were determined by ^{1}H-NMR spectroscopy. One-dimensional ^{1}H spectra of a 3mM ^{15}N-labelled alamethicin sample (provided by A. Yee) in CD_3OH were acquired over a temperature range from 230K to 340K using a spin-echo difference pulse program with pre-irradiation of the water resonance. The amide proton chemical shifts were plotted against temperature and their temperature-dependencies (slopes in ppb/deg K) were extracted from a least-squares fit of the data.

2.4 Curve Fitting of CD Temperature Titration Data

The CD titration data for RBP-1 and alamethicin were fitted to the equation :

$$\theta_{obs}=\frac{\theta_{100}+\theta_0 \cdot 10^{\frac{2(T-T_m)}{\Delta T}}}{1+10^{\frac{2(T-T_m)}{\Delta T}}} \qquad (6)$$

taken from Shalongo et al. (1994) This equation analyzes the thermal dependence of the ellipticity values at 222 nm at each temperature in terms of a 2-state helix/coil transition and calculates values for T_m , the midpoint temperature of the helix/coil transition of the peptides, and ΔT, the width of the thermal transition. Values for the constants used to represent the ellipticity values at 222 nm for 100% (θ_H) and 0% (θ_C) helix were obtained from Scholtz et al. (1991).

CHAPTER 3

RESULTS

3.1 Results of RBP-1 Studies

3.1.1 MASS SPECTROMETRY

The identity of the synthetic peptide RBP-1 was confirmed by fast atom bombardment time-of-flight mass spectrometry. A time-of-flight spectrum, showing the determination of the peptide mass is shown in Figure 6. Spectral analysis was done by N. Poppe-Schreimer of the Physics Department of the University of Manitoba. Mass spectrometry provided a molecular mass of 1864.7 ± .9 Daltons which matched the calculated mass of the peptide (1863 Daltons) based upon the sequence submitted to Chiron Mimotypes Pty. Ltd.

The sequence of residues 1-14 was obtained from the mass spectral data, however complete sequencing of the peptide was not possible, due to the lack of sufficient mass spectral data for the region comprising residues 15-20. Although the portion consisting of residues 15-20 could not be accurately sequenced, the molecular mass of a fragment corresponding to the mass of the last six residues of the sequence was observed. The difficulties could be due to the presence of proline at position 14. Bonds between Pro and another amino acid are easily fragmented in fast atom bombardment mass spectrometry, resulting in a complicated mass spectrum.

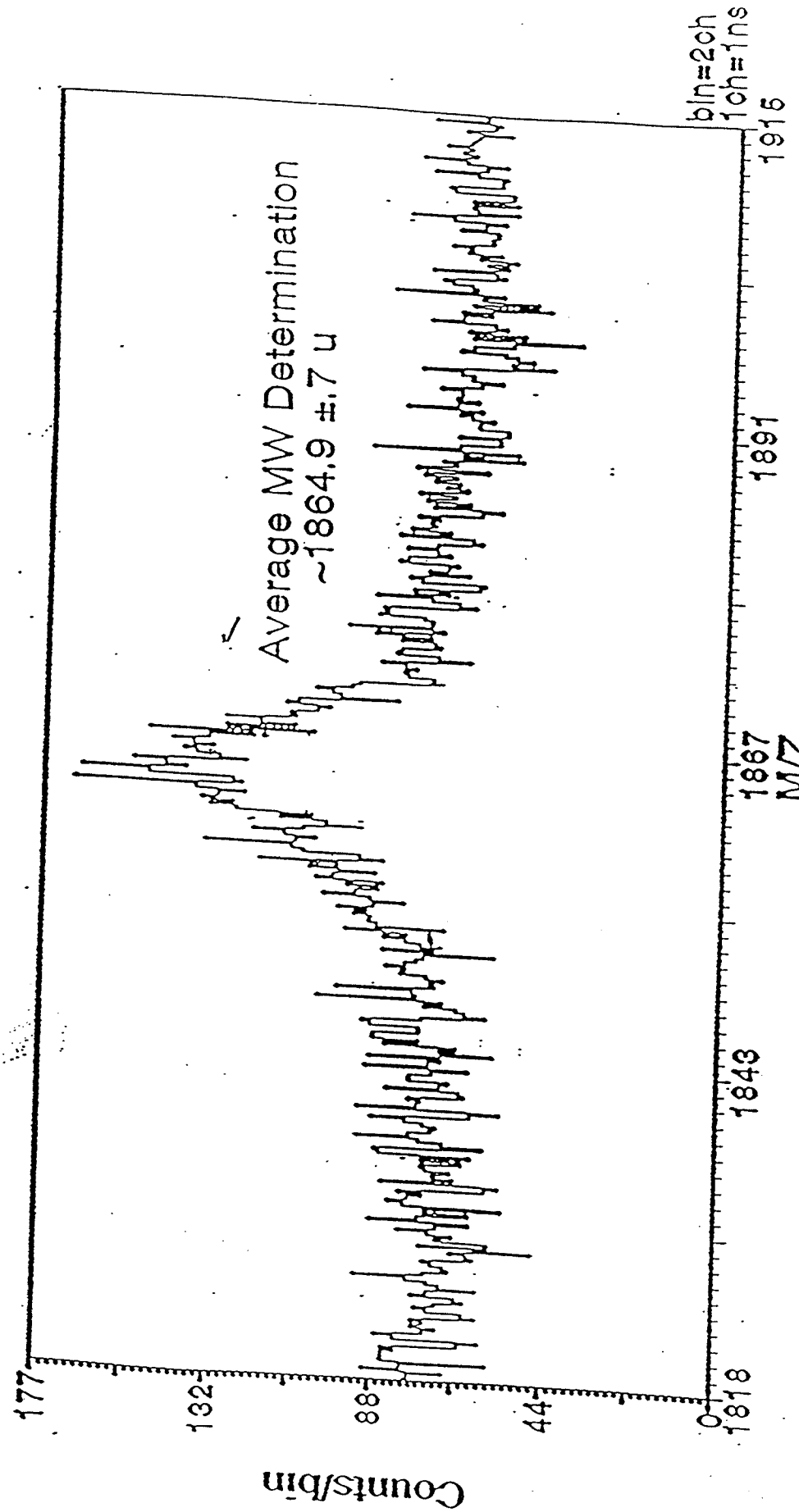

Figure 6: Time-of-flight mass spectrum for molecular weight determination of RBP-1

3.1.2 SOLUBILITY STUDY

Table 1 is a summary of the solubility of RBP-1 in various organic and aqueous solvents. In none of the solutions was the concentration of peptide great enough for NMR spectroscopy. The solvents tested differed greatly in their polarities. Solvents used in the study ranged from very polar, water, to extremely non-polar, carbon tetrachloride. The solubility of RBP-1 was greatest in the solvents which are relatively polar. Solubility was highest in trifluoroethanol and SDS. In methanol and ethanol, the peptide dissolved to a lesser degree. Of the solvents which displayed some facility in solubilizing the peptide, water, which has the greatest polarity of the different solvents tried, was the least effective.

Table 1: Solubility of RBP-1

Solvent	Dielectric Constant	Solubility
H_20 (D_2O)*	78	≤ 0.01 mg/ml
CH_3OH (CH_3OD/CD_3OH)*	32.7	≤ 0.01 mg/ml
CH_3CH_2OH	24.5	≤ 0.01 mg/ml
CH_3Cl	9	insoluble
$CHCl_3$	4.8	insoluble
CCl_4	2.2	insoluble
THF	7.6	insoluble
DMSO	47	insoluble
CH_3CN	38	insoluble
TFE	60	≥ 0.05 mg/ml
SDS	-----	≥ 0.05 mg/ml

* Attempts to prepare NMR solutions were made in these solvents, but no UV data were collected.

3.1.3 Concentration Determination by UV-VIS Absorption Spectrophotometry

The absorption spectra of all the peptide solutions were similar in shape and intensity. A single large peptide absorbance was observed between 195 - 208 nm in each solvent (Figure 7). The absorbance value of this large peak was used to calculate the solution concentration. Table 2 contains the peptide concentrations used for CD analysis in each solvent.

An experiment to investigate the temperature variation of the UV absorption spectra showed that the magnitude of the absorbance and the peak maximum position changed only slightly with temperature. Table 3 lists the results of this experiment. The UV spectra of the peptide solutions are shown in Figure 8.

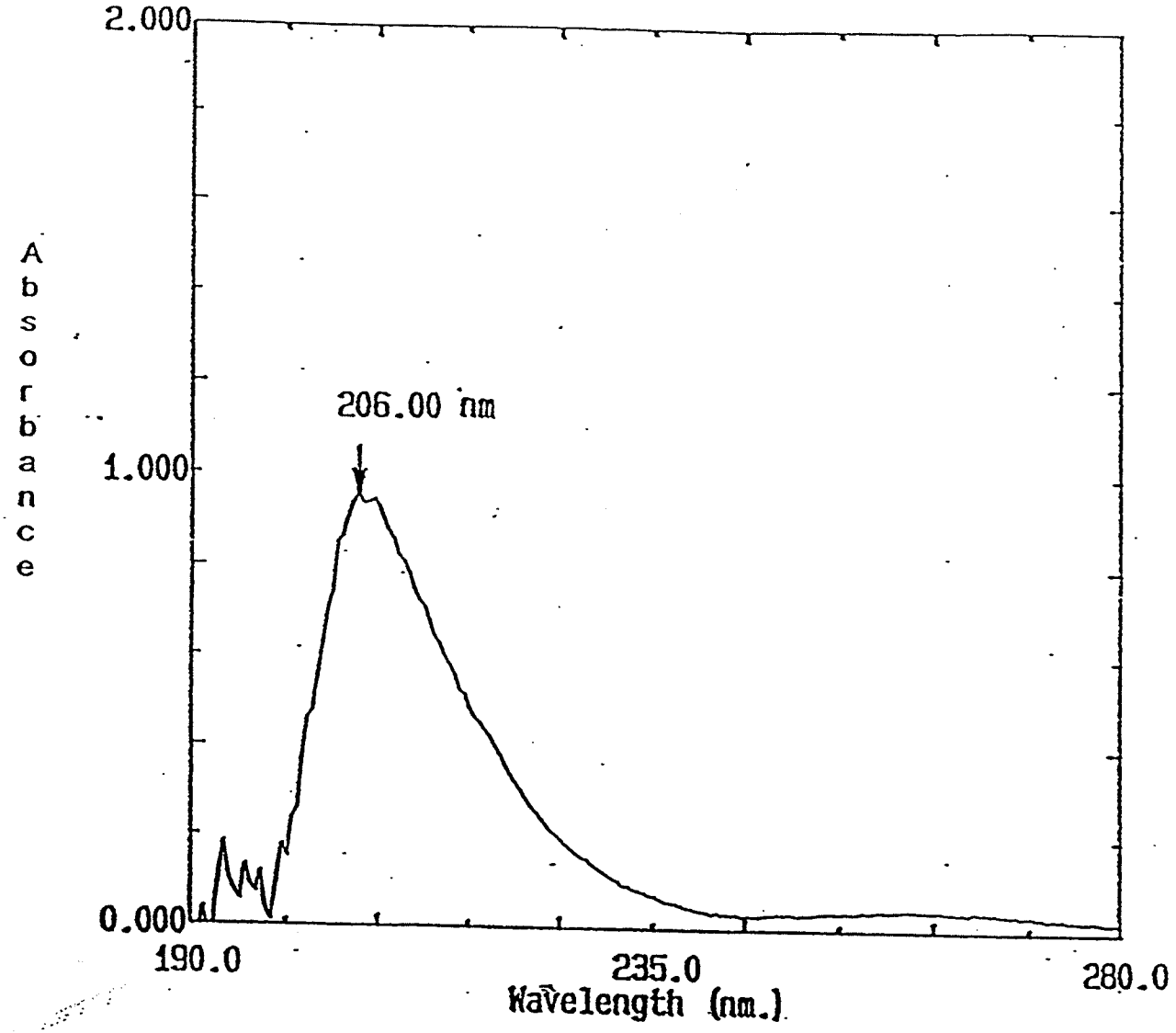

Figure 7: Absorption spectrum of RBP-1 in methanol at room temperature. The absorption of a solution of RBP-1 in methanol was measured as described under **Methods**. The concentration was calculated from the absorbance at 206 nm.

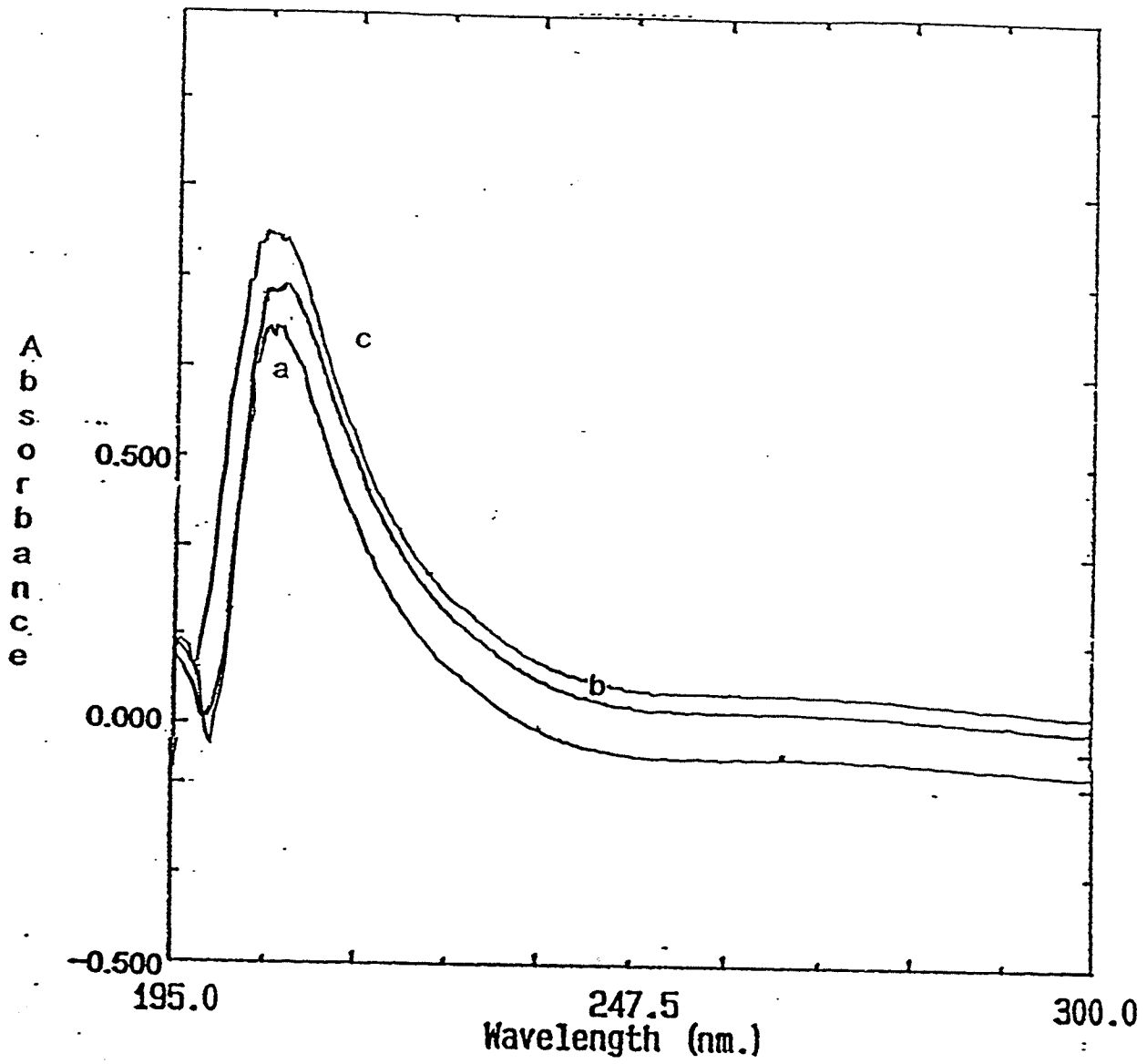

Figure 8: UV spectra of RBP-1 from the temperature study.

An investigation into possible effects of temperature on the spectral properties of RBP-1 was carried out by acquiring the spectrum at 3 temperatures of the peptide dissolved in methanol. Spectra at (a) 10°, (b) 23°, (c) 48°

Table 2: Concentrations Used for CD

Solution	Concentration (mg/ml)
Ethanol	0.0329
Methanol	0.0365
Trifluoroethanol	0.0342
Water	0.0328
SDS	0.0138

[calculated using $\varepsilon = 50950\ M^{-1} \cdot cm^{-1}$]

Table 3: Effect of Temperature on UV Absorbance of RBP-1

Temperature °C	Absorbance at λ_{Max}	λ_{Max} of major peak (nm)
10°	0.798	206.5
22°	0.801	207
41°	0.804	208

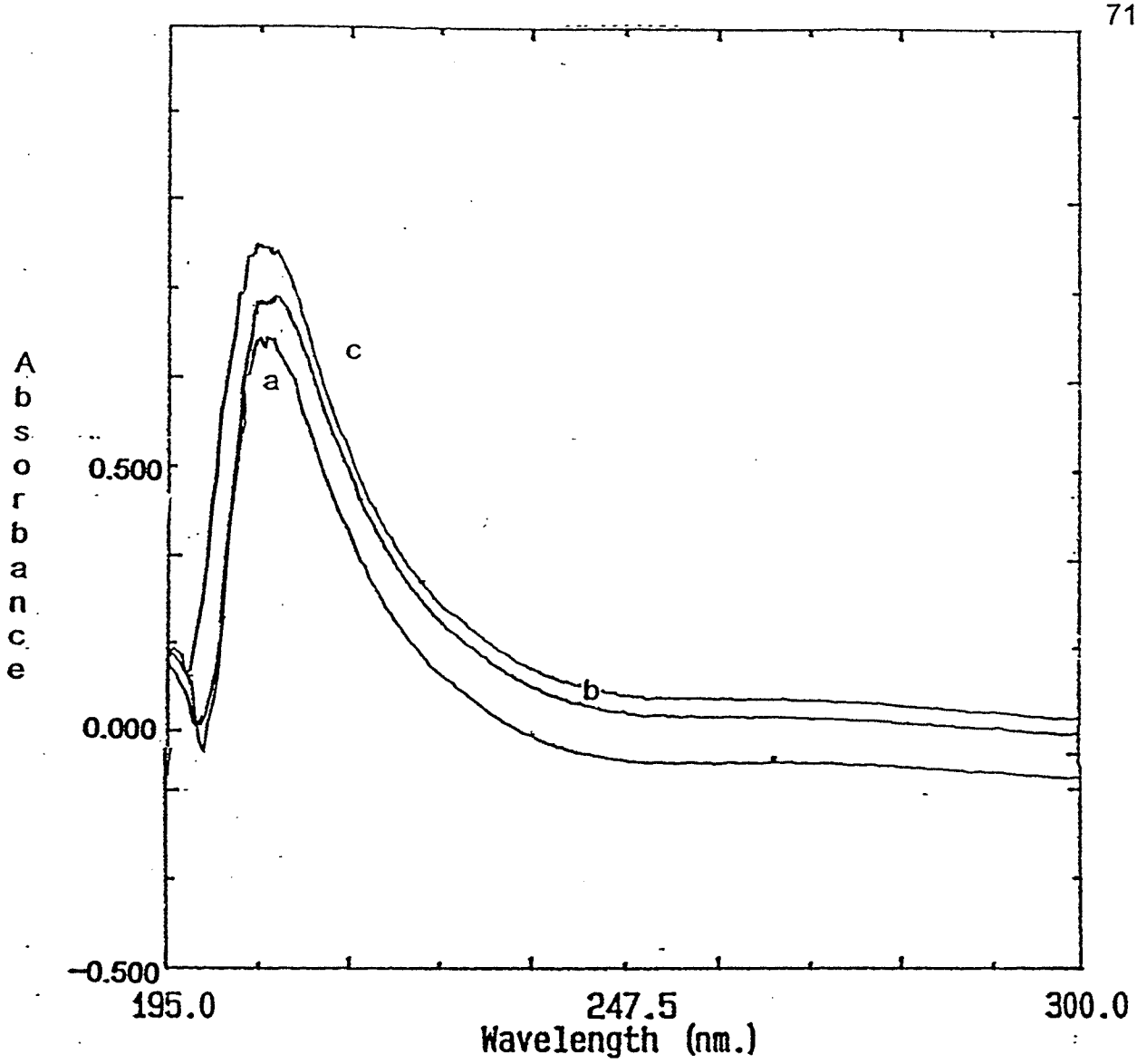

Figure 8: UV spectra of RBP-1 from the temperature study.

An investigation into possible effects of temperature on the spectral properties of RBP-1 was carried out by acquiring the spectrum at 3 temperatures of the peptide dissolved in methanol. Spectra at (a) 10°, (b) 23°, (c) 48°

3.1.4 CD USED TO INVESTIGATE PEPTIDE CONFORMATION

Figure 9a shows spectra obtained from a CD temperature titration in methanol. The main features are minima at 208 and 222 nm. These are strongly suggestive of a helical conformation (see **Introduction**). Figures 9a-d show that the peptide is helical in ethanol, TFE, and SDS. Temperature titrations of the peptide in which secondary structural content was monitored by CD were performed, as described in **Methods**. With increasing temperature of each solution, a decrease in ellipticity at the minima found at 222 and 208 nm is observed. The decrease may be considered to be an indication of a loss of helical structure.

Figure 9: CD temperature titrations of RBP-1 in (a) methanol, (b) ethanol, (c) TFE, and (d) SDS in water. The data sets in (a) and (d) are truncated at lower wavelengths due to severe noise. The symbols correspond to the temperatures used for the titrations.

a

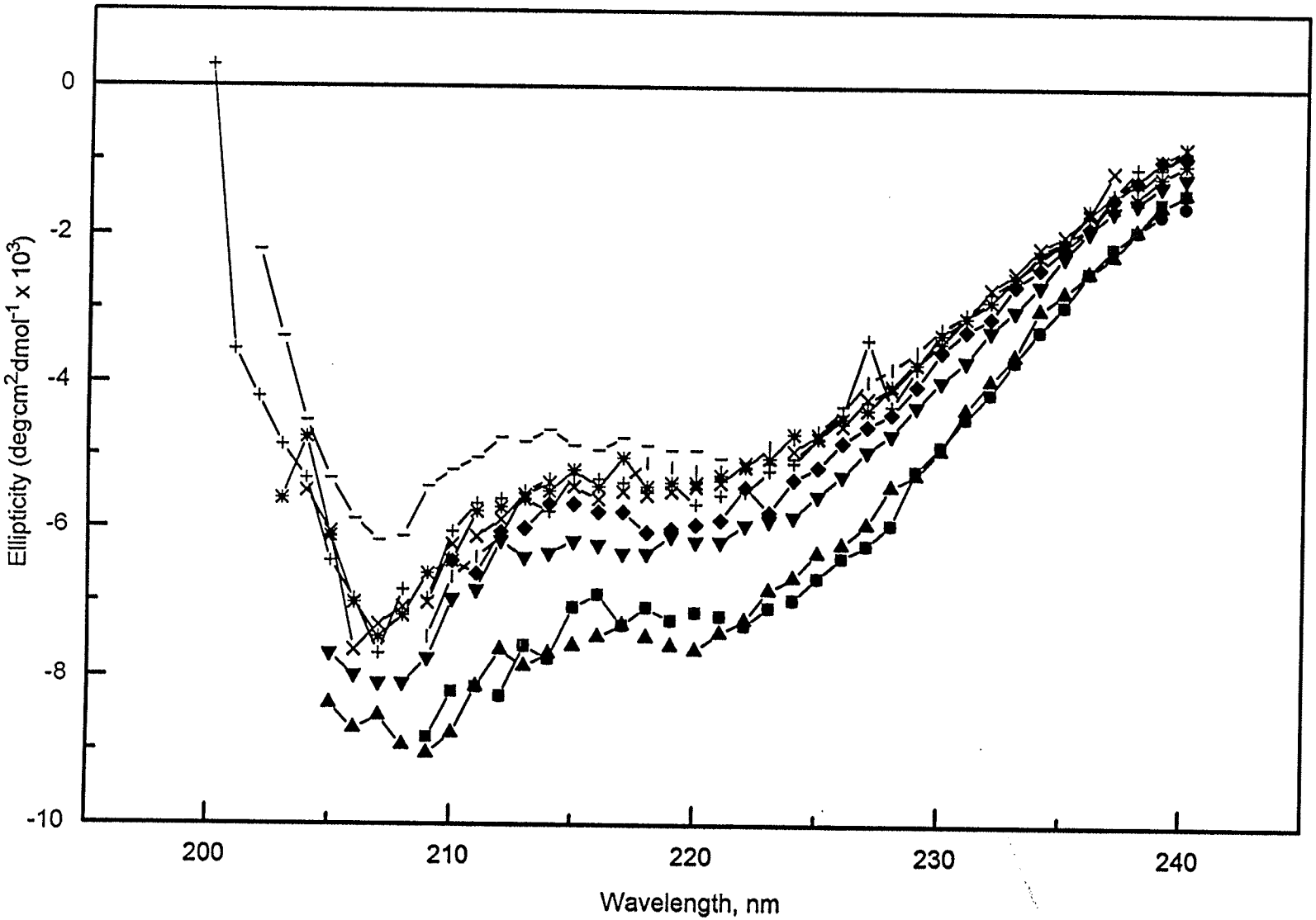
0
-2
-4
-6
-8
-10
Ellipticity (deg·cm²dmol⁻¹ x 10³)
200
210
220
230
240
Wavelength, nm

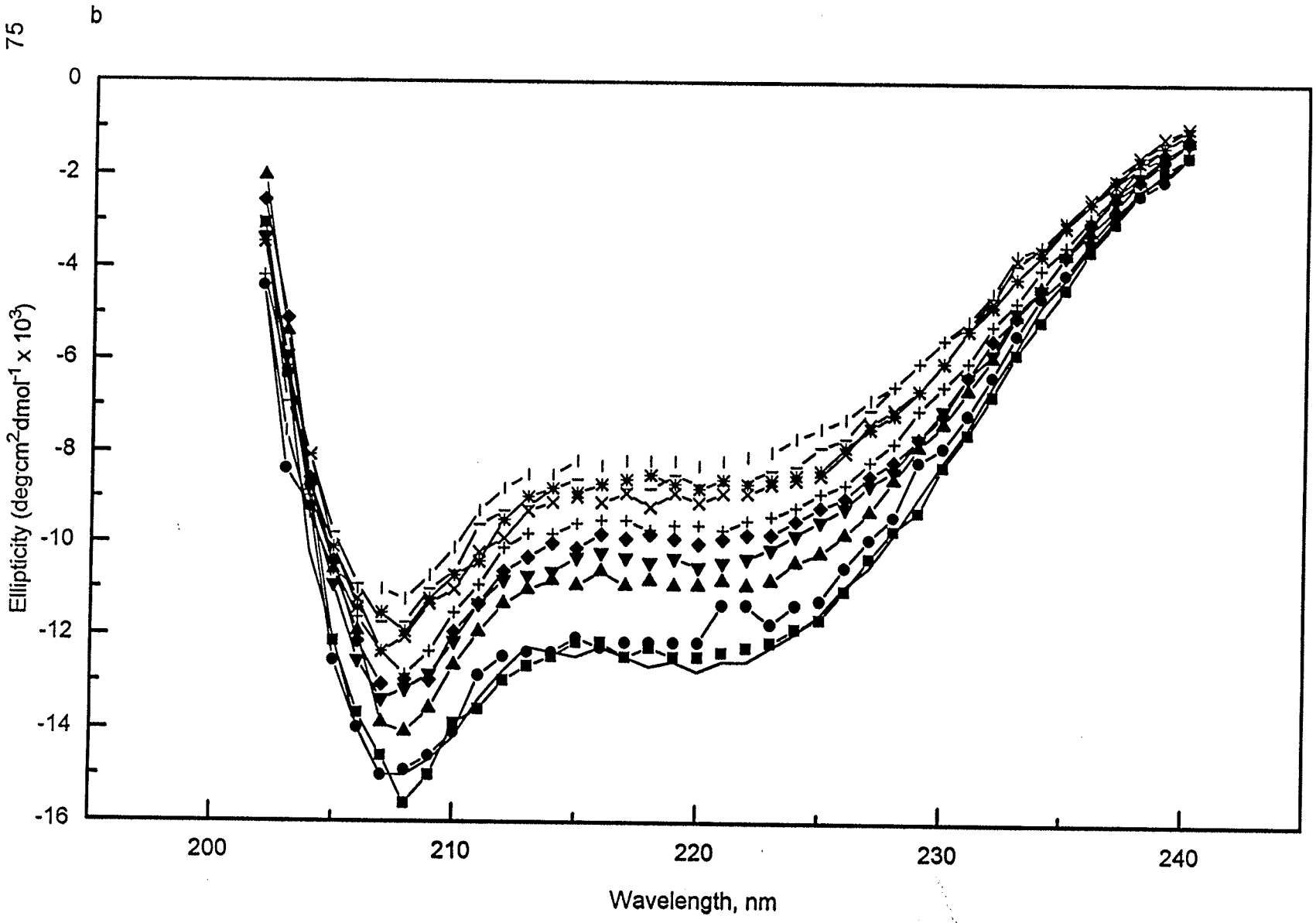
b
75
0
-2
-4
-6
-8
-10
-12
-14
-16
Ellipticity (deg·cm^{2}dmol^{-1} x 10^3)
200
210
220
230
240
Wavelength, nm

c

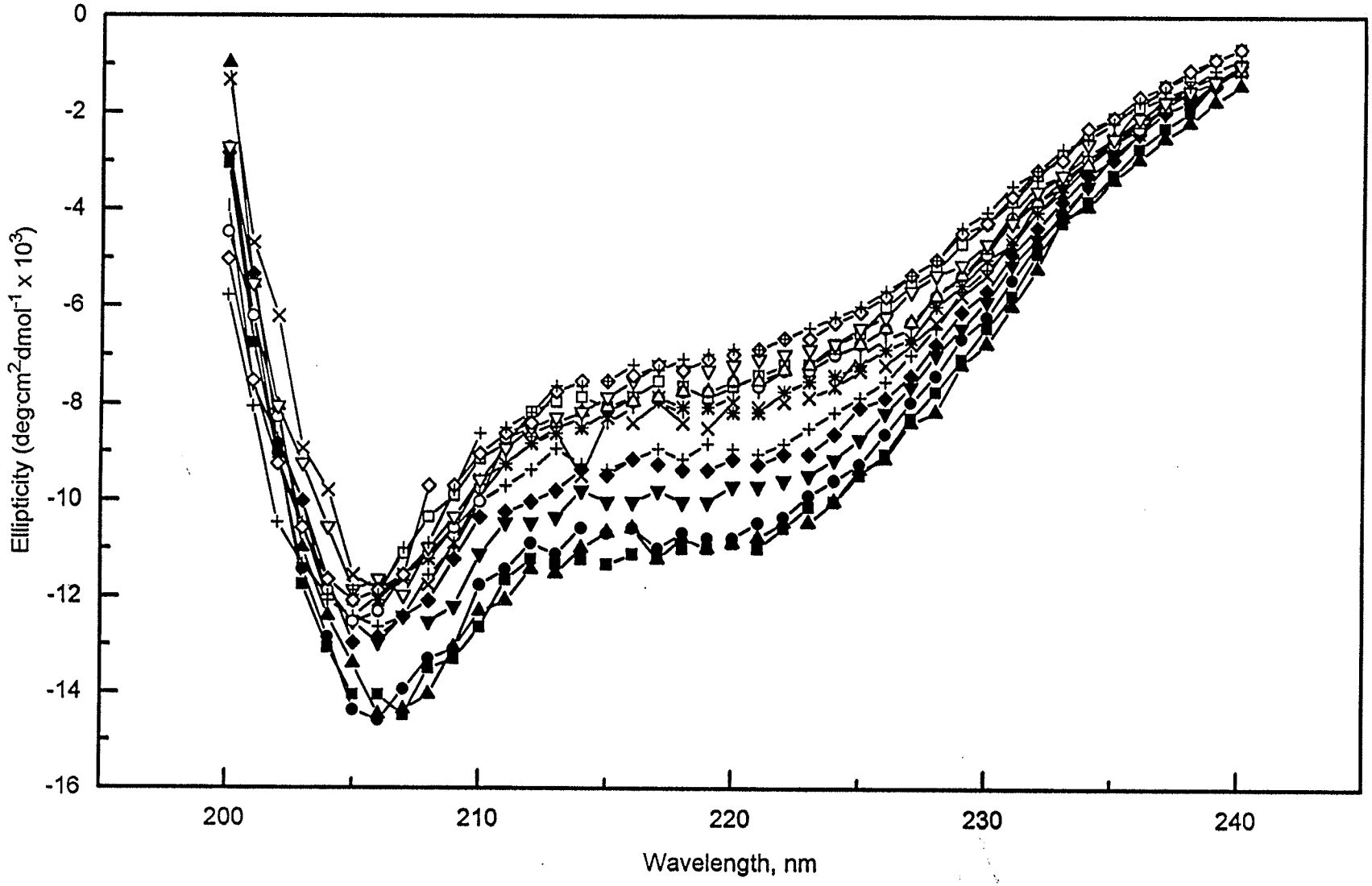
0
-2
-4
-6
-8
-10
-12
-14
-16
Ellipticity (degcm^{2}dmol^{-1} x 10^3)
200
210
220
230
240
Wavelength, nm

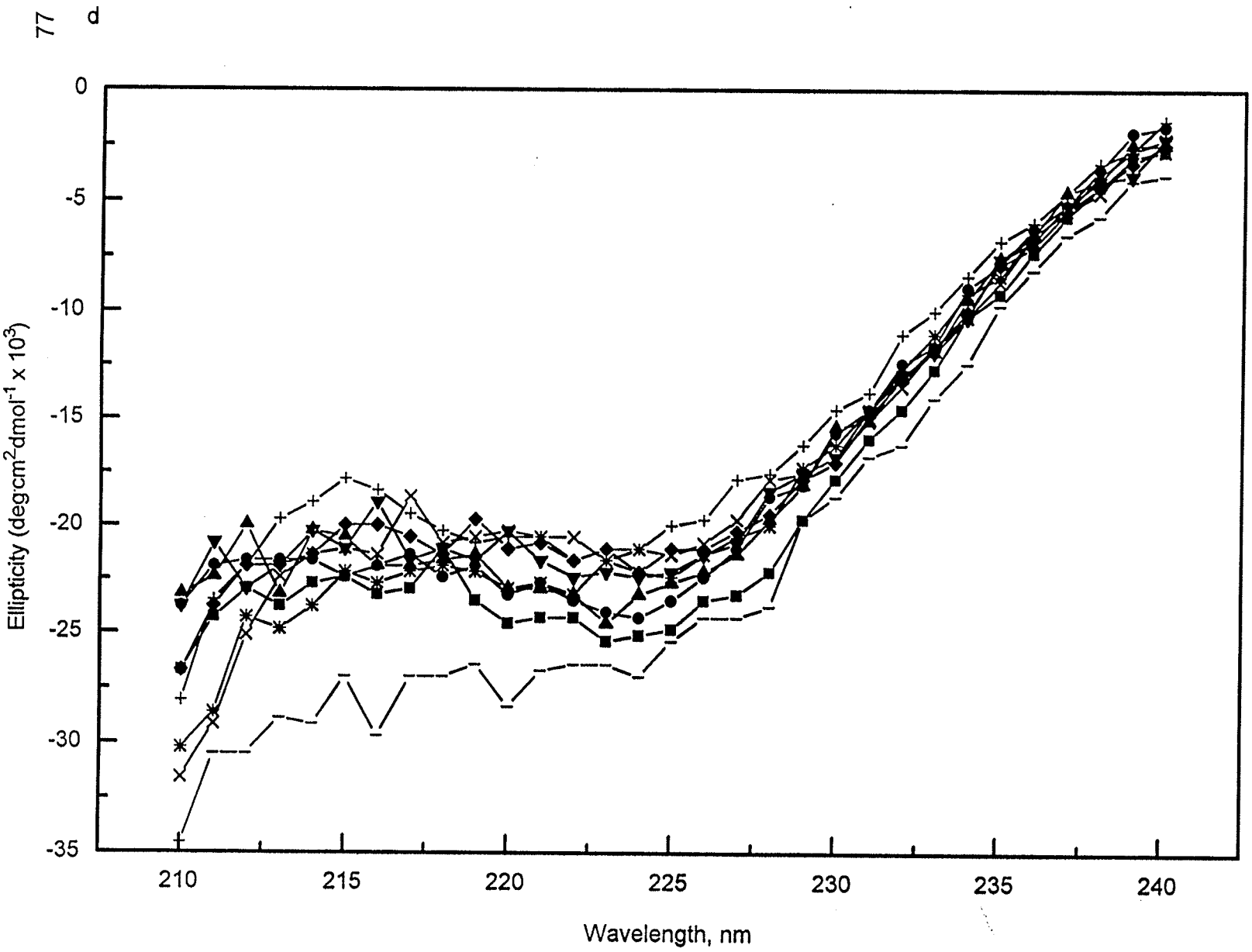
77 d
0
-5
-10
-15
-20
-25
-30
-35
Ellipticity (degcm2dmol-1 x 10^3)
210
215
220
225
230
235
240
Wavelength, nm

As can be seen in the plots in Figure 9, the intensities of the spectra in the different solvents decreases with changes from low to high temperatures, but the general shapes of the curves are retained. This suggests that a measurable amount of ordered structure (helical character) remains even at the highest temperatures reached. It is conceivable that at higher temperatures than those tested, complete unfolding of the peptide might occur, at which point the spectra would attain the shape corresponding to the random coil (Tiffany and Krimm, 1968).

For the titrations of RBP-1 in organic solvents and SDS, mean residue ellipticity at 222 nm was plotted against temperature to obtain curves for the temperature dependence. Figure 10 shows these curves for the peptide in methanol, ethanol, TFE, and SDS. The shape of the titration curve in methanol is similar to that observed for peptides which undergo cooperative two-state, thermal helix/coil transition. This sigmoidal shape was observed for a second titration in methanol using a freshly prepared solution. However, the steepness of the transition makes the data suspect. The transitions in ethanol, TFE, and SDS appear much less cooperative. Table 4 is a summary of some properties of the temperature titrations of RBP-1 in the different solvent systems.

The maximum ellipticity observed in each solvent varies significantly from solvent to solvent, and thus, the maximum amount of ordered structure found in the peptide also varies. The maximum ellipticity reached in methanol by RBP-1 is ~-7300 deg•cm^2•dmol^{-1}, whereas the maxima in ethanol and TFE are

considerably higher (-12000 and -23000 deg∘cm^2∘dmol^{-1}, respectively). Interestingly, in SDS, the maximum ellipticity attained is -29000 deg•cm^2•dmol^{-1}. Thus, the structure induced in each peptide in solution is strongly influenced by the solvent.

Figure 10: The effect of temperature on the mean residue ellipticity of RBP-1 at 222 nm in (a) methanol, (b) ethanol, (c) TFE, and (d) SDS.

a

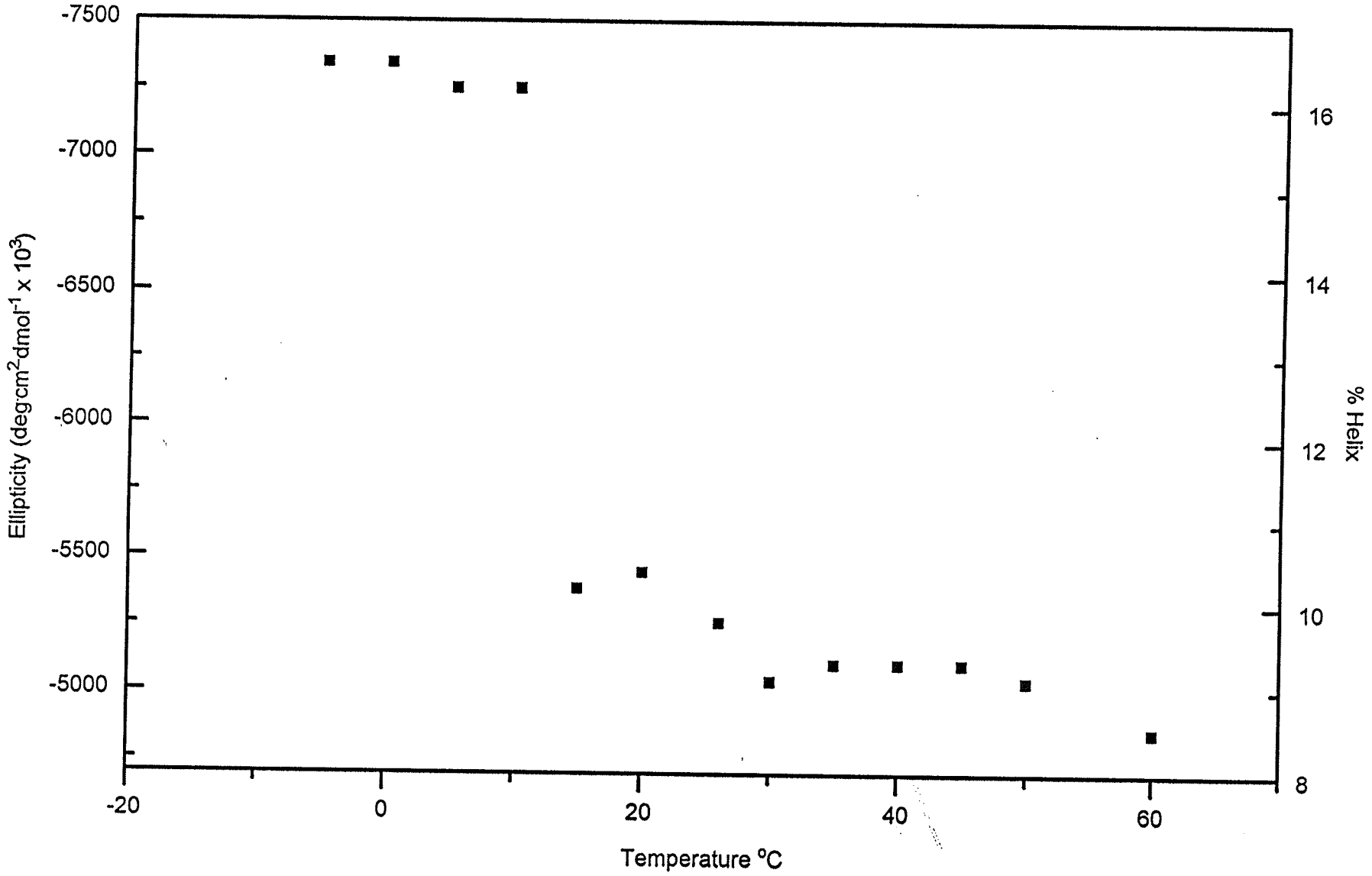
-7500
-7000
-6500
-6000
-5500
-5000
Ellipticity (deg·cm²dmol⁻¹ x 10³)
16
14
12
10
8
% Helix
-20
0
20
40
60
Temperature °C

b

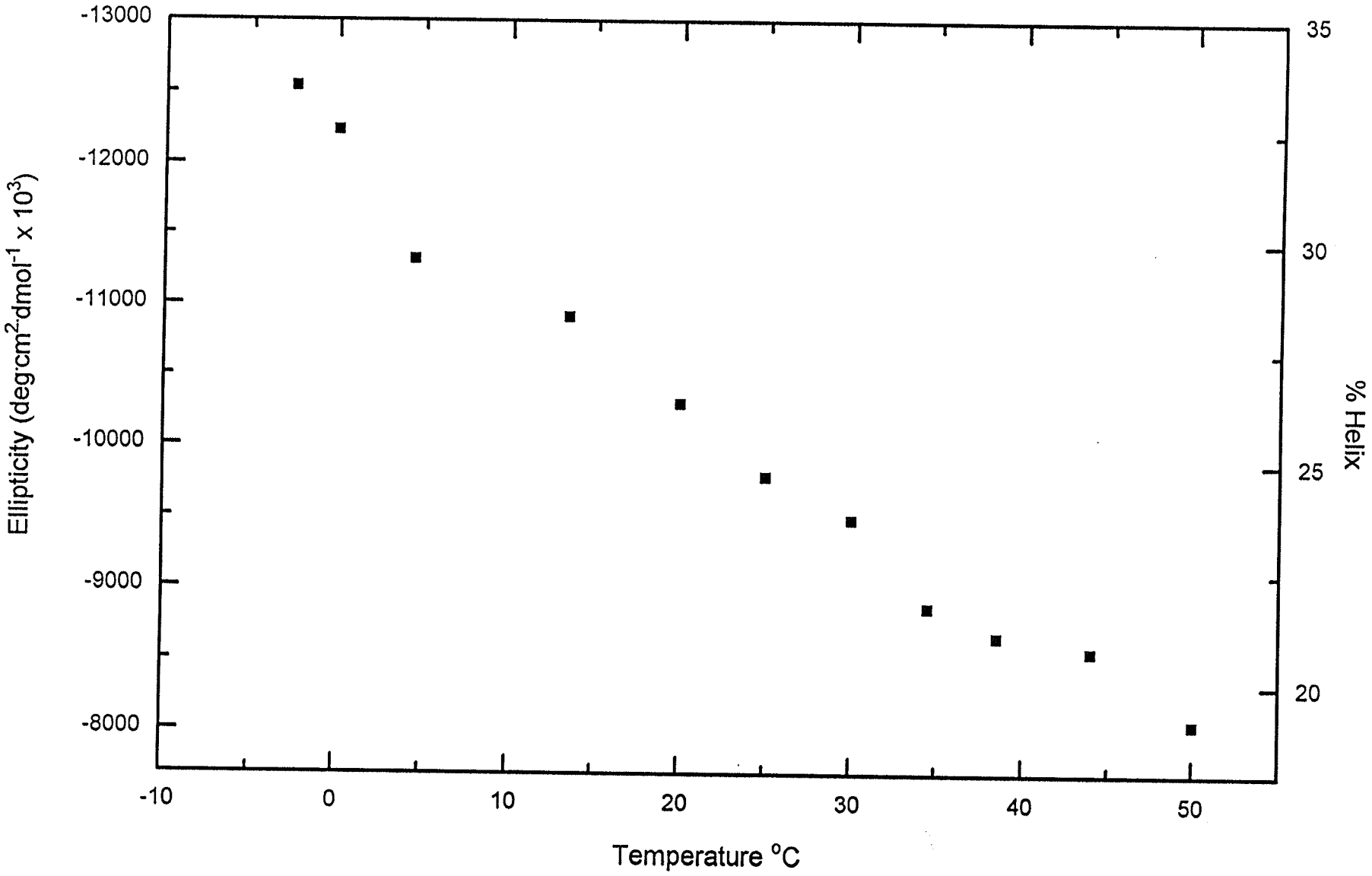
-13000
-12000
-11000
-10000
-9000
-8000
Ellipticity (degcm^{2}dmol^{-1} x 10^3)
35
30
25
20
% Helix
-10
0
10
20
30
40
50
Temperature °C

c

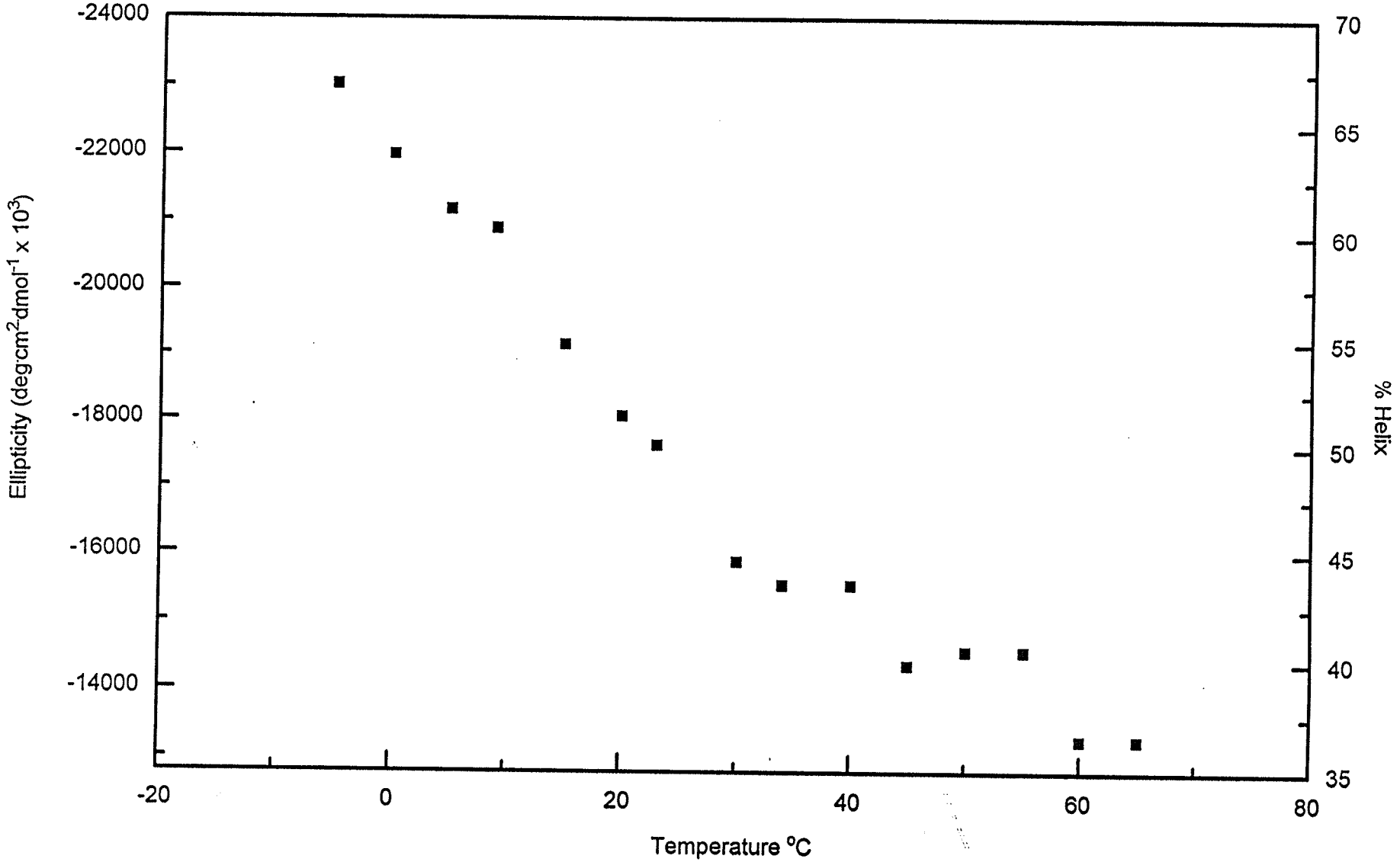
-24000
-22000
-20000
-18000
-16000
-14000
Ellipticity (degcm^{2}dmol^{-1} x 10^3)
70
65
60
55
50
45
40
35
% Helix
-20
0
20
40
60
80
Temperature °C

d

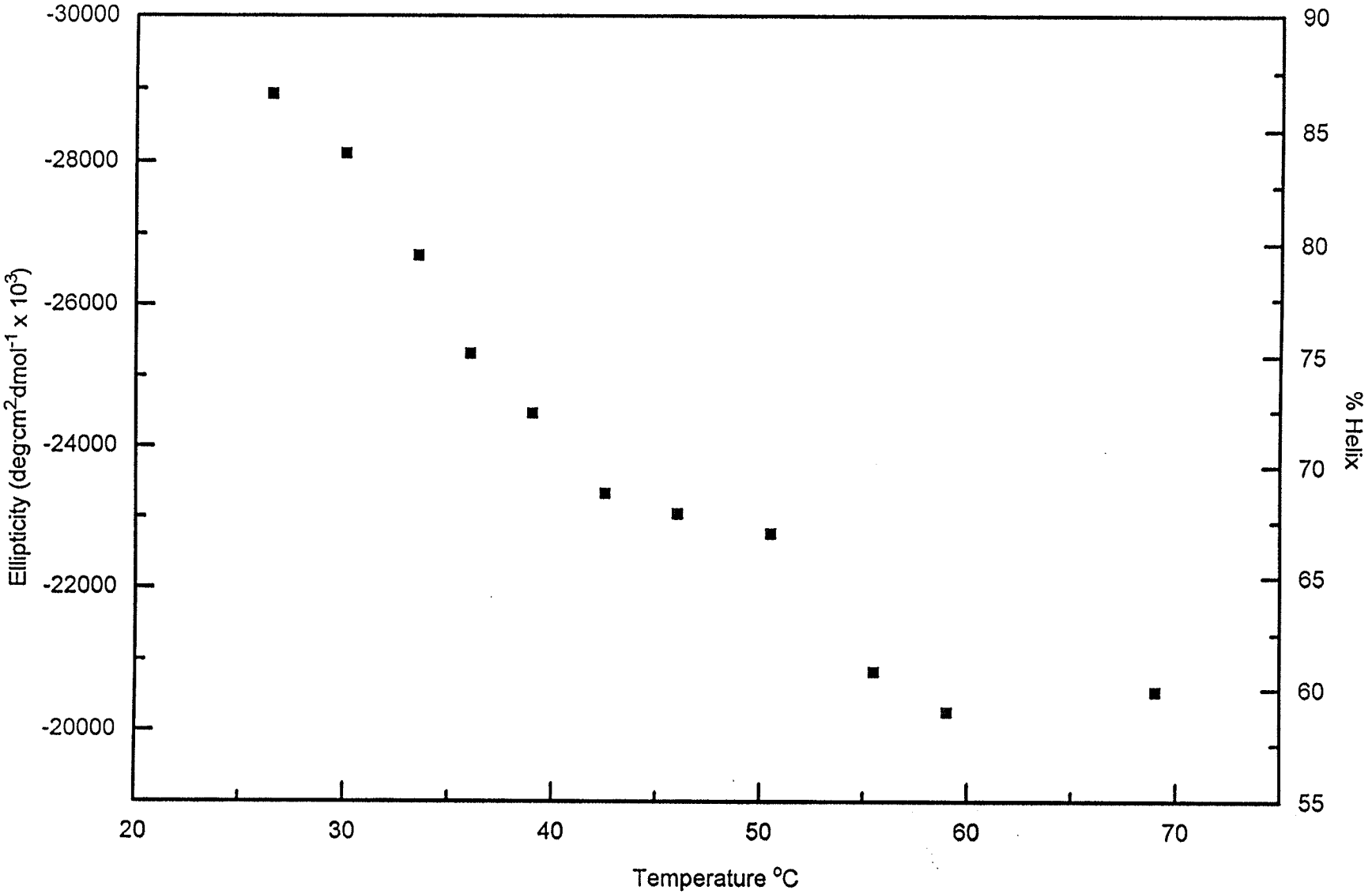
-30000
-28000
-26000
-24000
-22000
-20000
Ellipticity (degcm^{2}dmol^{-1} x 10^3)
90
85
80
75
70
65
60
55
% Helix
20
30
40
50
60
70
Temperature °C

The above results are in contrast with the results of CD experiments on RBP-1 dissolved in water. At low temperatures, the CD spectrum of RBP-1 in water displays a very minor amount of ordered structure which is apparent from the shape of the curve and the negative ellipticity at 222 nm. At higher temperatures, shapes of the spectra (Figure 11) are very similar to those of completely disordered polypeptides found in the literature (see **Introduction**). Spectra exhibiting similar shapes were observed by Merutka et al. (1990) in their central residue replacement experiments on a 17-residue peptide when Pro was placed at position 9. At low temperature, the spectrum did not display any significant helical character. This suggested that the central Pro residue interrupts helix formation, and the flanking regions are too short to form the α-helices. They observed peptide CD spectra which resembled the spectrum of a random coil molecule. An isodichroic point around 207 nm (not ~202 nm, as for an α-helix) was seen in the spectra taken over a range of temperatures. These properties are similar to those of the spectra for a left-handed poly(L-proline) II helix (Tiffany and Krimm, 1968).

Table 4: Temperature Titration Properties of RBP-1

Solvent	Isodichroic Point	Maximum Ellipticity $deg \cdot cm^2 \cdot dmol^{-1}$	% helix[1]	Sigmoidal transition at 222 nm
Methanol	no	-7297	16.5	yes
Ethanol	yes	-12542	33.4	no
TFE	possibly	-23019	68.4	no
SDS	no	-28589	86.0	no
Water	no	-2500	0.52	no

[1]calculated from Equation 4

Figure 11: Temperature titration of RBP-1 in water.The CD curves have a characteristic disordered form. The curves show a small positive ellipticity in the region around 218 nm and a large negative ellipticity at about 198 nm.

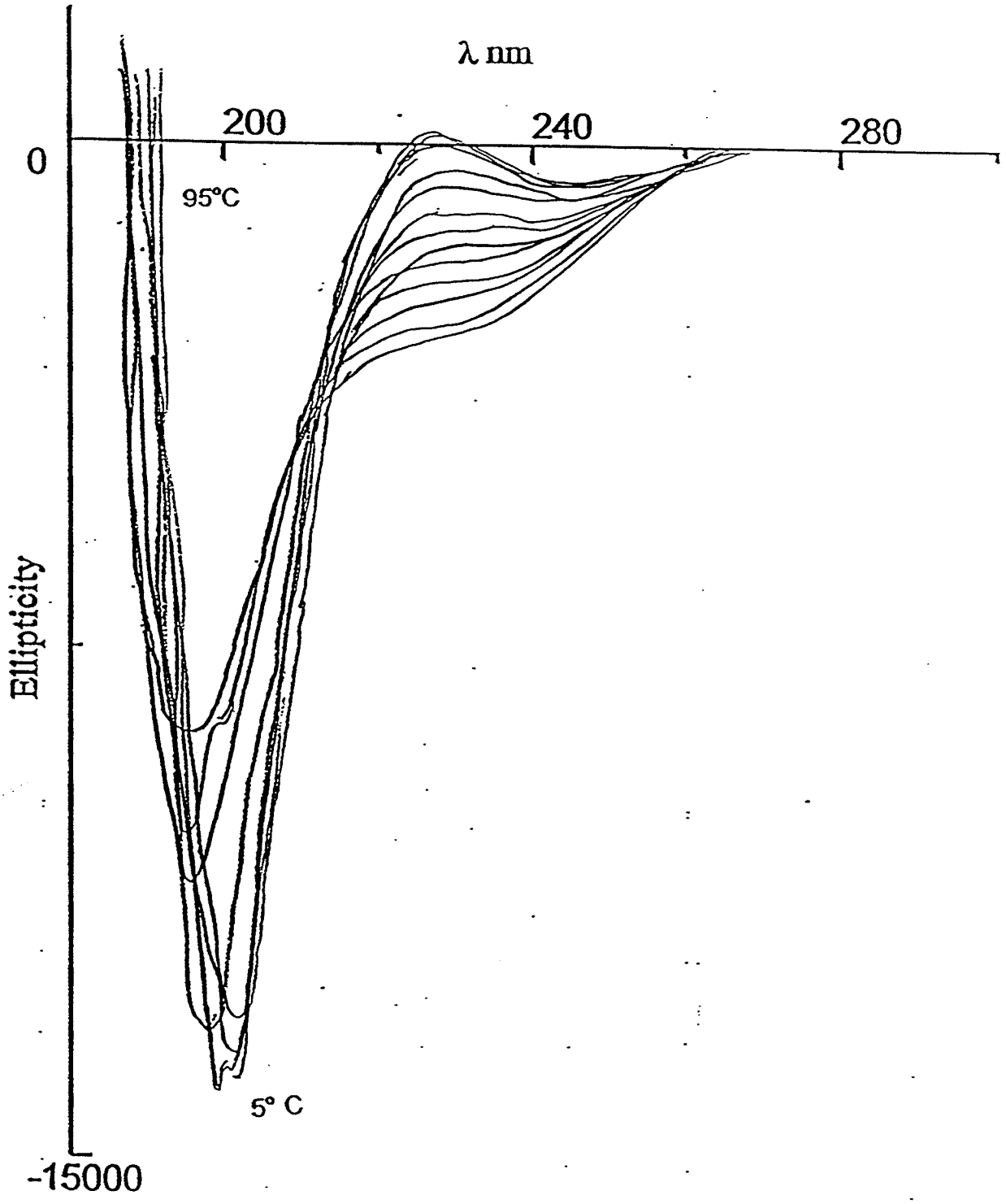
λ nm
200
240
280
0
95°C
Ellipticity
5° C
-15000

3.2 Secondary Structure Determination

3.2.1 HELIX CONTENT CALCULATED BY EQUATION (4)

The CD spectra were analyzed to obtain the degree to which the individual pure secondary structural types contribute to the experimental spectra in each solvent system. This analysis was accomplished using three different methods, each requiring different amounts of information from the experimental spectra. The values for the helix content calculated from equations 4 and 5, and by the CCA program are found in **Appendices A** and **B**.

The helix content was calculated from Equation 4 using the the mean residue ellipticity of each spectrum of the temperature titrations determined at the diagnostic wavelength of 222 nm by Equation 2. Helix content graphed as a function of temperature for each peptide system may be seen in Figures 10 a-d.

3.2.2 CONVEX CONSTRAINT ANALYSIS

The second method used to analyze the CD data was Convex Constraint Analysis (Fasman et al., 1991). This is an algorithm designed to deduce the chiral contributions to an experimental spectrum of a set of common secondary structures which are obtained directly from the experimental CD curves of reference proteins (26 proteins with structures solved by X-ray diffraction). The CD spectrum is measured as a function of the wavelength, $f(\lambda)$, with other factors such as concentration being held constant. Thus, the spectrum can be

secondary structures present in the total spectrum.

The data treatment necessary to make use of the program is outlined in **Methods**. Once the algorithm has been completed, an output data file is produced with the results of each of the *n* iterations performed (usually $n = 30$) in the form of matrices. Choosing a solution from these pure CD curves is determined by picking the iteration where the standard deviation, σ, and the volume of the simplexes are at a minimum. When a solution has been found meeting the above criteria, the values in the matrix for the pure structural components may be plotted (either without further treatment, or after a multiplication of the individual matrix columns with the corresponding conformational weight) to see the shape of the respective curves. These curves are assigned to pure secondary structural conformations by comparison with the CD curves for secondary structures in the literature (Perczel et al., 1991, Perczel and Fasman, 1992). A calculated spectrum, wherein the individual contributions combine additively to produce a theoretical spectrum for the molecule under study is obtained by multiplying the pure curves by their confomational weights and adding these values. This spectrum can be compared to the experimental CD spectrum which was originally used for deconvolution by the CCA algorithm. On the basis of the "fit" between the calculated and experimental spectra (by eye), an assessment of the success of the deconvolution with the number of pure components chosen may be made. Some of these analyses were unreasonable as some yielded high values for

some components such as the aromatic contribution whereas the peptide contains only one aromatic residue, phenylalaninol. In addition, in the deconvolutions of the temperature titrations, the helix or unordered weights do not steadily decrease or increase, respectively, with increasing temperature. It is also interesting to note that, in the case of RBP-1 in SDS, when 5, 4, or 3 pure components were used for the deconvolution parameters, from one to three of the resulting conformational weights had zero for the magnitude. This indicates that there is no contribution to the spectrum of RBP-1 from some components in the analysis. The conformational weight assigned to the helix contribution in numerous cases for RBP-1 in SDS was 100%.

A two-component analysis of each data set gave results that did not exhibit any of the peculiarities of the 5, 4, or 3 component fits. The 2 components were always helical and random coil (or indeterminant). Given the small size of the peptide, the two component fits seemed reasonable and only these are discussed in what follows.

The conformational weights of the pure components as determined by CCA for RBP-1 in each solvent system are tabulated, at least in part in **Appendix A**. Sample graphs of pure component spectra, experimental spectra and spectra calculated from CCA using pure component spectra and their corresponding weights are shown in Figures12 and 13.

Figure 12: Plots of the output generated by CCA for RBP-1 in (A) Methanol, (B) Ethanol, (C) TFE, and (D) SDS at the lowest temperature at which spectra were obtained for each solvent (-5, -2.5, -5 and 21° C,respectively). The resulting pure component curves are plotted for (a) 2 and (b) 3 components. The different unique secondary structural components are designated by the following symbols: ● α-helix, ■ unordered, ▲ ↑↓β, and, ♦ residual or undefined.

A RBP-1 in methanol

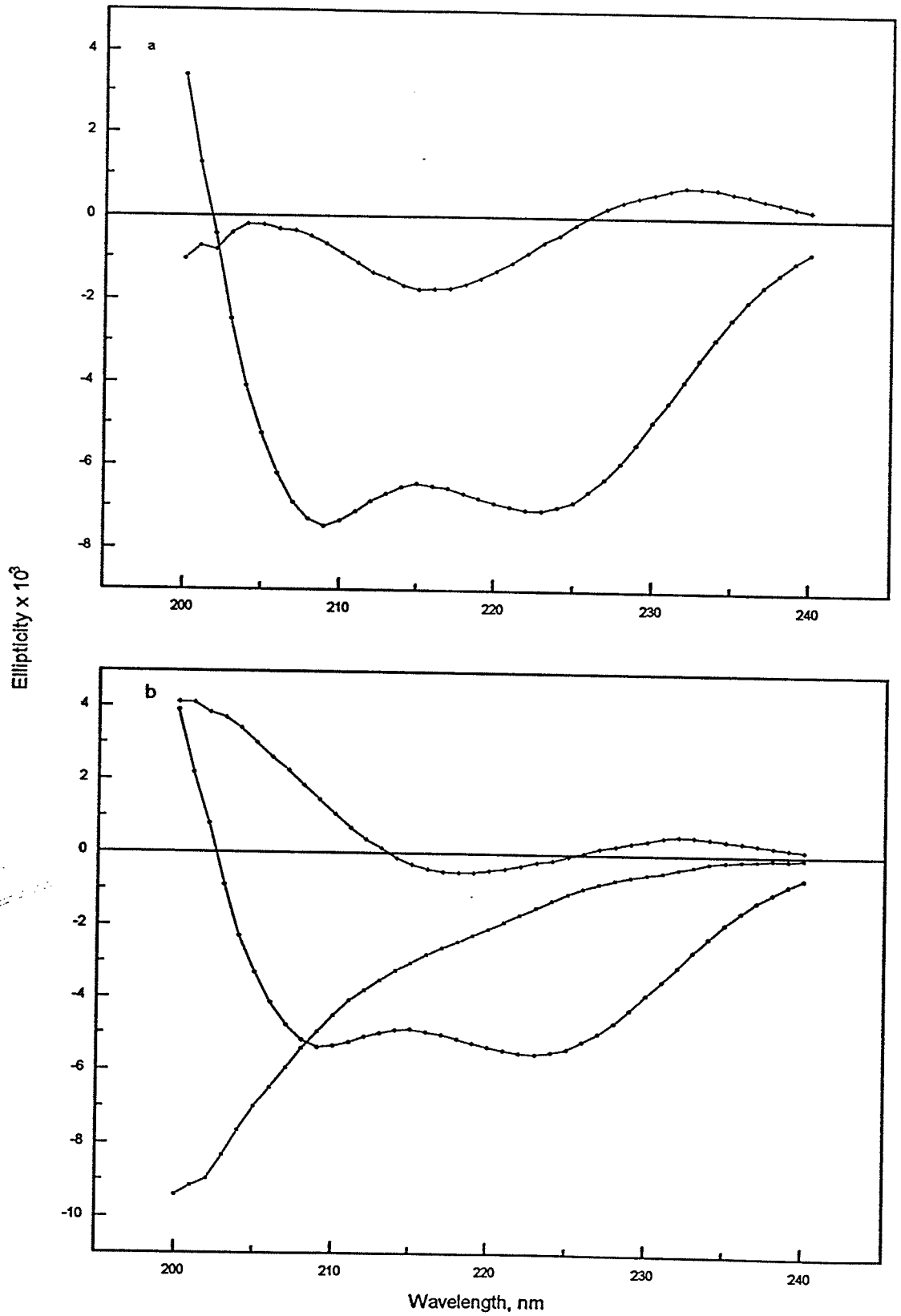

B RBP-1 in ethanol

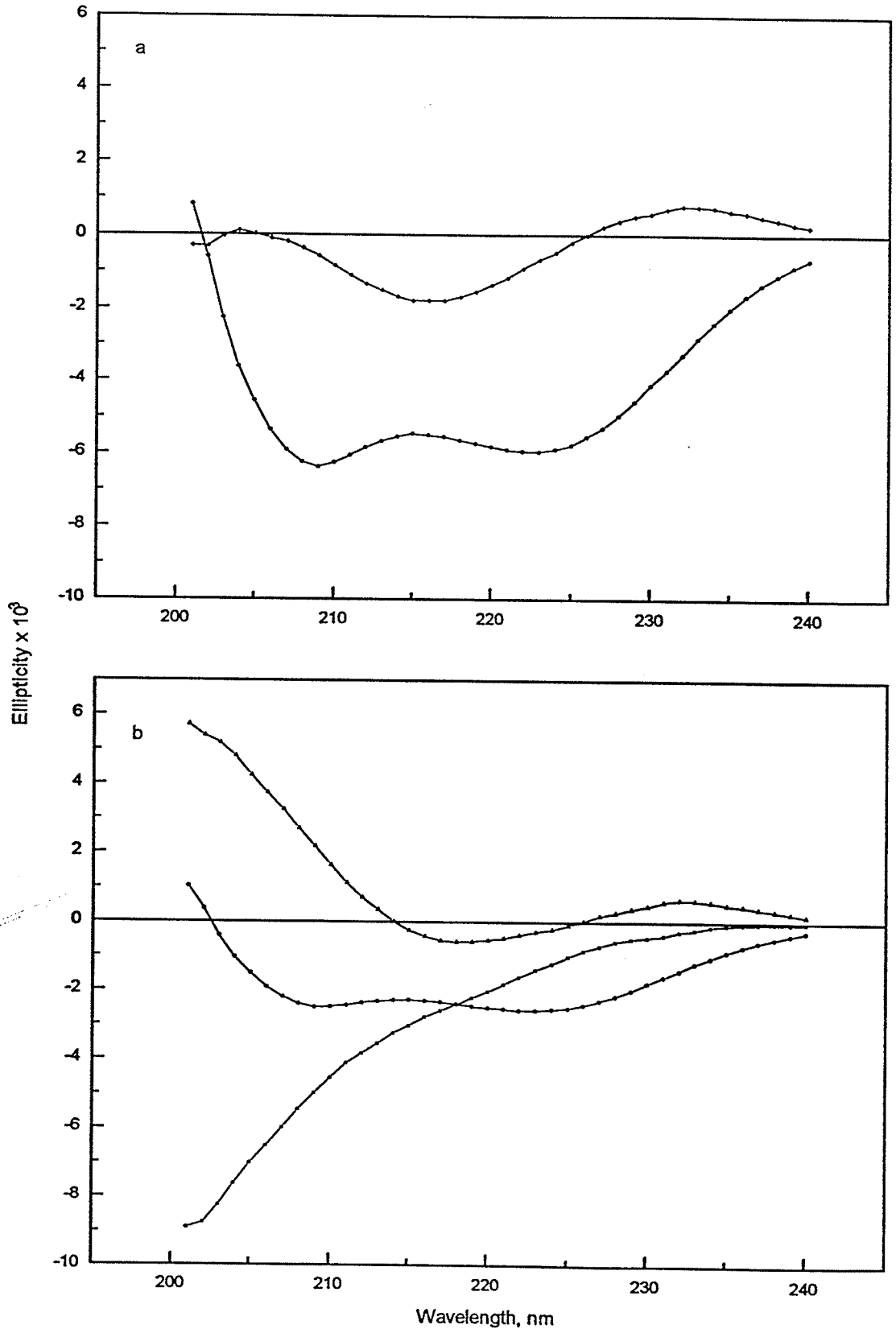

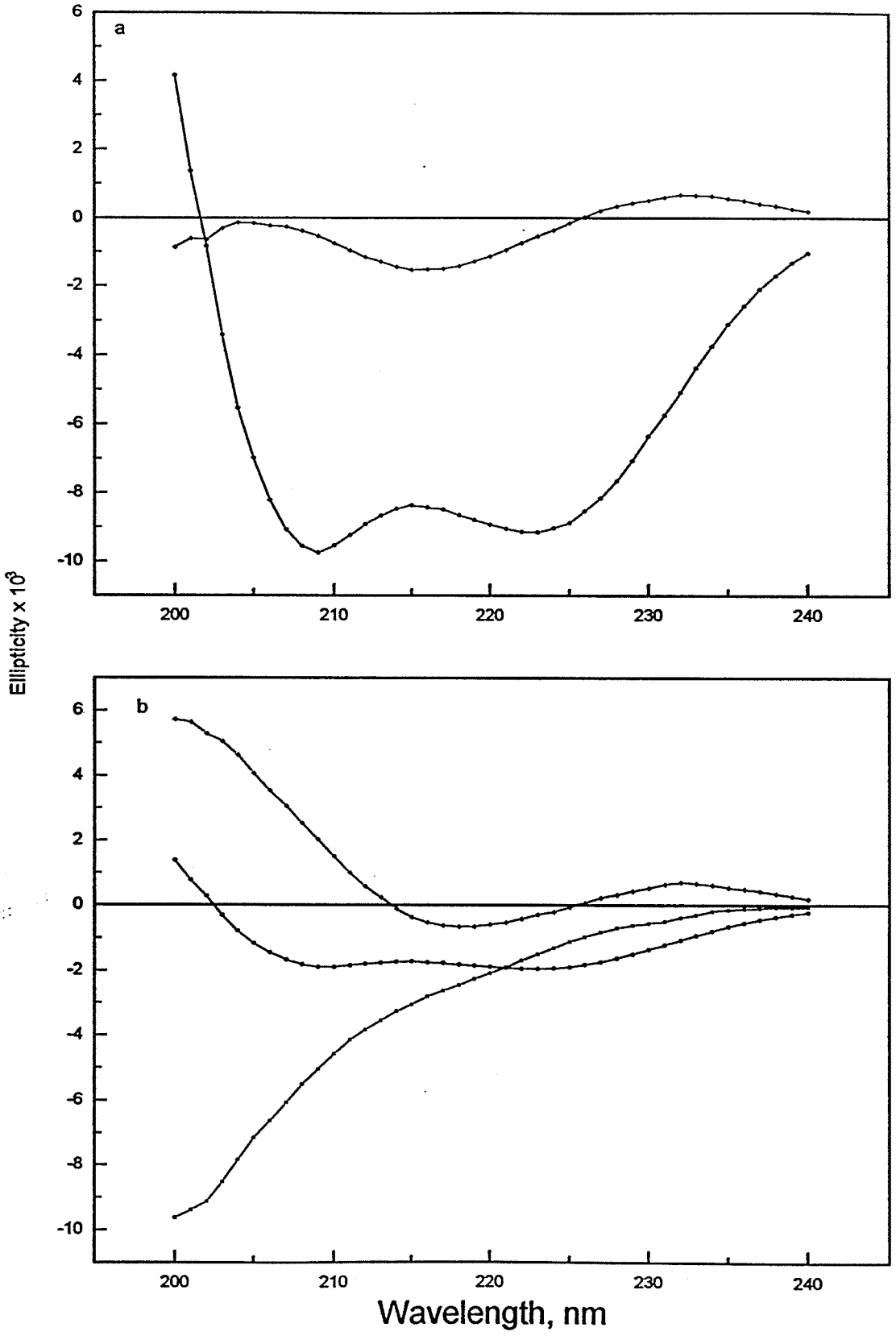
a
b
6
4
2
0
-2
-4
-6
-8
-10
200
210
220
230
240
Ellipticity x 10³
Wavelength, nm

D RBP-1 in SDS

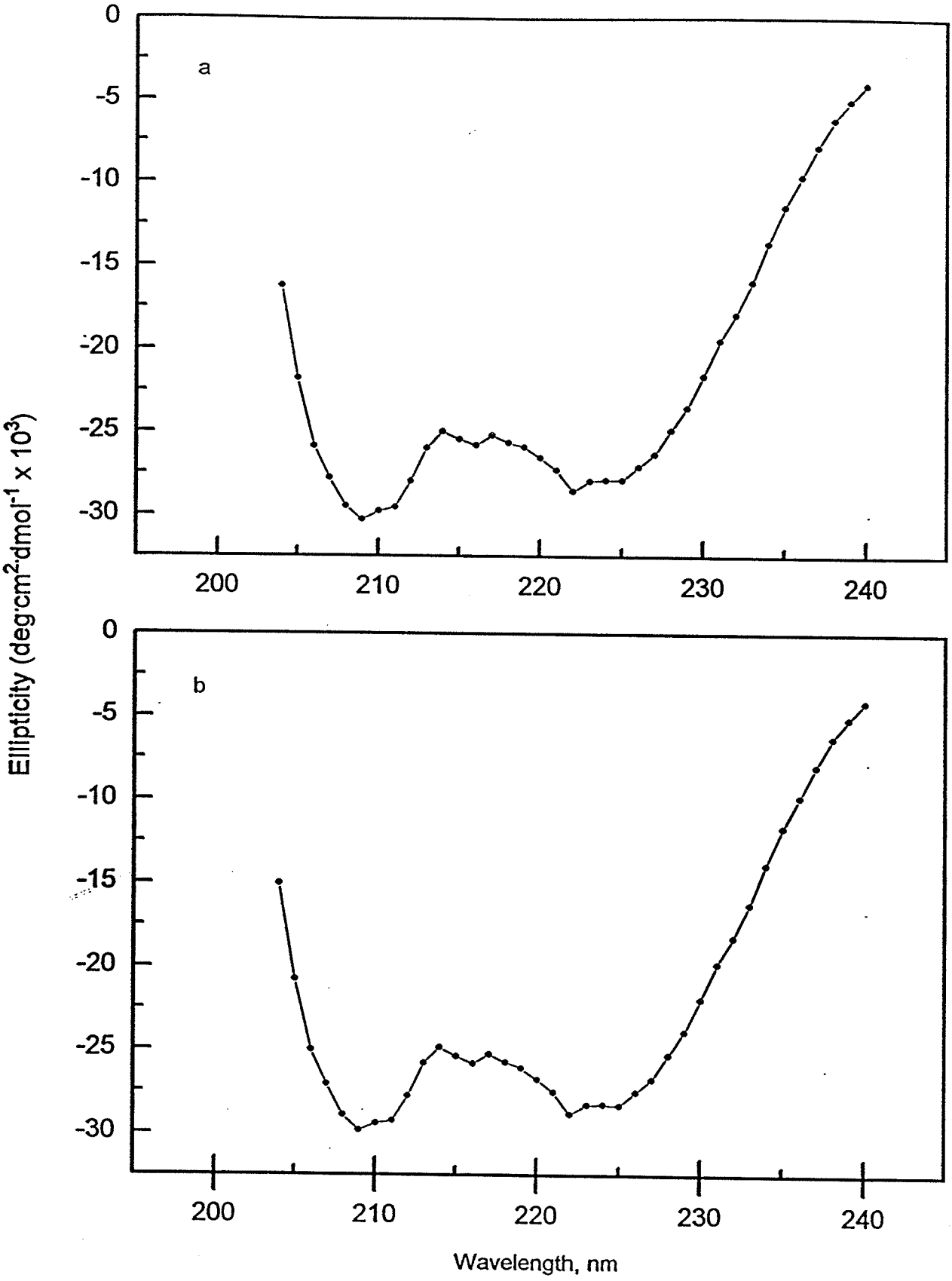
a
b
0
-5
-10
-15
-20
-25
-30
200
210
220
230
240
Ellipticity (deg·cm²·dmol⁻¹ x 10³)
Wavelength, nm

Figure 13: Experimental (●) and CCA-calculated (■) spectra at the same temperatures given in Figure 12 deconvoluted into 2 (a) and 3 (b) components in (A) methanol, (B) ethanol, (C) TFE, and (D) SDS.

A

a

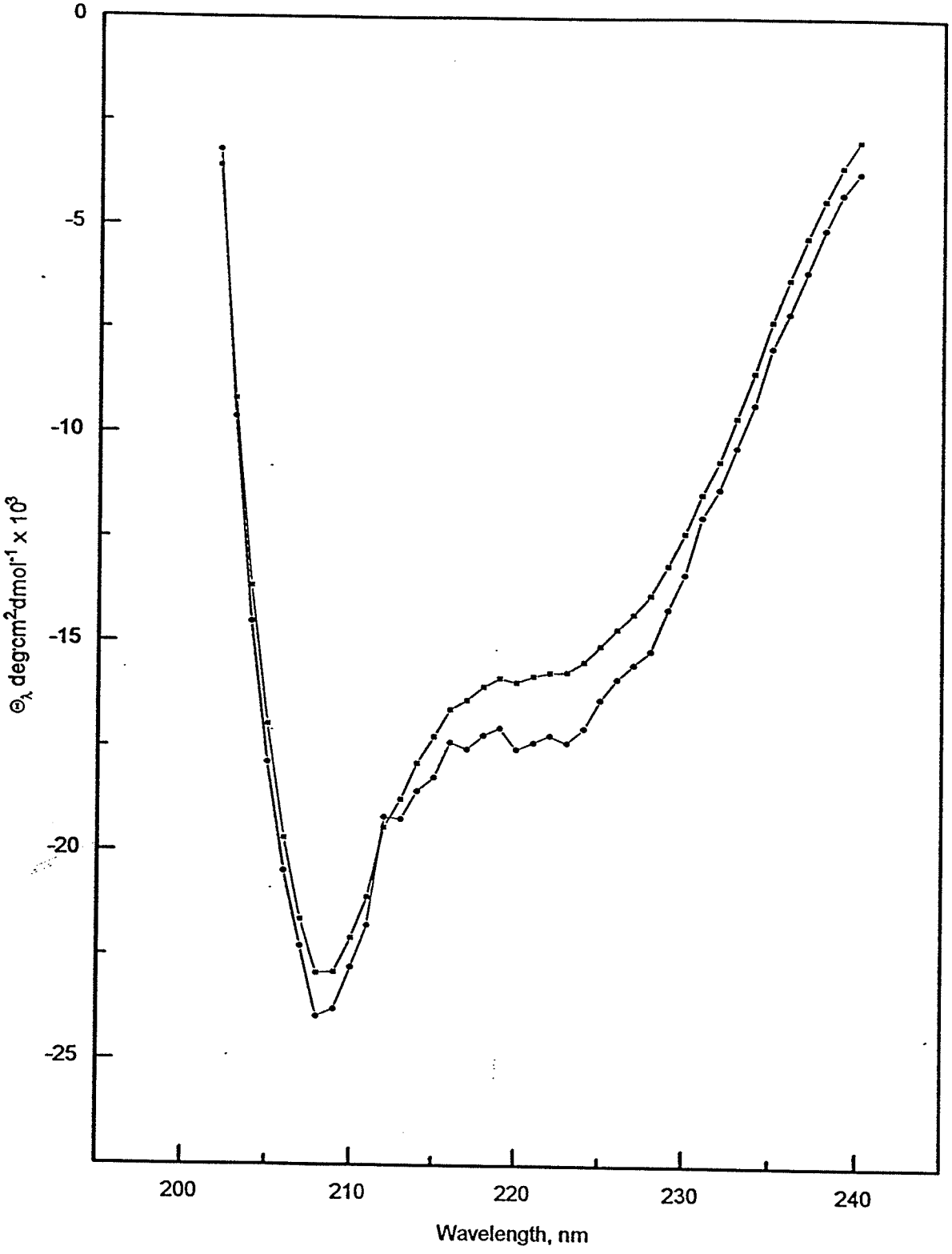
0
-5
-10
-15
-20
-25
Θ_λ degcm^{2}dmol^{-1} x 10^3
200
210
220
230
240
Wavelength, nm

A

100

b

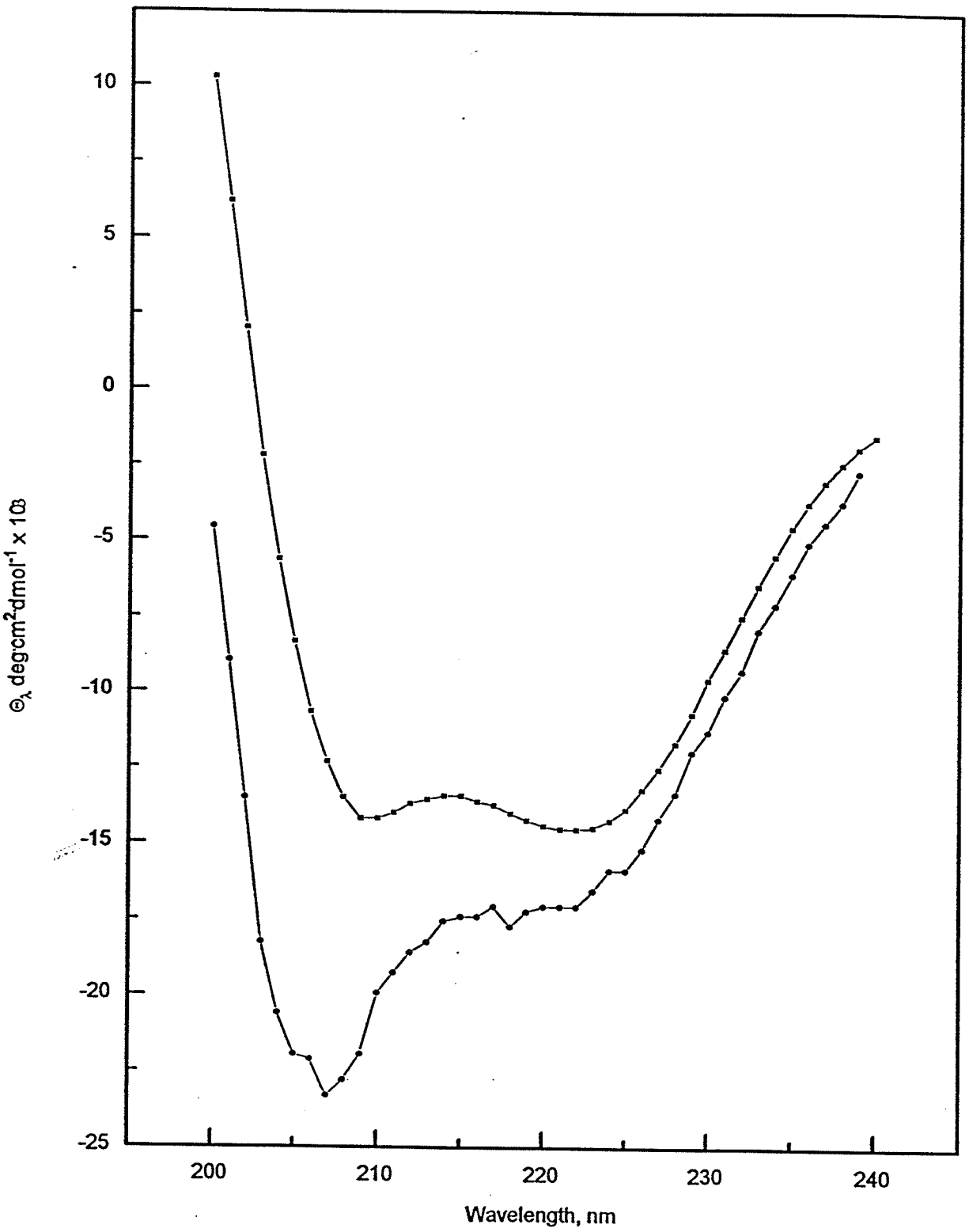
10
5
0
-5
-10
-15
-20
-25
200
210
220
230
240
Wavelength, nm
Θλ deg·cm²·dmol⁻¹ x 10³

B

a

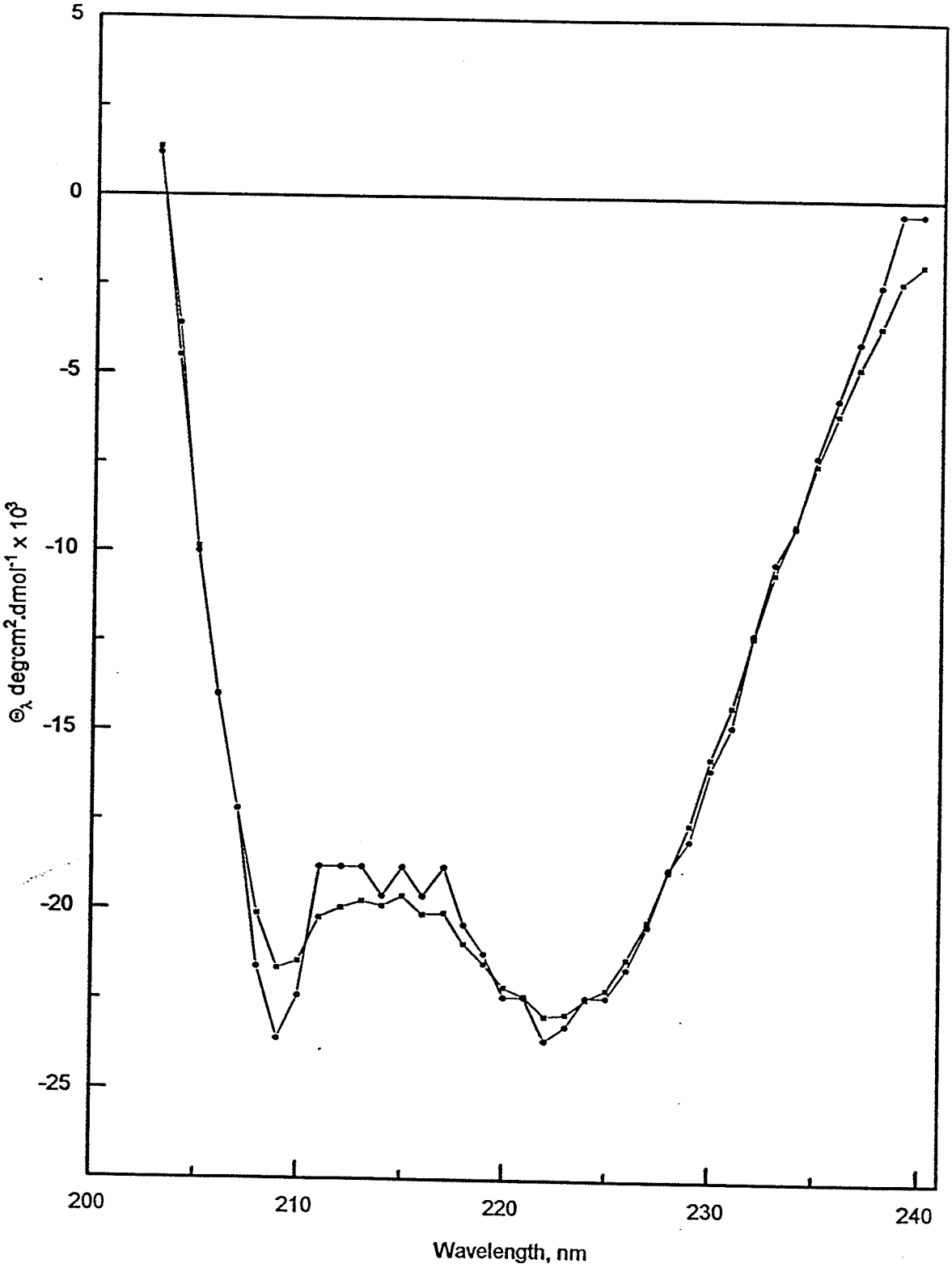
5
0
-5
-10
-15
-20
-25
Θ_λ deg·cm^2.dmol^{-1} x 10^3
200
210
220
230
240
Wavelength, nm

B

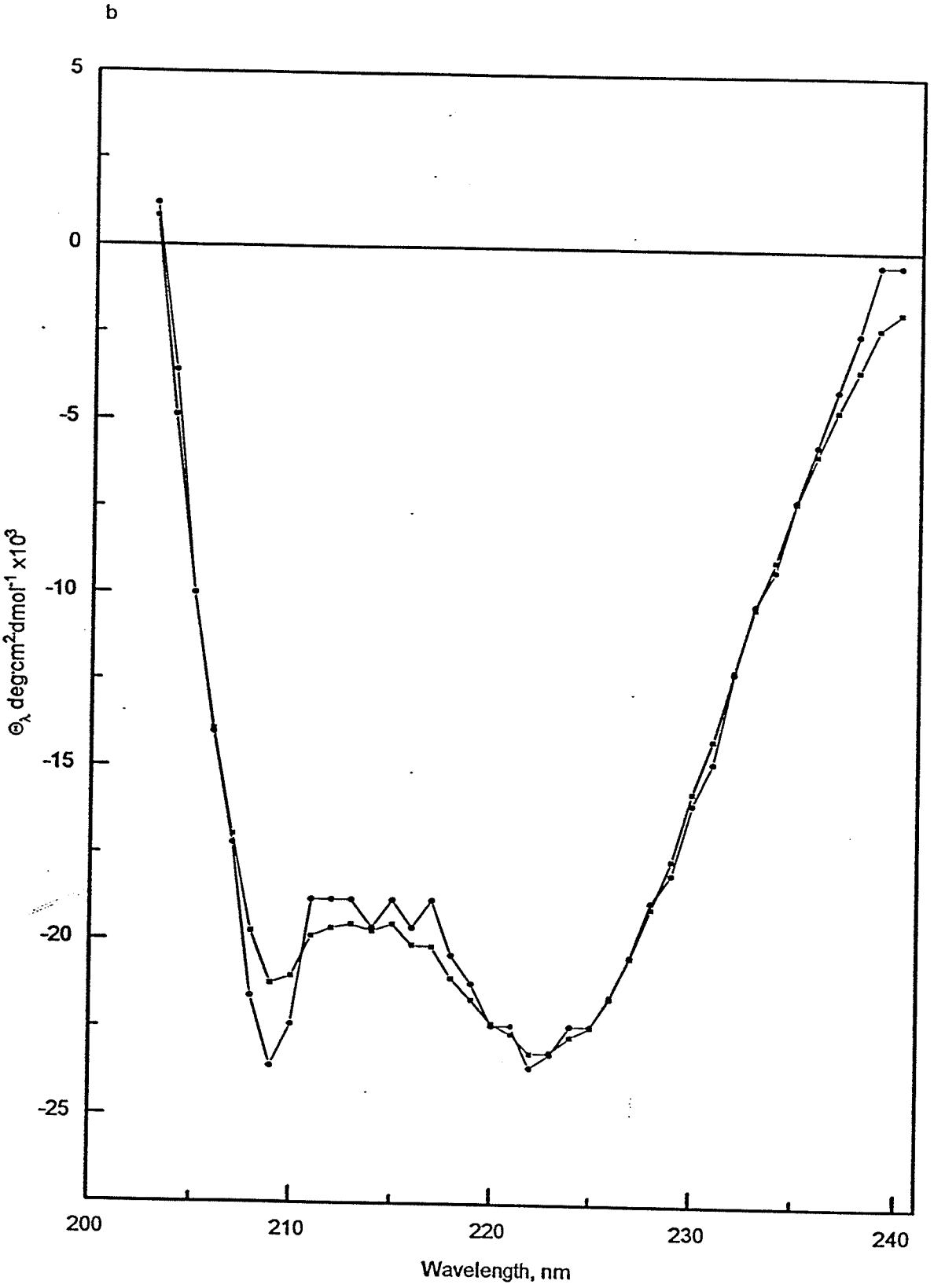
b
5
0
-5
-10
-15
-20
-25
Θ_λ deg·cm^2·dmol^{-1} x10^3
200
210
220
230
240
Wavelength, nm

C

a

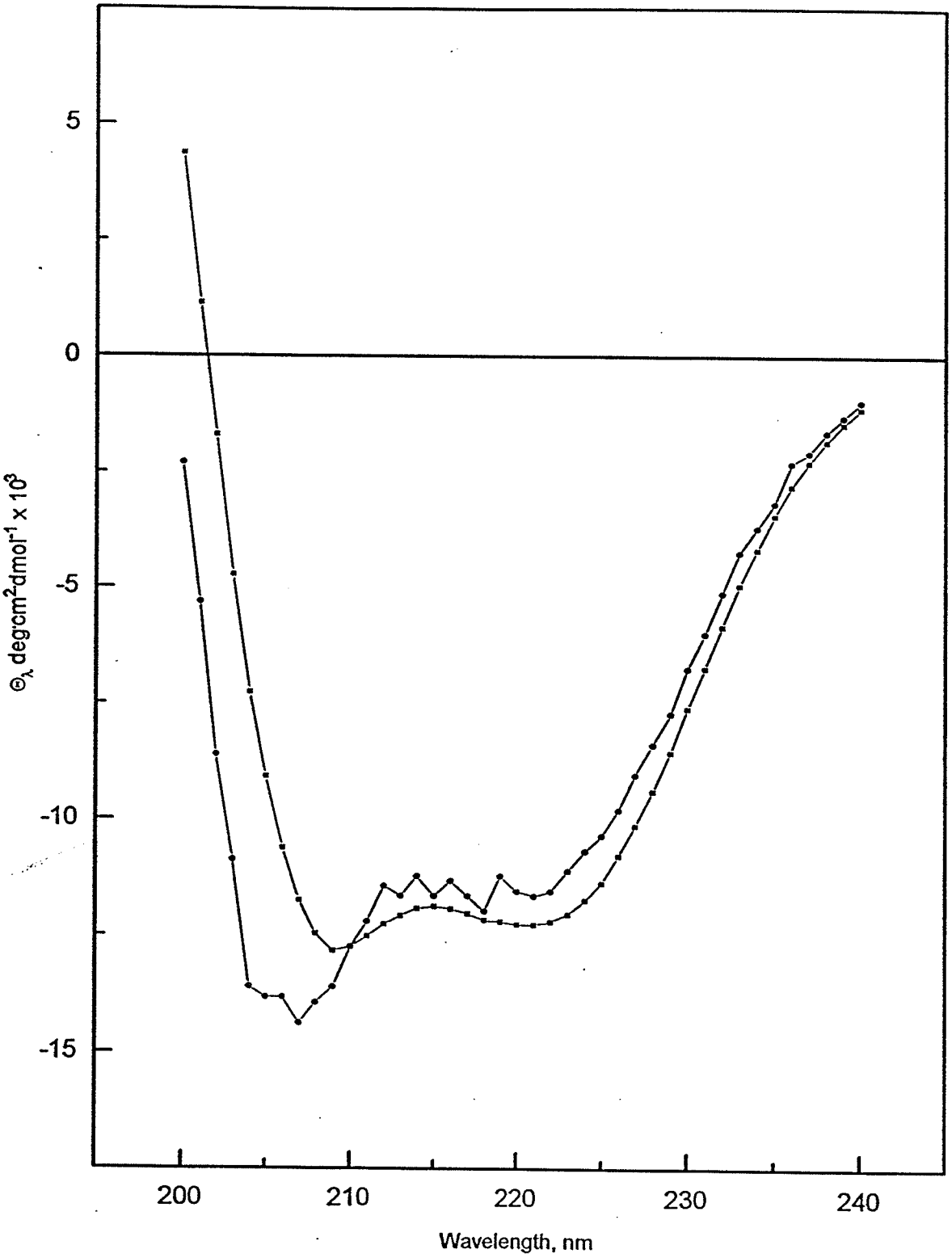
5
0
-5
-10
-15
Θ_λ degcm^{2}dmol^{-1} x 10^3
200
210
220
230
240
Wavelength, nm

C

b

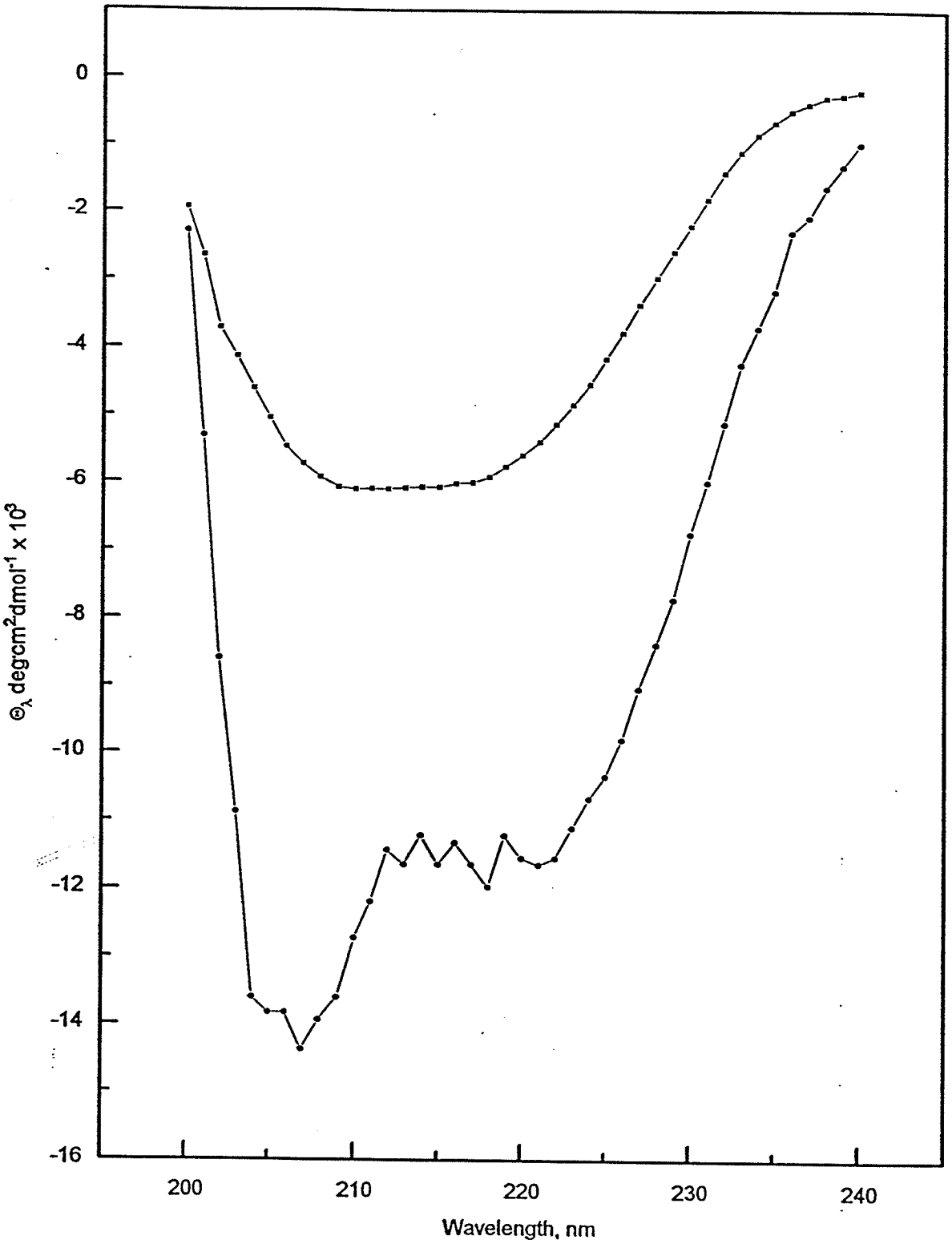
0
-2
-4
-6
-8
-10
-12
-14
-16
200
210
220
230
240
Wavelength, nm
Θλ degrcm2dmol-1 x 10³

D

a

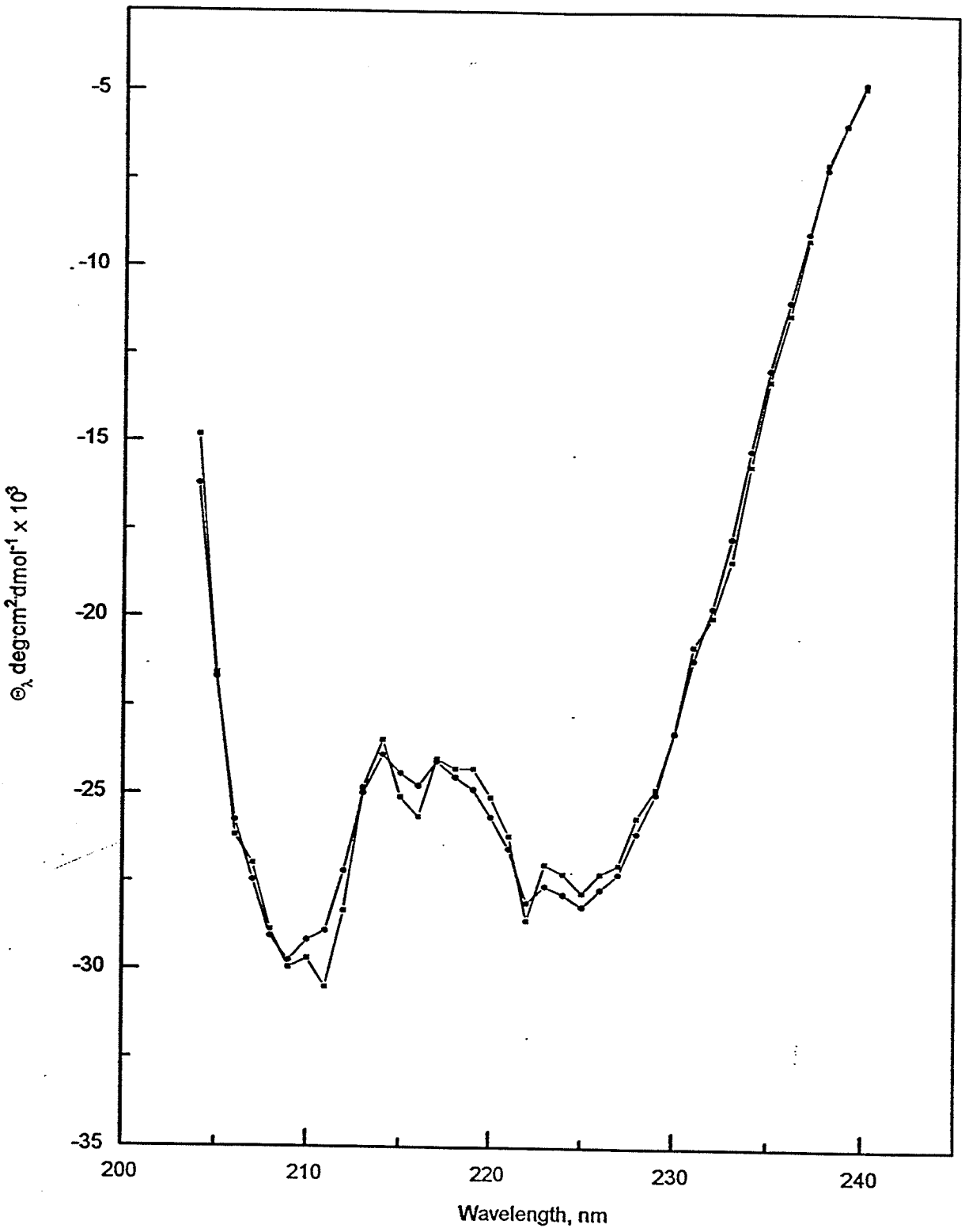
-5
-10
-15
-20
-25
-30
-35
200
210
220
230
240
Wavelength, nm
Θ_λ degcm^{2}dmol^{-1} x 10^3

b

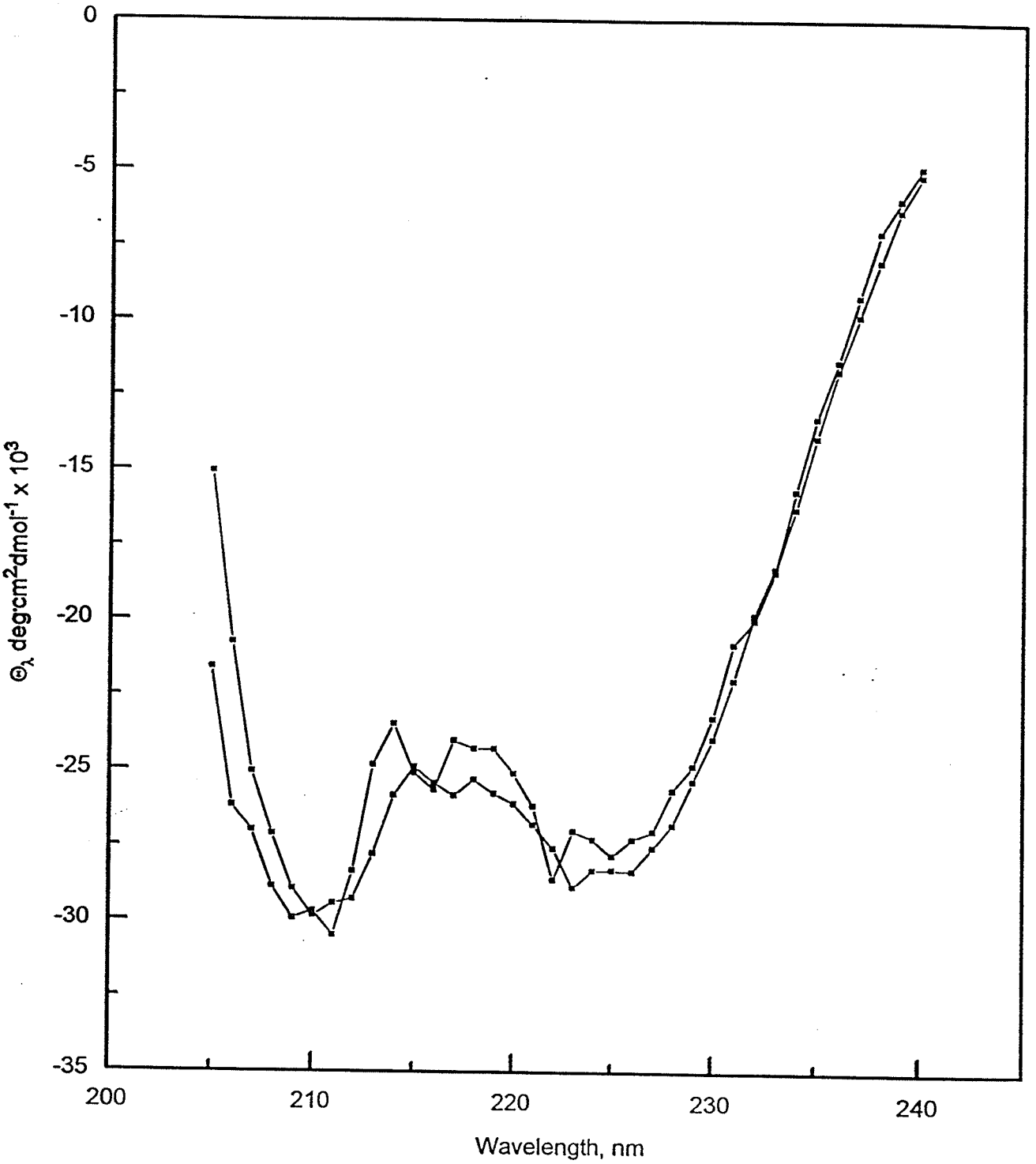
0
-5
-10
-15
-20
-25
-30
-35
200
210
220
230
240
Wavelength, nm
Θλ degcm2dmol-1 x 10³

3.3 Non-Linear Least Squares Fits of Temperature Dependence of CD Ellipticity Values

3.3.1 RESULTS FOR RBP-1 CD TEMPERATURE TITRATIONS

Temperature titrations of the peptide RBP-1 in methanol, ethanol, trifluoroethanol and SDS were fit to Equation 6 derived as described in **Methods**. These fits assume that the peptide exists in only two states, the helix and random coil. Appendix A contains the temperature and ellipticity values used. The Marquart-Levenbery algorithm in the program *Mathematica* determined values for the T_m and ΔT variables of the equation. The fitted data are shown in Figure 15. The values of T_m, ΔT and χ^2 goodness of fit are given below in Table 5. The information or implications given by these sets of values will be discussed in the next chapter. Note that there is generally good agreement between the calculations of percent helix content shown in Figures 10a -d calculated using equation 4, and the helix content shown in Figures 14 a - d calculated using equation 5. Table 5 illustrates that as the correlation between the maximum inducible helix (Table 4) and the melting point of the helices (Table 5).

Figure 14: *Mathematica* output of fitting procedure. The graphs a - d are the results of fitting the CD data for RBP-1 in methanol, ethanol, TFE and SDS to equation 6. The top graphs show the ellipticities over the range of temperatures measured. The bottom graphs indicate where the data fall in a two-state helix coil model of the transition.

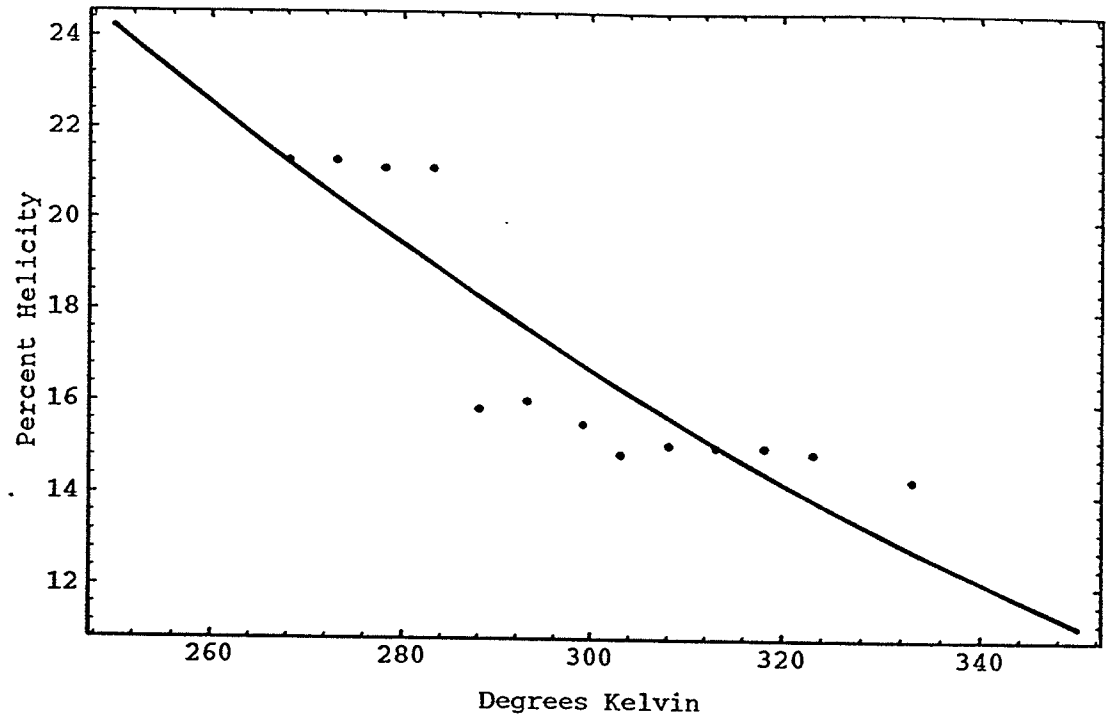
Percent Helicity
24
22
20
18
16
14
12
260
280
300
320
340
Degrees Kelvin

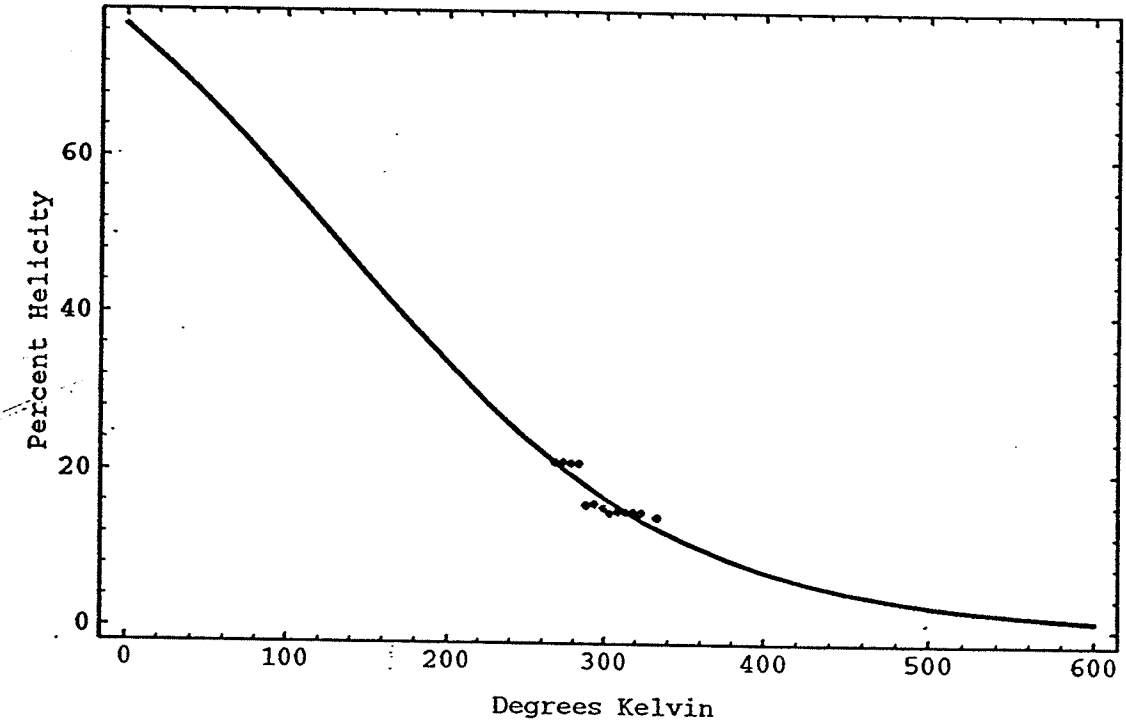
Percent Helicity
60
40
20
0
0
100
200
300
400
500
600
Degrees Kelvin

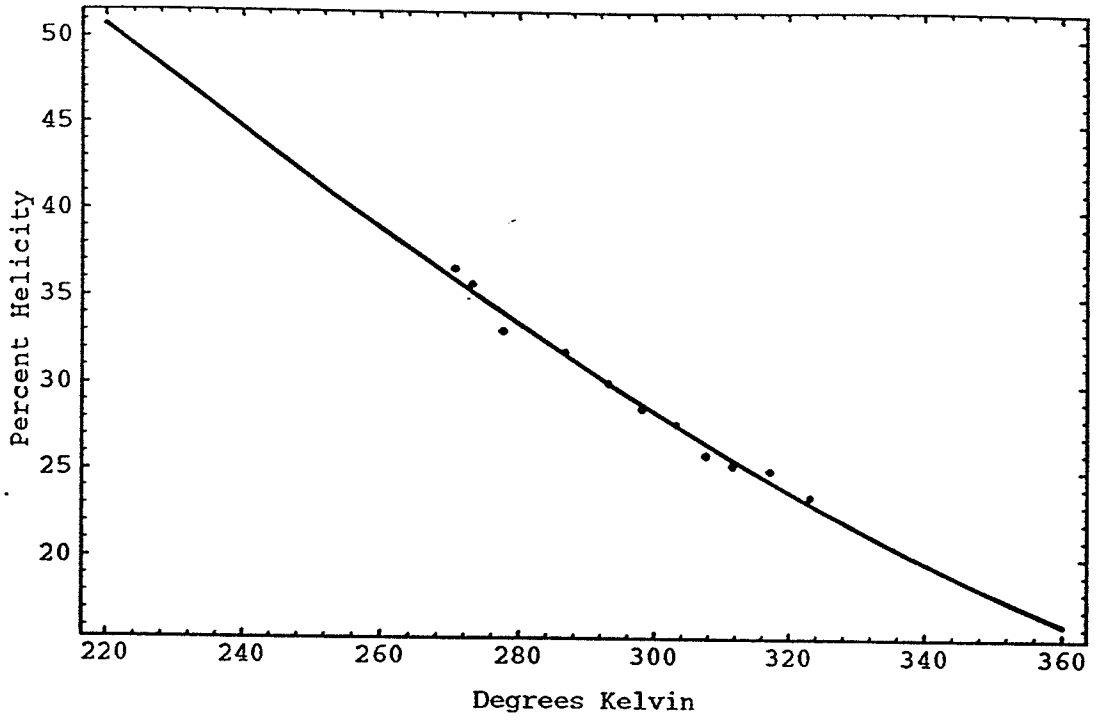
Percent Helicity
50
45
40
35
30
25
20
220
240
260
280
300
320
340
360
Degrees Kelvin

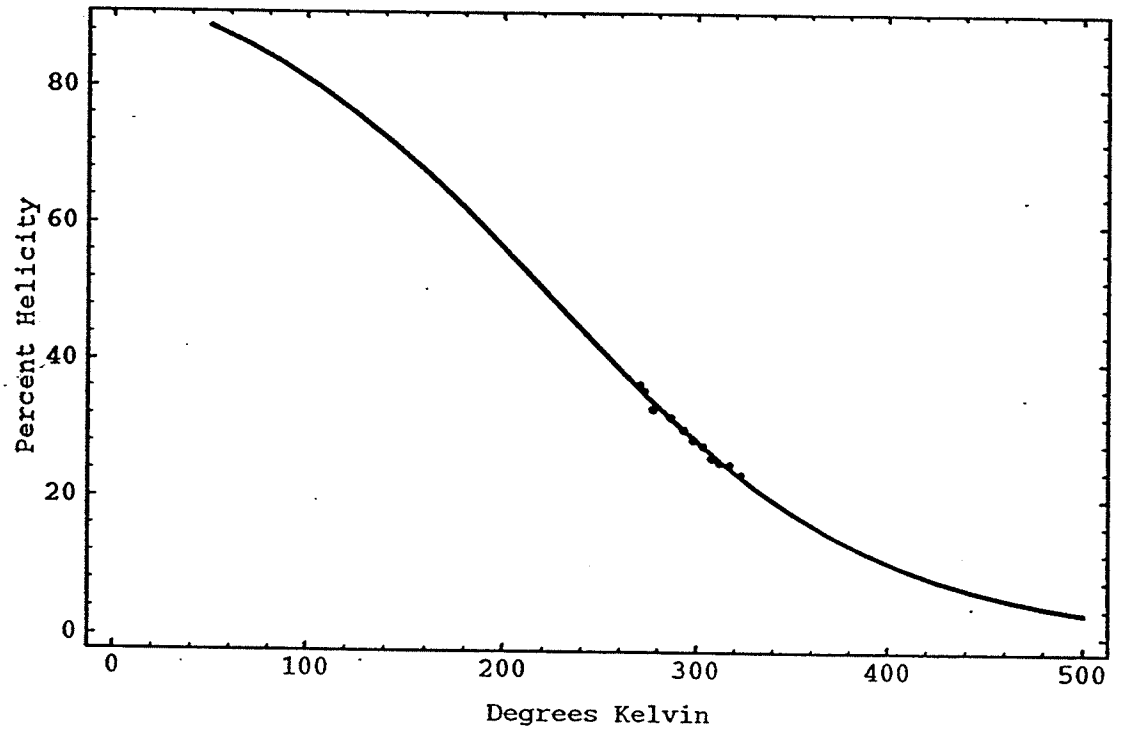
Percent Helicity
80
60
40
20
0
0
100
200
300
400
500
Degrees Kelvin

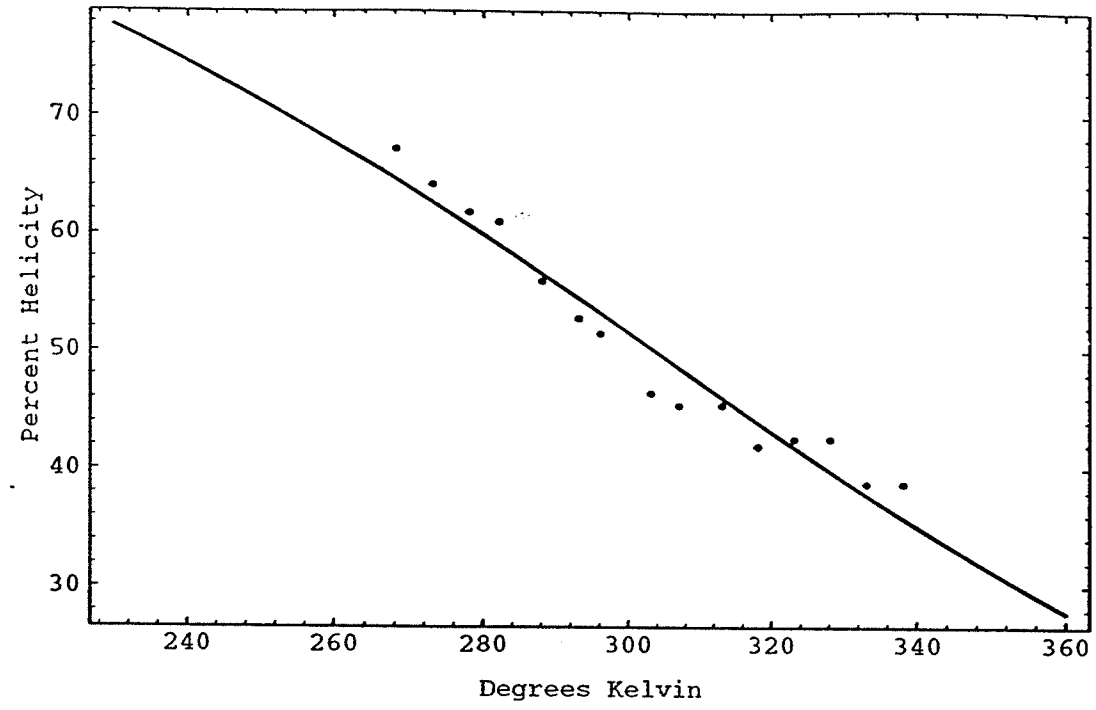
Percent Helicity
70
60
50
40
30
240
260
280
300
320
340
360
Degrees Kelvin

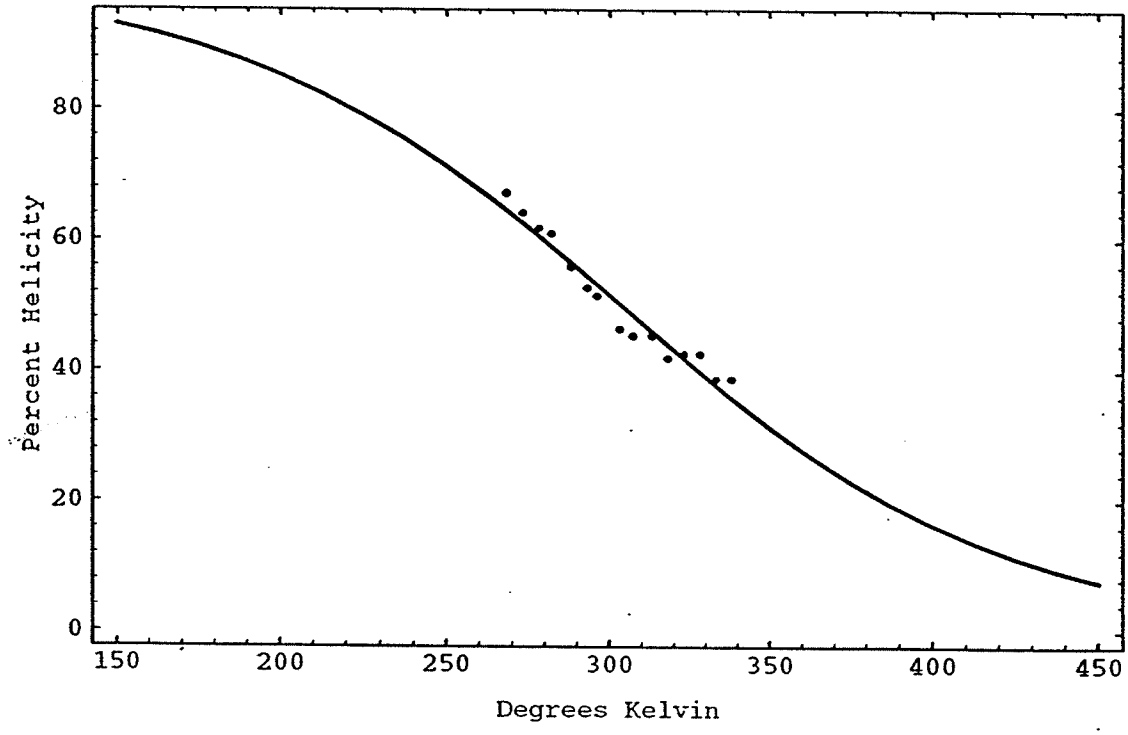
Percent Helicity
80
60
40
20
0
150
200
250
300
350
400
450
Degrees Kelvin

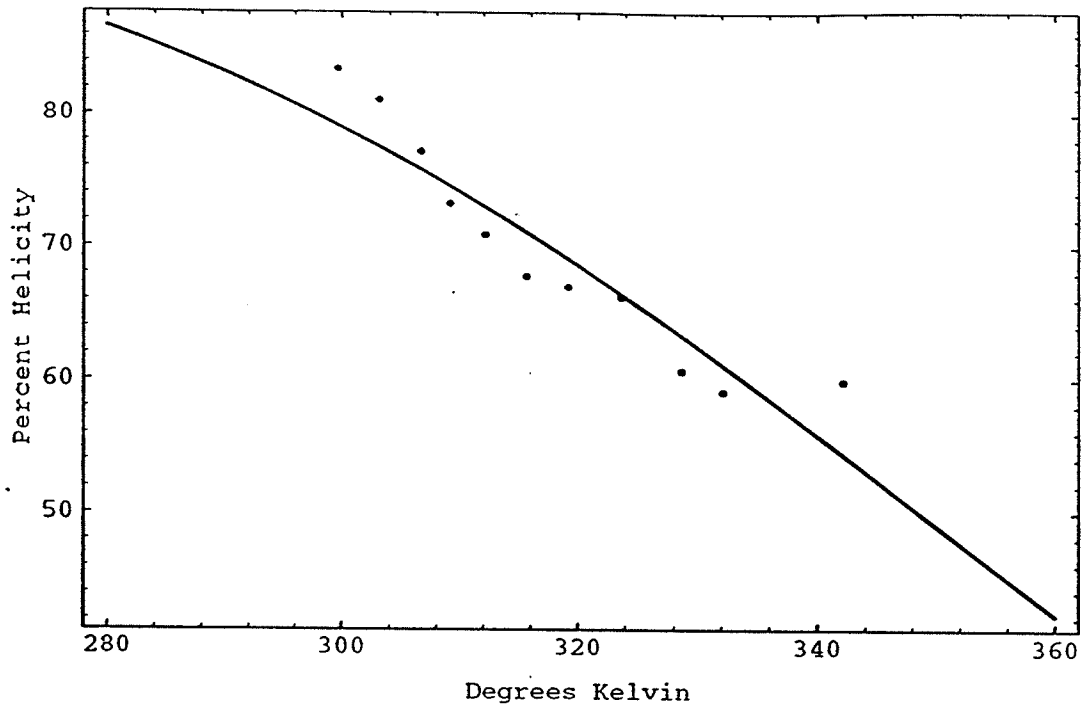
Percent Helicity
80
70
60
50
280
300
320
340
360
Degrees Kelvin

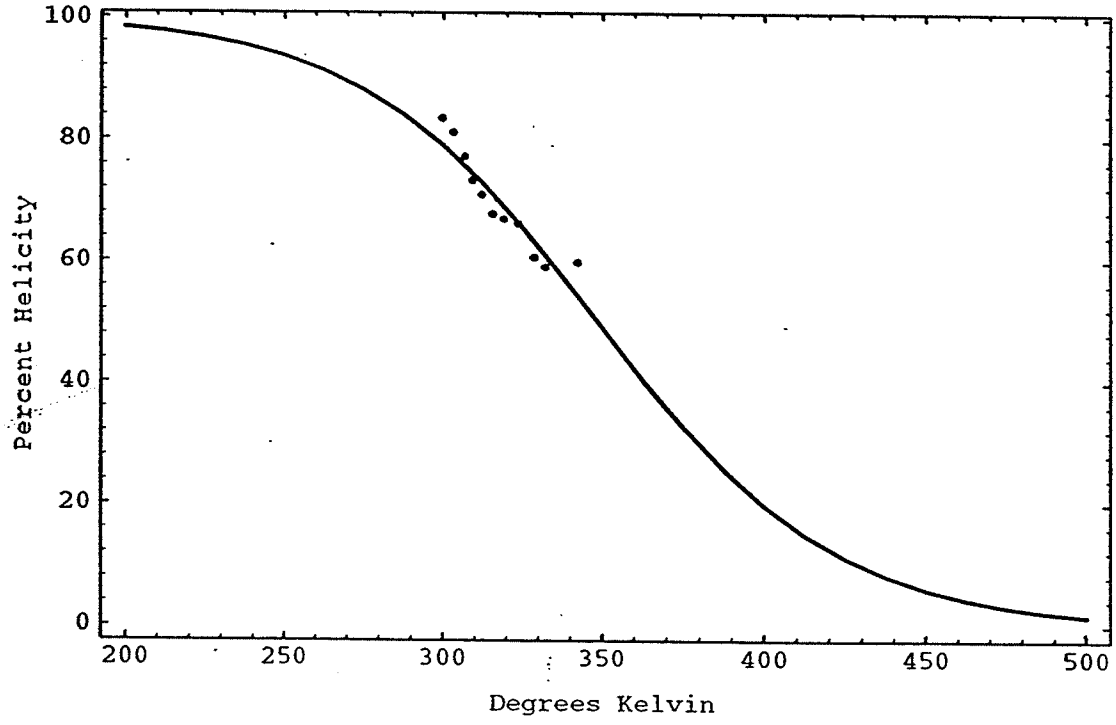
Percent Helicity
100
80
60
40
20
0
200
250
300
350
400
450
500
Degrees Kelvin

Table 5: Fitted Values for RBP-1

Solvent	T_m, K	ΔT, K	χ^2
Methanol	128	493	23.3
Ethanol	222	386	2.8
TFE	304	272	67.3
SDS	349	169	95.6

3.4 Results of Alamethicin Study

3.4.1 CD EXPERIMENTS

CD temperature titrations of alamethicin in methanol and SDS were performed by another student, A.A. Yee. I analyzed her data form these experiments in the same fashion as for RBP-1. Spectra of the CD temperature titrations of alamethicin in methanol and SDS are shown in Figure 15. A graph relating the helix content calculated from Equation 4 and the experimental temperatures is shown in Figure 16. Representative plots of the CCA outputs are shown in Figures 17 and 18. A plot of the ellipticity versus temperature displays an almost linear relationship, rather than the sigmoidal shape of the analogous plot for RBP-1 in methanol. This suggests a noncooperative helix-coil transition.

The shapes of the CD spectra of alamethicin in methanol are very similar to the shapes of the curves for RBP-1 in methanol, ethanol, and TFE. The spectra for both peptides show the characteristic helical shape. However, the curves for alamethicin and the synthetic peptide in SDS are different in one respect. Alamethicin shows a more intense negative ellipticity around 222 nm than it does near 208 nm. The reverse is seen in the spectra for RBP-1 in SDS.

Figure 15: Temperature titrations of alamethicin in (a) methanol, and (b) SDS.

a

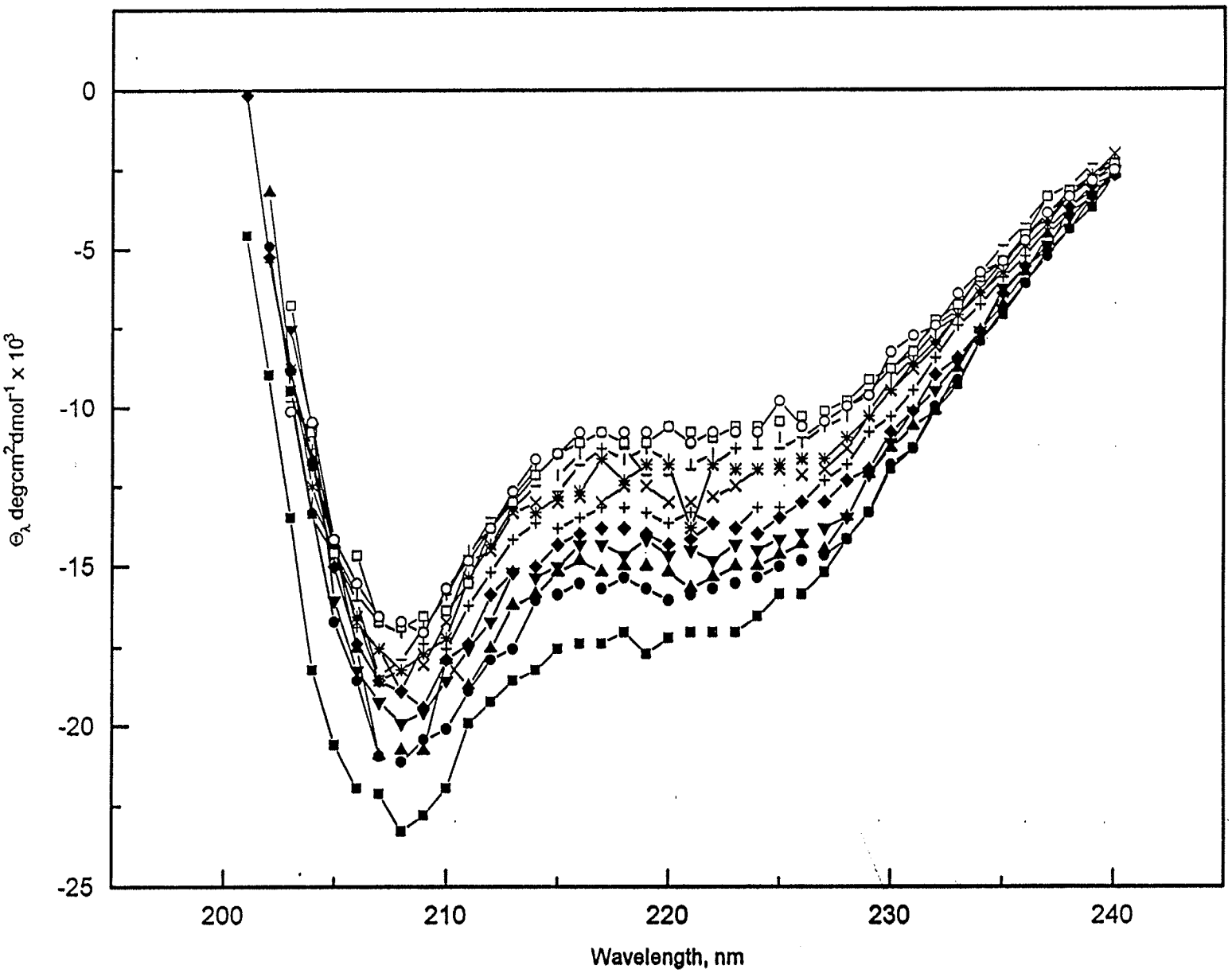
0
-5
-10
-15
-20
-25
200
210
220
230
240
Wavelength, nm
Θ_λ degcm^{2}dmol^{-1} x 10^3

b

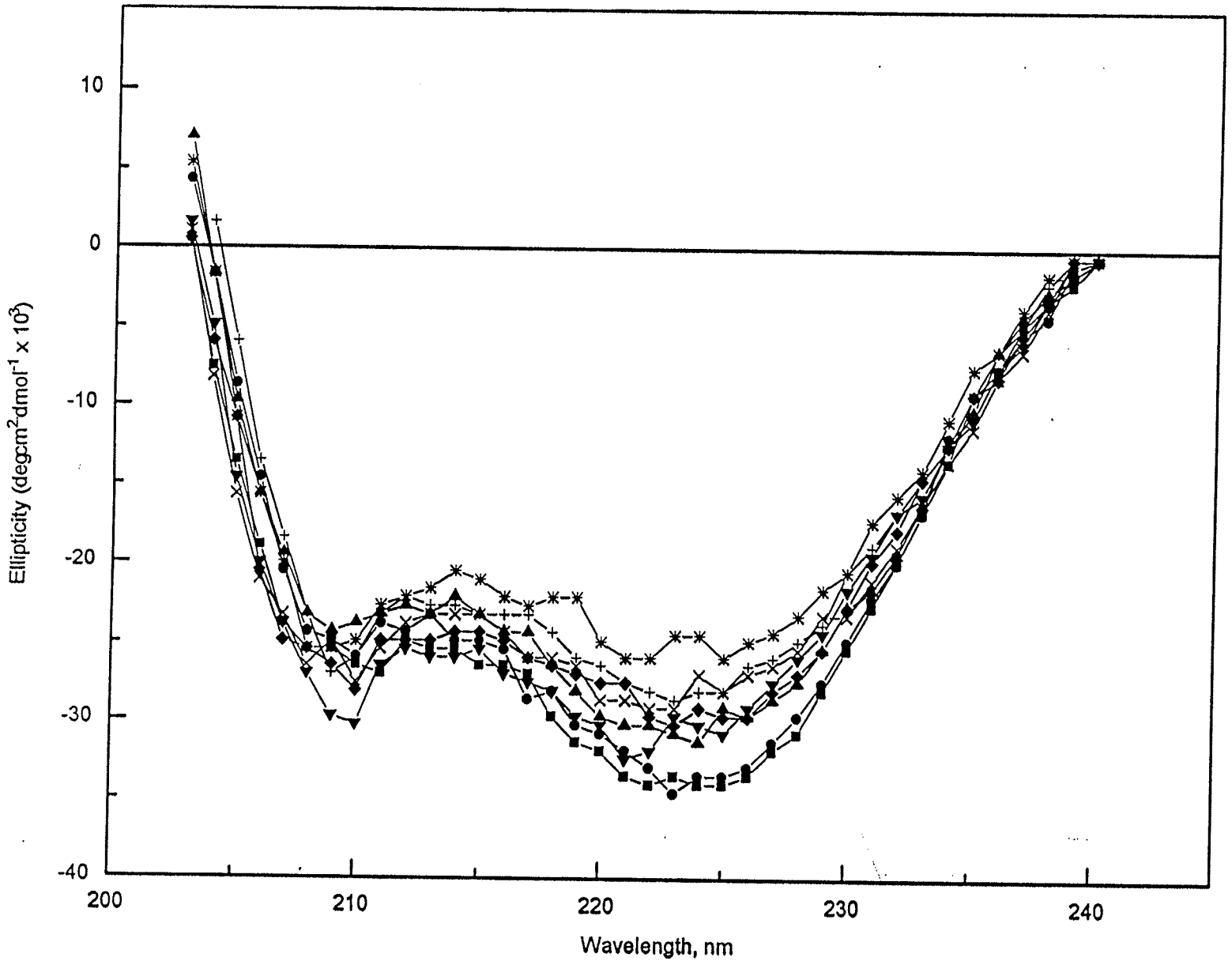
10
0
-10
-20
-30
-40
200
210
220
230
240
Ellipticity (degcm2dmol-1 x 10³)
Wavelength, nm

Similar spectra to that of alamethicin in SDS have been observed in bacteriorhodopsin in the purple membrane (Gibson and Cassim, 1989). RBP-1 exhibits the characteristic helical character in both methanol and SDS. There is a considerable difference in the maximum ellipticity shown by the two peptides in methanol. Alamethicin has a maximum ellipticity value of -17000 $deg \cdot cm^2 \cdot dmol^{-1}$, while RBP-1 has an ellipticity of only -7300 $deg \cdot cm^2 \cdot dmol^{-1}$. In SDS, the peptides have similar ellipticities, -33000 $deg \cdot cm^2 \cdot dmol^{-1}$ for alamethicin and -29000 $deg \cdot cm^2 \cdot dmol^{-1}$ for the synthetic analog. The differences in methanol are strong evidence for a significant influence of the Aib residues on helical conformation. Similar results in SDS indicates that the solvent has a stronger effect on conformation than a factor like helix propensity. The helix content of alamethicin in methanol ranged from 49% at low temperature to 28% at the highest temperature. In SDS, the helix content went from 100% at low temperature to 60%.

Figure 16: Helix content of alamethicin as a function of temperature in (a) methanol, and (b) SDS.

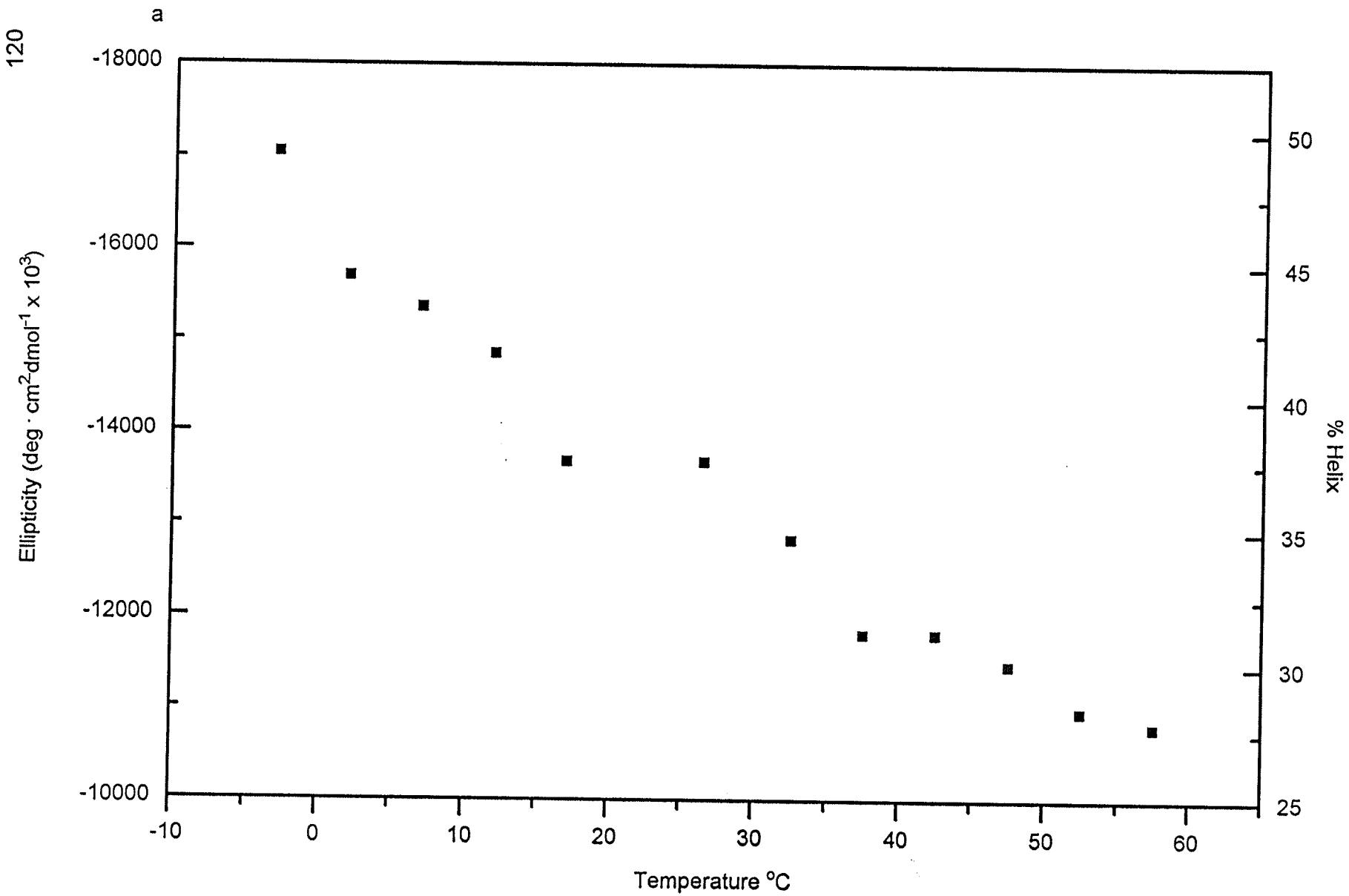
a
120
-18000
-16000
-14000
-12000
-10000
Ellipticity (deg · cm2dmol-1 x 10^3)
50
45
40
35
30
25
% Helix
-10
0
10
20
30
40
50
60
Temperature °C

b

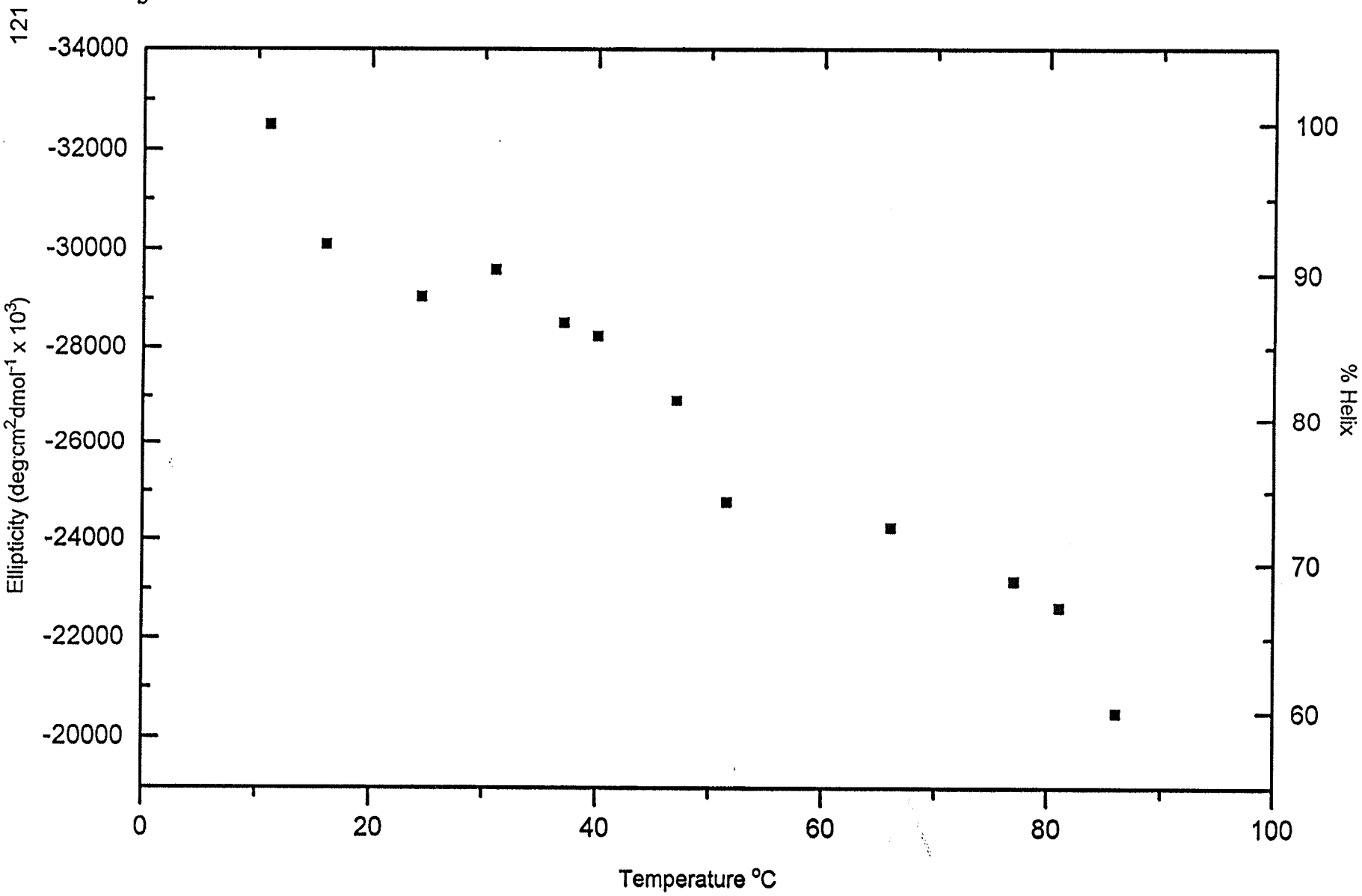
-34000
-32000
-30000
-28000
-26000
-24000
-22000
-20000
Ellipticity (degcm^{2}dmol^{-1} x 10^3)
100
90
80
70
60
% Helix
0
20
40
60
80
100
Temperature °C

Figure 17: Resulting pure component curves are plotted for CCA analyses for (a) 2 and (b) 3 components for alamethicin in (A) methanol and (B) SDS at the lowest temperature used in each solvent (-5, 13 °C, respectively). The different unique secondary structural components are designated by the following symbols:● α-helix, ■ unordered, ▲ ↑↓β, ♦ residual or undefined.

A Alamethicin in methanol

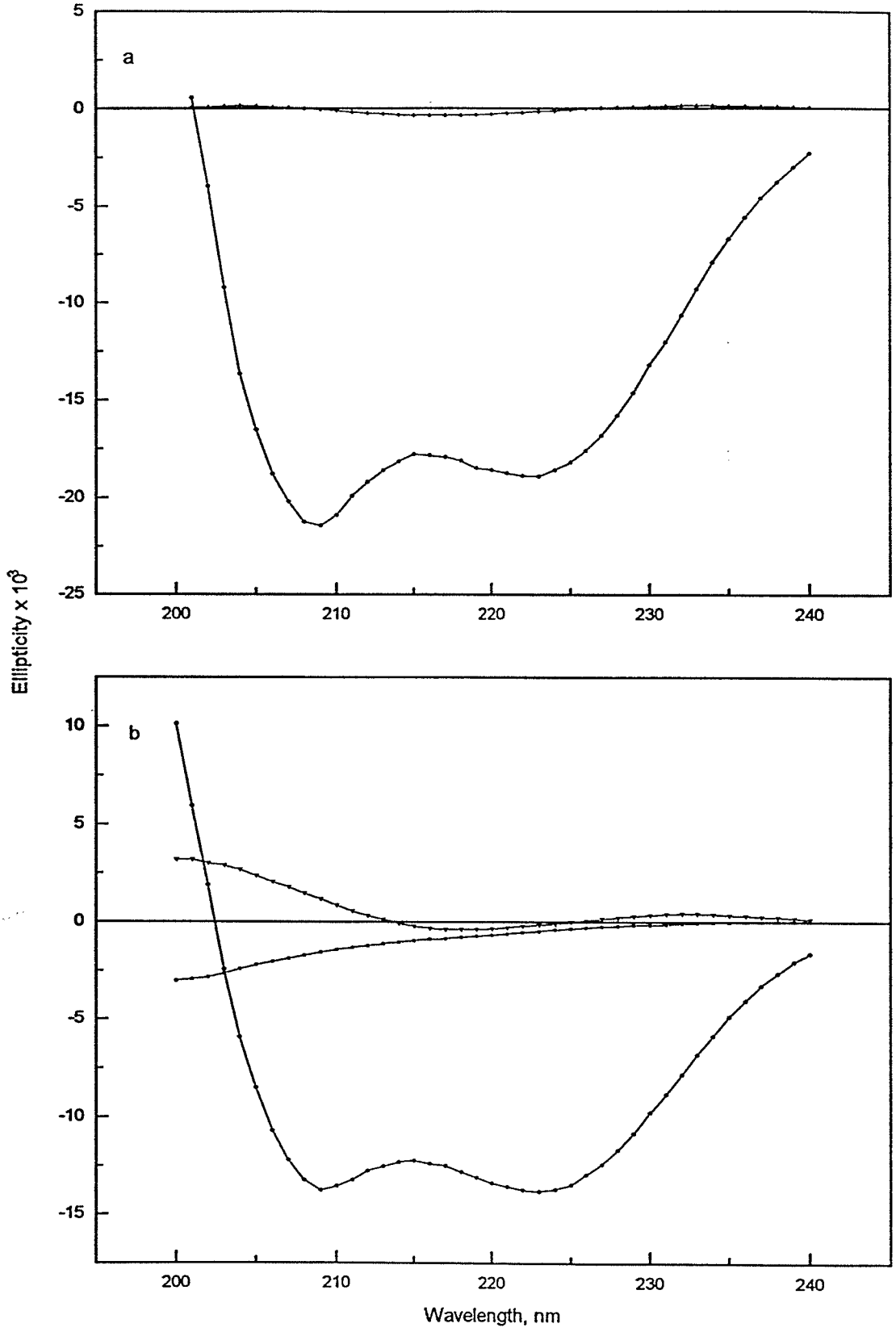

B Alamethicin in SDS

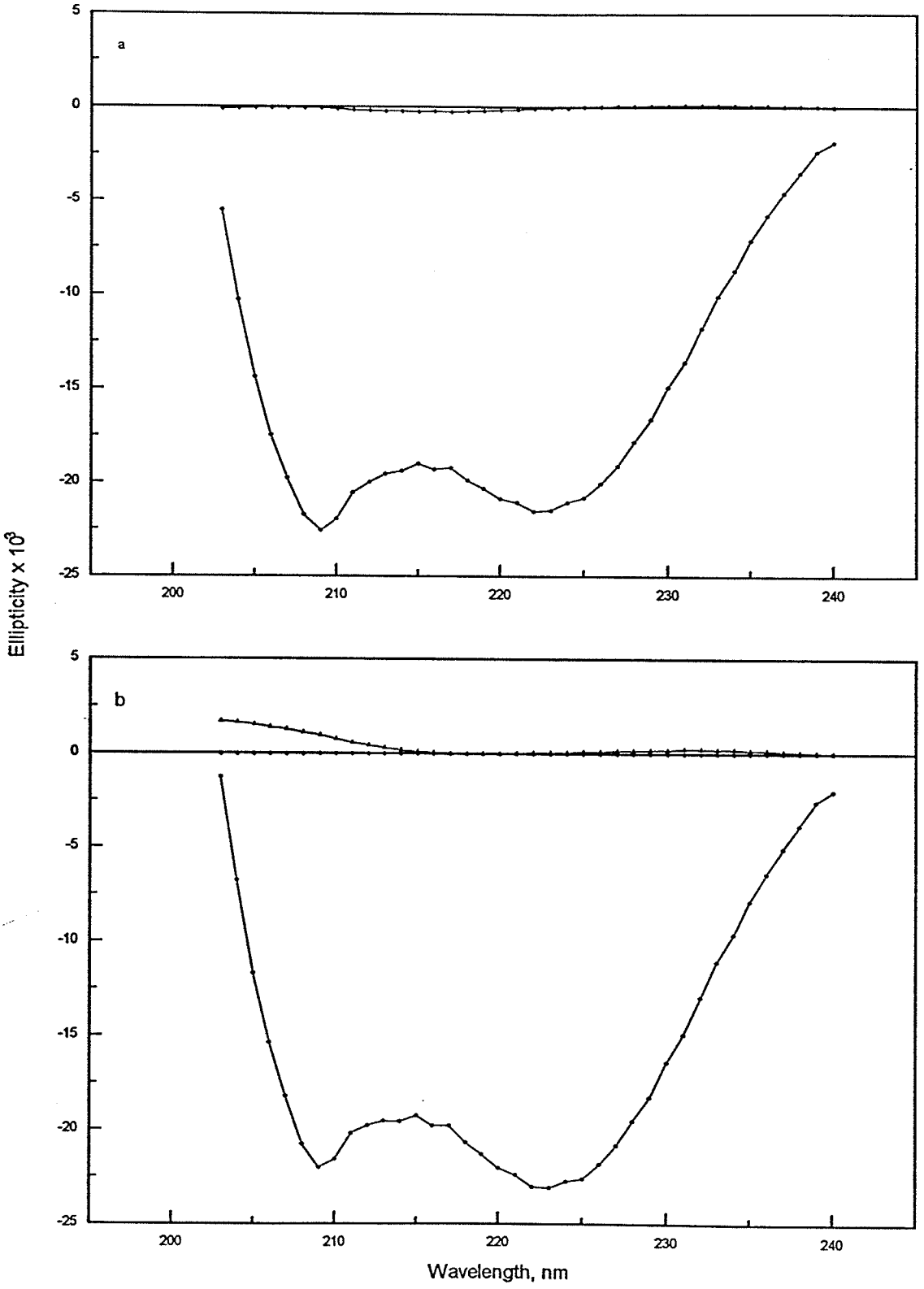

Figure 18: The weighted sums of the component spectra from the CCA deconvolutions compared to the experimental spectrum for each analysis of alamethicin in each solvent system is plotted here for each set of pure component analysis in Figure 18. The calculated spectrum in each plot is represented by ■. The measured spectrum is defined by the symbol ●.

A

a

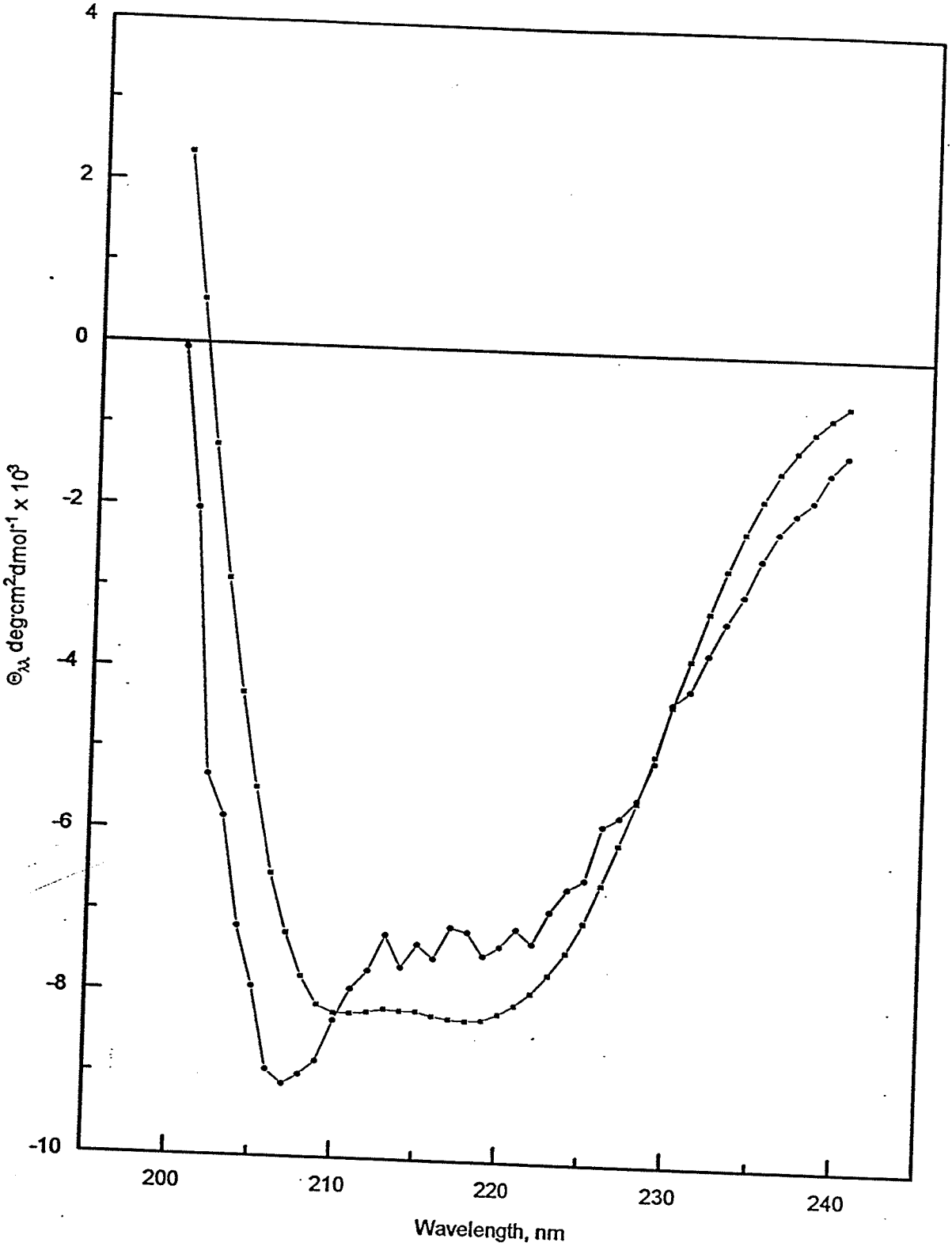
4
2
0
-2
-4
-6
-8
-10
200
210
220
230
240
Wavelength, nm
Θ_λ deg·cm^2·dmol^{-1} x 10^3

A

b

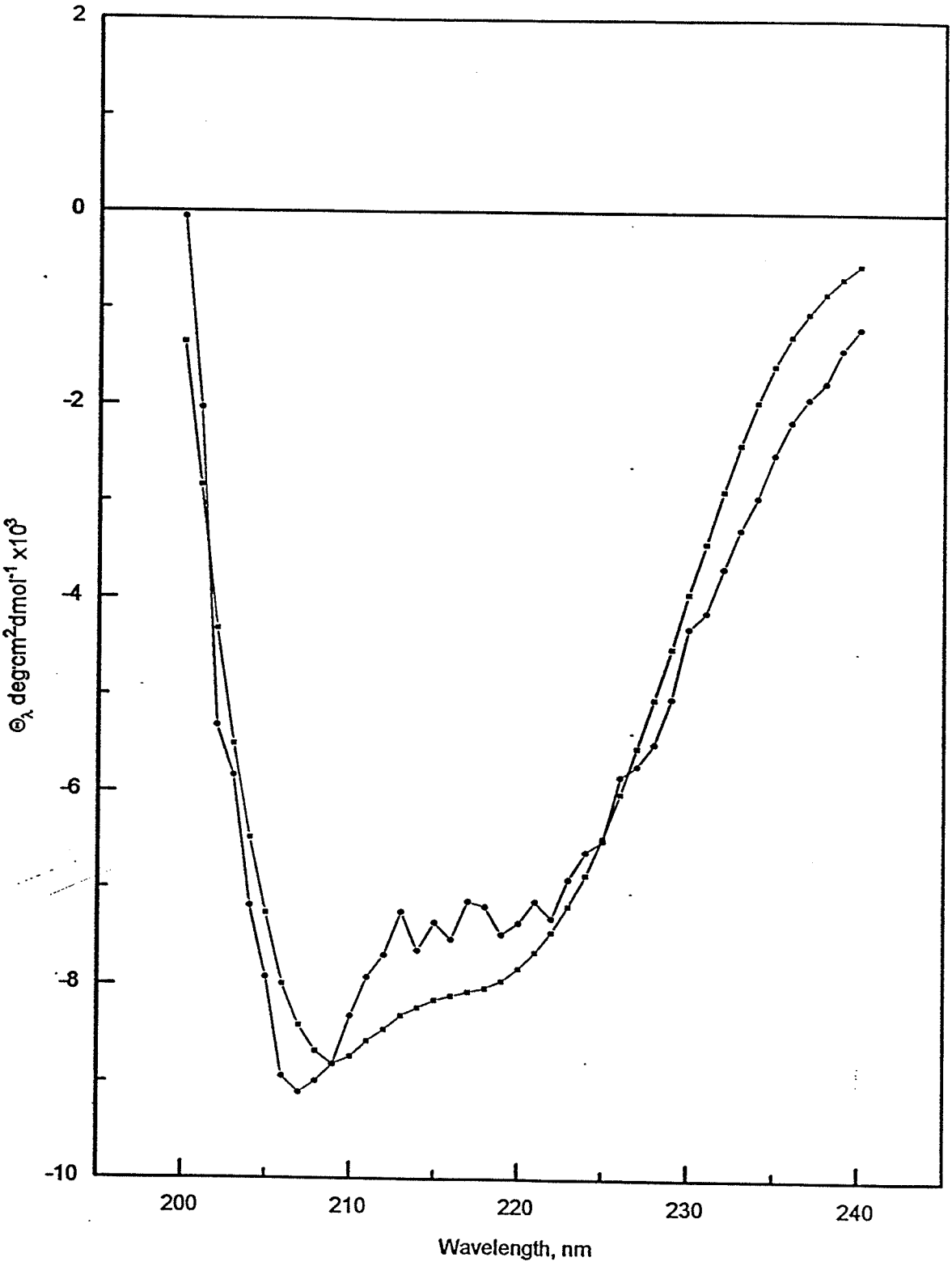
2
0
-2
-4
-6
-8
-10
200
210
220
230
240
Wavelength, nm
Θ_λ degcm^{2}dmol^{-1} x10^3

a

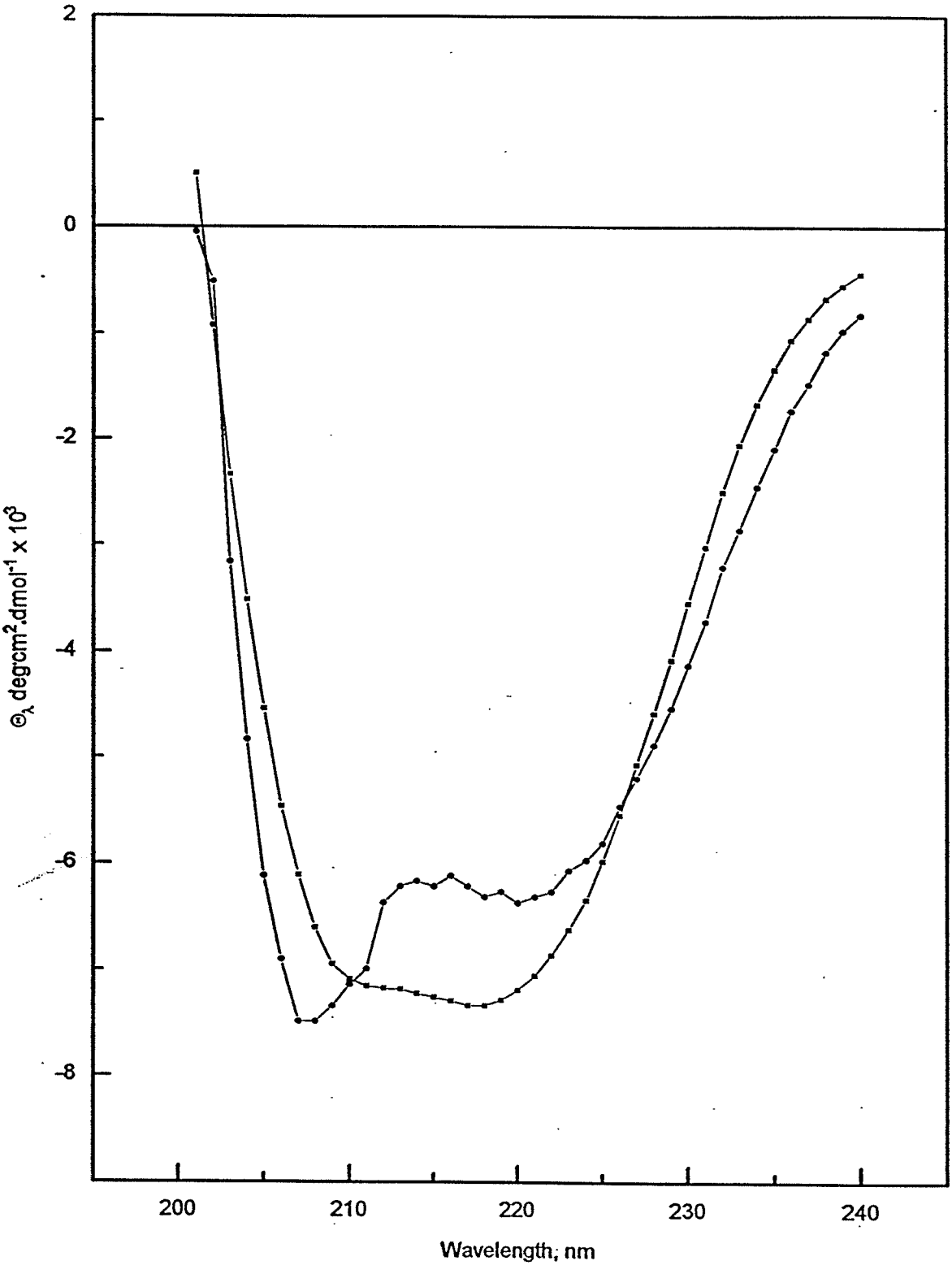
2
0
-2
-4
-6
-8
Θ_λ degcm^2.dmol^{-1} x 10^3
200
210
220
230
240
Wavelength, nm

b

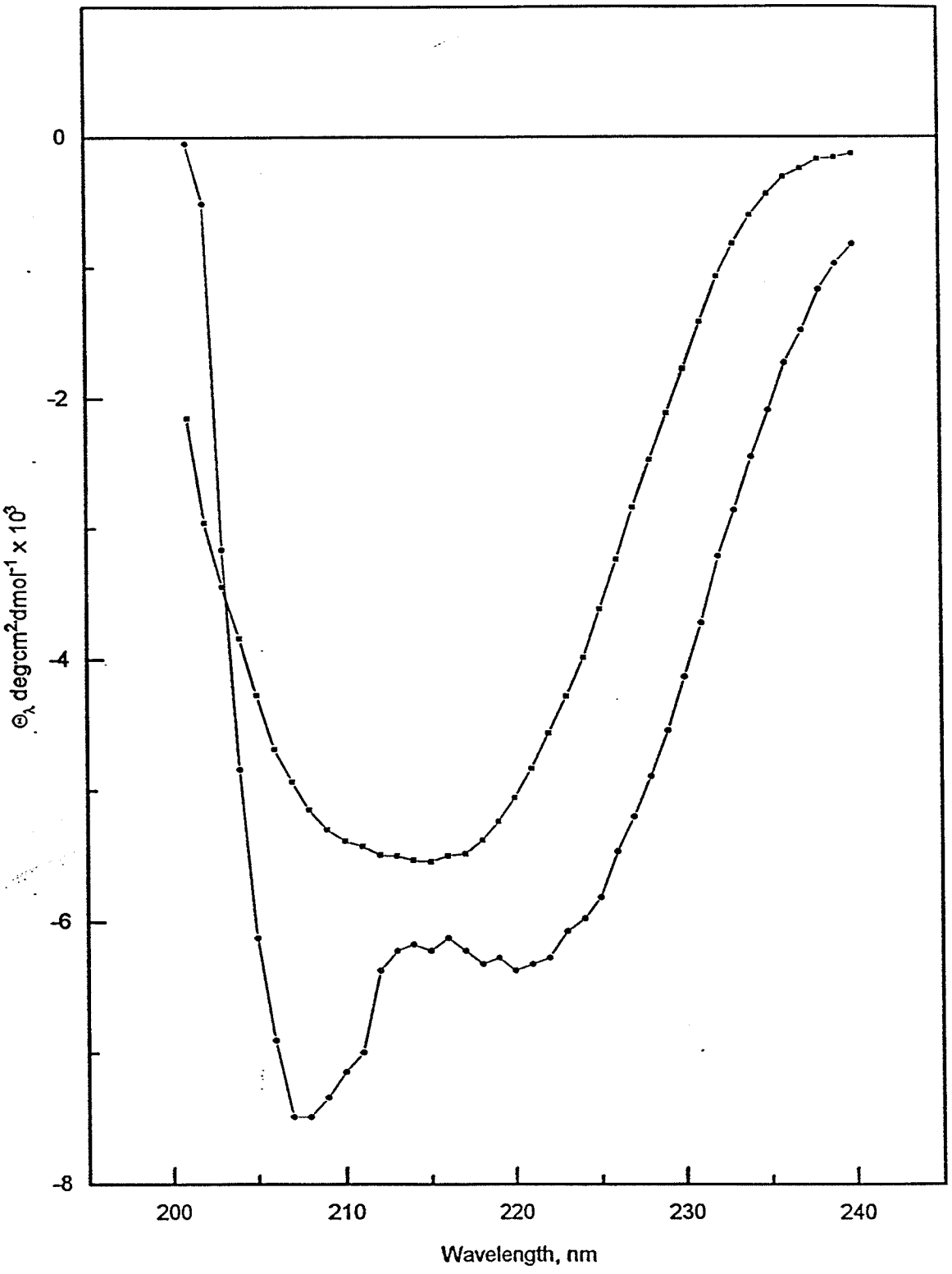

3.4.2 RESULTS FOR ALAMETHICIN CD TEMPERATURE DEPENDENCE FITTING

θ_{222} values and corresponding temperatures for the methanol and SDS temperature titrations of alamethicin are found in Appendix A. The results of fitting the temperature titrations to a two-state helix/coil transition (equation 6) are given in Table 6. Similar to the results with RBP-1, the calculations of the % helicity in alamethicin using equation 4 (Figure 16) and equation 5 (Figure 19) give similar results. Note as well that methanol induces a maximum of 51% helicity in alamethicin with a transition midpoint of 261 K. SDS induces much greater helicity, 97%, and the midpoint of the melting curve is much higher at 378 K.

Table 6: Fitted Values for Alamethicin

Solvent	T_m, K	ΔT, K	χ^2
Methanol	128	493	23.3
SDS	349	169	95.6

Figure 19: *Mathematica* output of fitting procedure. The graphs a and b are the results of fitting the CD data from alamethicin in methanol and SDS to equation 6; The top graphs show the ellipticities over the range of temperatures measured. The bottom graphs indicate where the data fall in a two-state helix coil model of the transition.

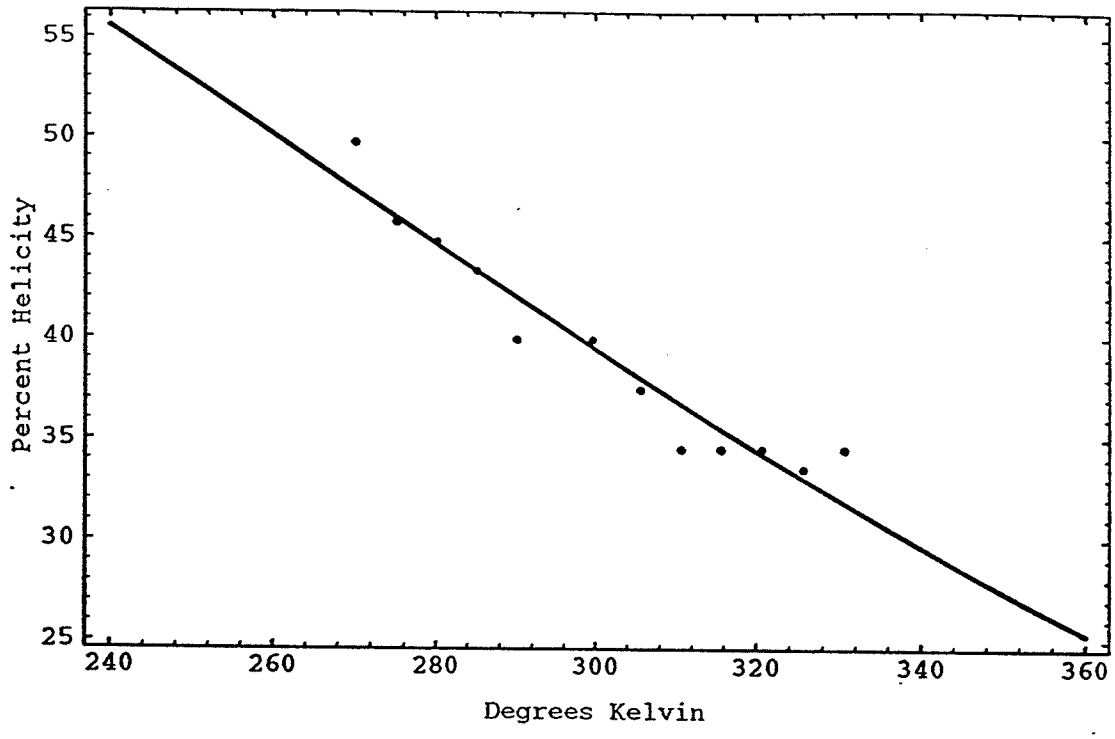
Percent Helicity
55
50
45
40
35
30
25
240
260
280
300
320
340
360
Degrees Kelvin

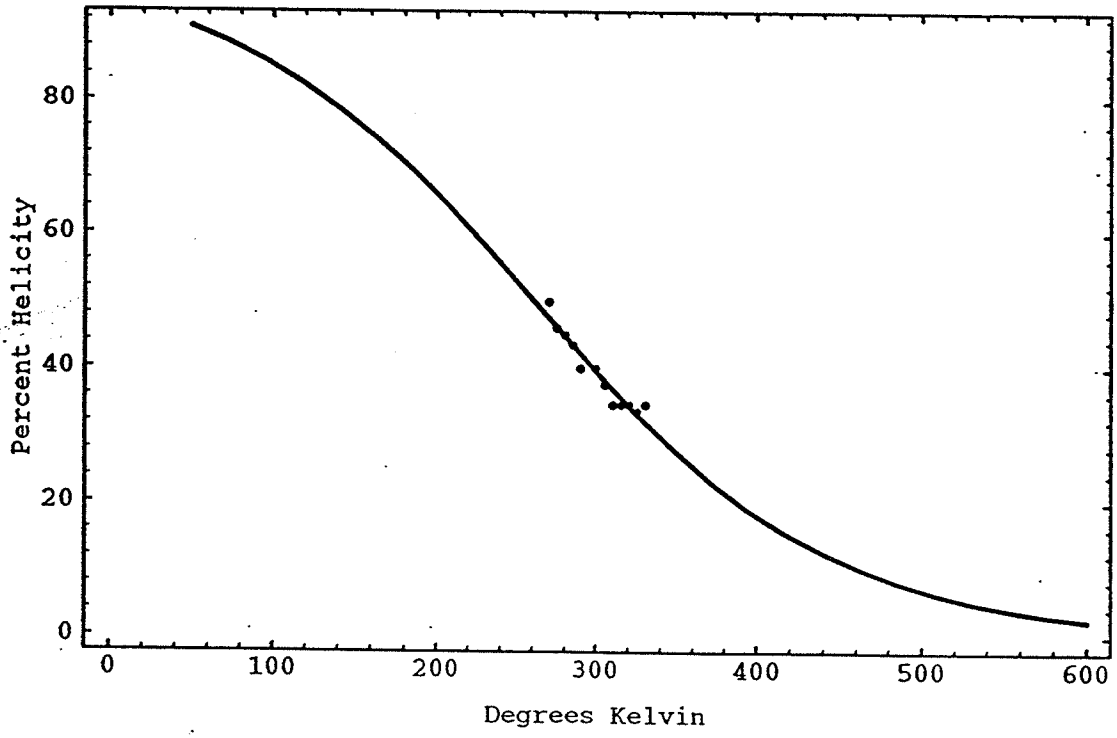
Percent Helicity
80
60
40
20
0
0
100
200
300
400
500
600
Degrees Kelvin

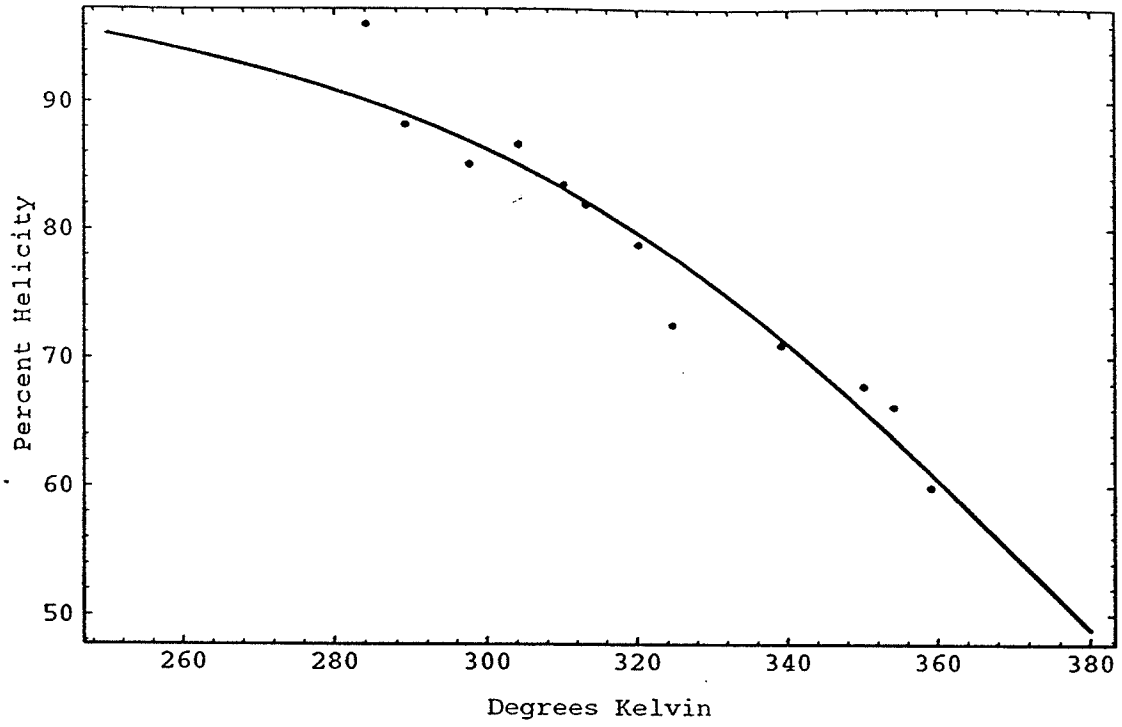
Percent Helicity
90
80
70
60
50
260
280
300
320
340
360
380
Degrees Kelvin

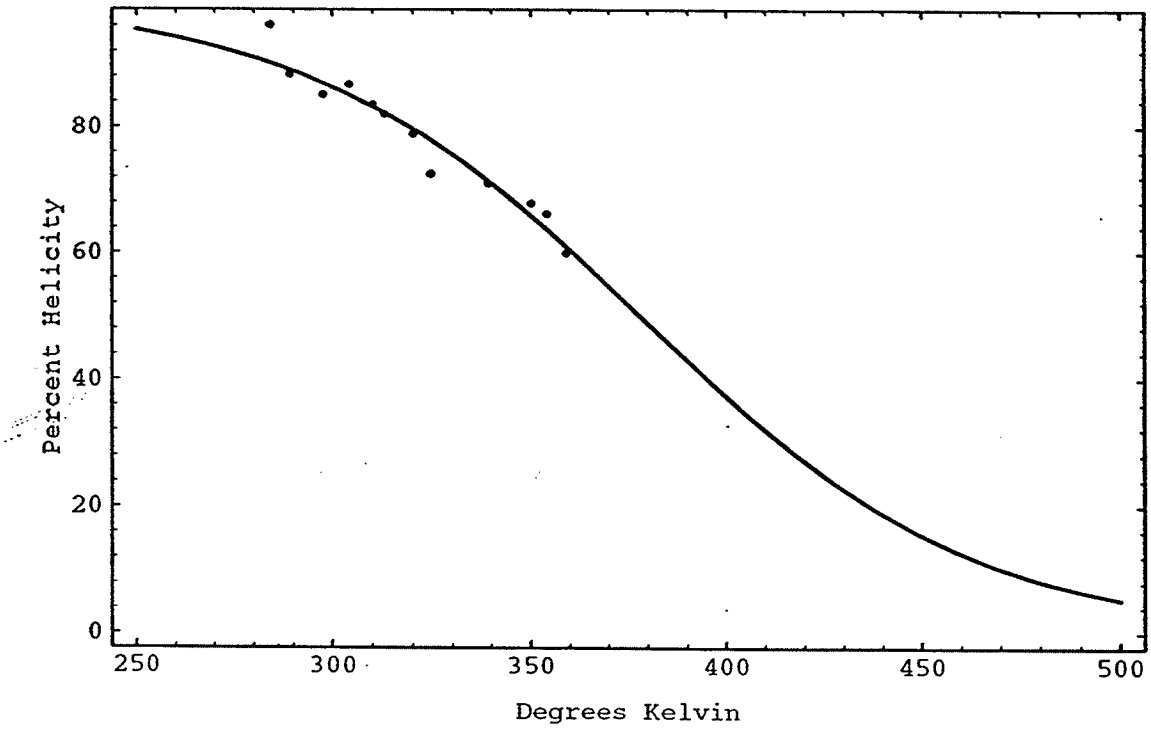
Percent Helicity
80
60
40
20
0
250
300
350
400
450
500
Degrees Kelvin

3.3.2 NMR EXPERIMENTS

^{15}N-labelled alamethicin was studied on the 500 MHz NMR spectrometer. A temperature experiment was carried out to study the temperature-dependence of the amide protons of alamethicin. Figure 20 shows a typical ^{1}H spin-echo difference NMR spectrum of the amide region of ^{15}N-labelled alamethicin. the positive peaks belong to protons directly attached to ^{15}N atoms. The negative peaks belong to protons directly attached to other atoms such as ^{12}C. The chemical shift of each alpha proton was determined at each temperature used. These chemical shifts are shown in Appendix C. Figure 21shows the slopes of the chemical shifts of (a) the backbone amide protons and (b) the glutamine side-chain amide protons.

For an explanation of the interpretation of the meaning of the magnitude of the slopes, see the Introduction (Basu et al., 1991). The $\Delta\delta/\Delta T$ values for the side-chain amides and that of the Aib-1 backbone amide are the largest (-5.3 to -6.4 ppb/deg), suggesting that these protons are not involved in intramolecular hydrogen bonds. The slopes of the backbone amides of the portion of the molecule from Aib-8 to Aib-13 range from -3 to -4.5 ppb/deg which suggest that the protons are weakly hydrogen bonded in the middle of the alamethicin molecule. A stronger H-bonded state is indicated by the range of slopes (-2 to -3 ppb/deg) shown by the amide protons of residues Aib-5 to Gln-7 and Aib-16 to Pho-20. The two residues following both Pro-2 and Pro-14

(Aib-3 and Ala-4, and Aib-15 and Val-16, respectively) have slopes ≥ -1.3 ppb/deg. In fact, Aib-3 and Ala-4 have positive slopes. The size of these slopes suggest involvement of the amide protons in strong intramolecular H-bonds.

Figure 20: The spectrum showing the amide proton region of alamethicin acquired with the 500 MHz spectrometer

Alamethicin N-15 Labelled at 295K

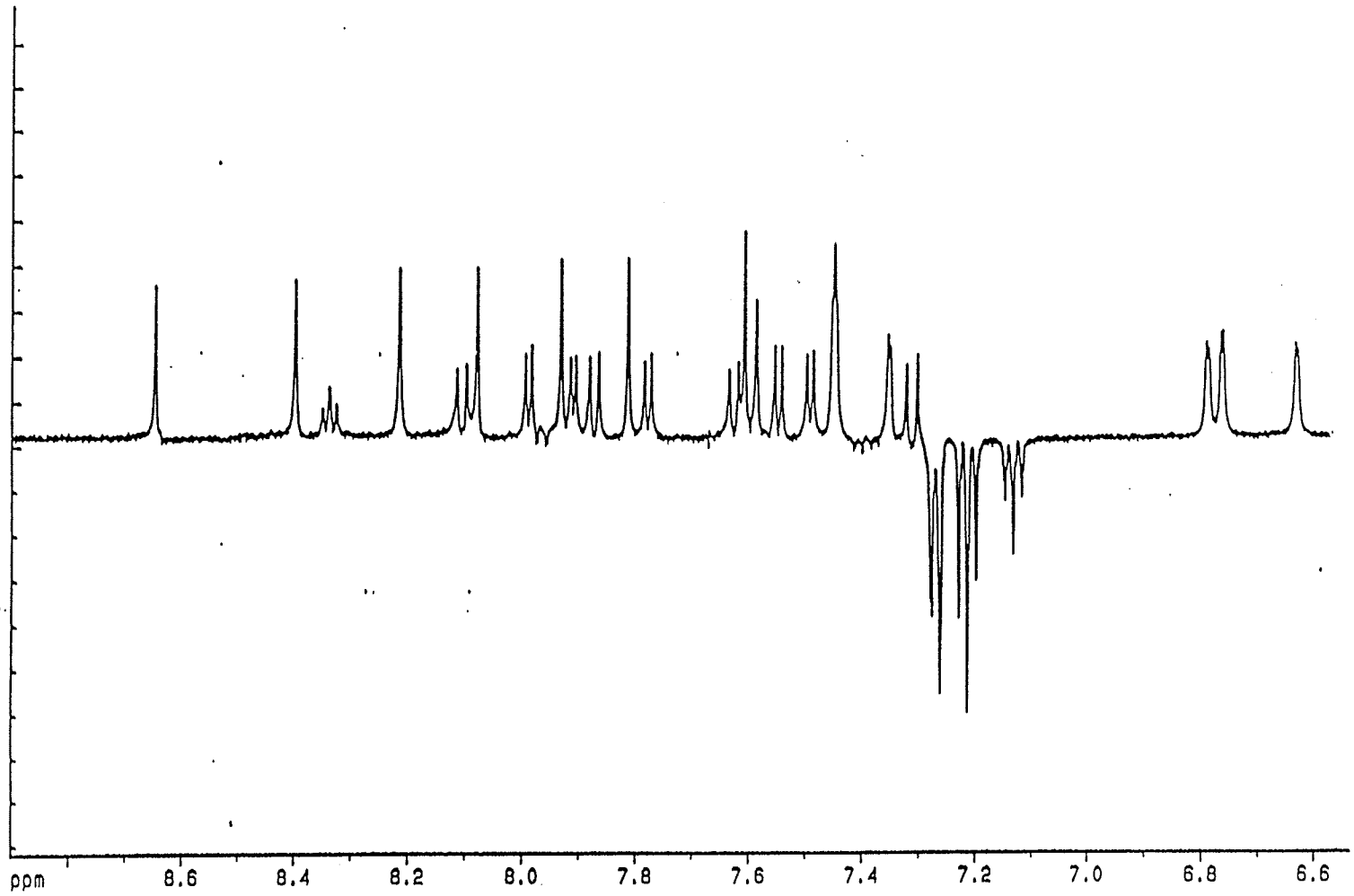

Figure 21: The slopes of the chemical shift changes of the (a) amide protons and (b) glutamines side-chain protons of alamethicin.

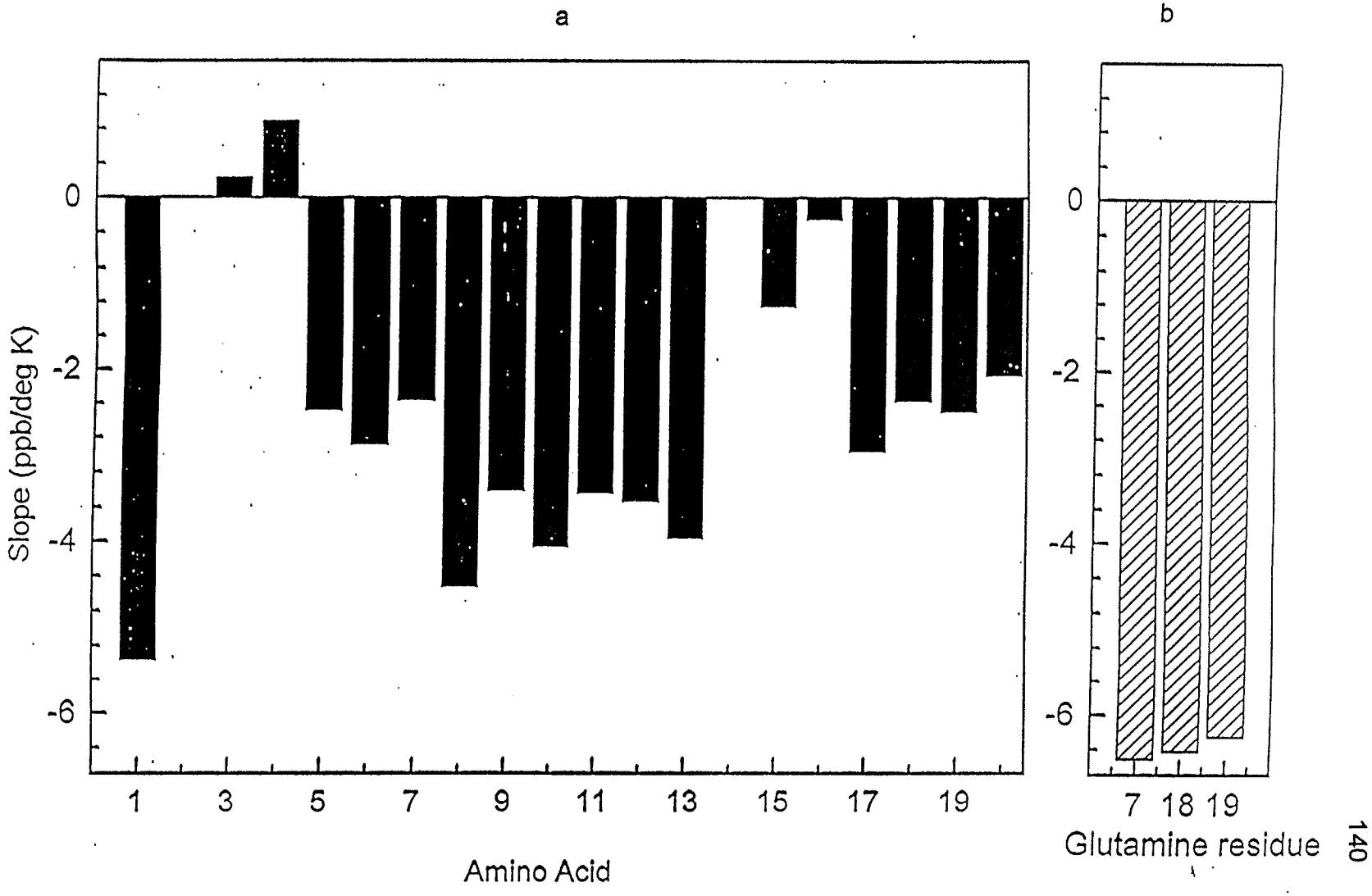
a
b
0
-2
-4
-6
Slope (ppb/deg K)
1
3
5
7
9
11
13
15
17
19
Amino Acid
7
18
19
Glutamine residue

CHAPTER 4

DISCUSSION

4.1 Physical Properties of RBP-1

4.1.1 SOLUBILITY OF RBP-1

Initially, attempts were made to dissolve the synthetic peptide RBP-1 in several solvents to sufficient concentrations for structural studies using NMR. These efforts were unsuccessful in obtaining samples for NMR experiments. The peptide proved to have very low solubility in numerous organic solvents, as well as in pure H_2O and detergent solutions. Such a finding was perplexing, in light of the fact that the peptide is a very close analog of the natural fungal peptide alamethicin (see **Introduction**). Alamethicin had been shown to be quite soluble in methanol (Yee and O'Neil, 1992) and in SDS solution (Yee, unpublished results). This suggested the possibility that the peptide sample contained impurities which lowered its solubility or that the peptide did not match the sequence submitted for synthesis. In order to verify the sequence and the presence or absence of impurities, a small amount of sample was provided to the Physics Department for mass spectral analysis. The molecular weight and parts of the sequence were determined to match the expected amino acid sequence. Also, the mass spectrum (see Figure 4 in **Results**) appeared to be free of any substantial contamination.

Since the mass spectral analysis verifies the identity of the peptide, the question of the solubility problems remains to be answered. One explanation for RBP-1's low solubility in polar organic solvents may lie in the amino acid sequence in some way. The sequence shows the peptide to be extremely hydrophobic. However, this does not explain the low solubility in organic solvents, such as chloroform and CCl_4. RBP-1 should prefer to be dissolved in these non-polar solvents if hydrophobicity is the main criterion. The sequence of the natural counterpart, alamethicin, would appear somewhat more hydrophobic due to the structure of the Aib residues, and alamethicin is also substantially soluble in several organic solvents. However, RBP-1 showed only limited solubility in several alcohols (see Table 1), whereas alamethicin is quite soluble. Possibly, the amino acid residues of the synthetic peptide are arranged in some way which lowers its solubility. That alamethicin is significantly more soluble than RBP-1 in several alcohols may be due to the strong helix-inducing capacities of the Aib residues. Formation of a helix might be expected to increase the polarity of a peptide due to the partial "burial" of hydrophobic residues and due to the formation of a helix macrodipole. Our CD results suggest that RBP-1 adopts a significantly less ordered conformation in methanol and ethanol than does alamethicin. Exposed hydrophobic residues in a predominantly random coil structure may be the reason why the peptide is so insoluble in alcohols. However, we observe only small increases in solubility in both TFE and SDS which, despite the large increase in helix content in those

solvents, suggests that other factors may play a role in the solubility of the peptide.

4.1.2 UV ABSORPTION CHARACTERISTICS OF RBP-1

Due to its lack of complete solubility at suitable levels in all solvents, determination of the concentration of RBP-1 in experimental solutions by weight of peptide added was not possible. The small amount of peptide sample available made it necessary to use a non-destructive UV absorption method to calculate the concentrations. An extinction coefficient was calculated using values obtained from the literature as described in the **Methods**. The derived value was used to determine the solution concentrations of RBP-1.

The existence of any temperature dependence of the absorption spectra of RBP-1 was also tested by recording the spectrum of a solution of RBP-1 in methanol at three distinct temperatures. All three spectra displayed only minor differences in wavelength of maximum absorbance and maximum absorbance values (see Figure 8, **Results**).

In general, the absorption characteristics of the peptide agreed with expectations from the literature. The maxima observed in the different solvents was within the range of wavelengths given for peptides or amino acids in the literature (195 - 209 nm). Temperature and solvent did not show any significant effect on the spectra of the peptide solutions. Noticeable changes would have suggested a structural change or a chemical reaction occurring between the

peptide and solvent.

4.2 CD Spectroscopic Findings for RBP-1

4.2.1 GENERAL COMMENTS ON THE CD RESULTS

Circular dichroism spectroscopy is a powerful tool for semi-quantitative assessment of the secondary structural properties of biological molecules, as described in the **Introduction**. It is very easy to determine what the major secondary structural component of a protein or peptide is by obtaining its CD spectrum in the range 240 to 190 nm. This region contains the wavelengths in which the major transitions of the peptide bonds of the molecule occur.

From the shapes of the CD spectra of RBP-1 in methanol, ethanol, TFE, and SDS (at "room temperature", for example), it is obvious that the α-helix is the predominant secondary structure existing in the peptide in all the solvents. The strong peaks at 222 and 208 nm are very characteristic of the α-helix.

Similarly, the CD spectra of alamethicin in methanol and SDS also show a large α-helical component. An interesting note may be made, for alamethicin in SDS, that the intensities of the two extrema for the helix structure are reversed in comparison to the spectra for RBP-1 in SDS as well as for RBP-1 and alamethicin in organic solvents. This has been observed in studies of alamethicin in lipid membranes (Vogel, 1987; Woolley and Wallace, 1993). This reversal of the intensities of the two peaks has been attributed to peptide-

peptide interactions such as formation of two-stranded coiled-coil conformations (Woolley and Wallace, 1993). This coiled-coil conformation causes distortions in the backbone conformations of the alamethicin molecules which produce shifts and increases (or decreases) in the intensities of the transitions.

If one assumes that the difference in shape between the spectra of alamethicin in SDS and RBP-1 in SDS is a result of peptide-peptide interactions within the SDS micelles, then there must be a reason why this effect is only observed for alamethicin and not its very similar synthetic analog. The only fact that stands out is the Aib content of alamethicin. Perhaps the presence of Aib residues directly stabilizes interactions between peptide helices, while alanine residues in the analog do not provide sufficient stabilization for long-lasting, strong peptide-peptide interactions. Another possibility is that the Aib residues stabilize helical structure and that the helices interact, perhaps via their macrodipoles. The less helical alanine-based RBP-1 peptides would interact to a smaller extent because they are less helical.

It is also quite apparent that the shapes of the spectra of RBP-1 in water do not indicate any significant helical content (see Figure11 in **Results**). The spectrum, even at low temperatures, does not possess the characteristic double minima denoting a helical structure. It does correspond nearly exactly with the shape found for samples of disordered peptides.

Observation of the shapes of the CD spectra for the two peptides studied qualitatively informs an observer that a helical conformation is common to both

in solvents other than pure water. This does not give any numerical value to the amount of secondary structure possessed by the peptides in the different solvents. Such information requires more detailed analysis of the individual spectra based upon the calculated ellipticities.

4.2.2 HELIX CONTENT CALCULATED USING EQUATION 4

The amount of helix content (%) in the peptide at each assay temperature in each solvent was calculated using Equation 4 (see **Results**). This equation was obtained from the literature and although it was initially designed for use with large proteins, a good idea of the extent of the helix structure was obtained in the present study. Therefore, the absolute accuracy of the values that were calculated is not certain, but a good idea of the extent of helix structure is obtained. For RBP-1, the helix content ranges from 16.5% in methanol, to 33.4% in ethanol, to 68.4% in TFE. The helicogenic strengths of the organic solvent are made plain, with the helix content slightly more than doubling as the progression is made from methanol to TFE. This agrees with previous ideas regarding the solvents' strengths; as well, in SDS, RBP-1 has 86.6% helicity which attests to the high helicogenicity of SDS. Similar results were obtained using an equation derived for small peptides (see **Equation 5**).

Helix content in alamethicin was analyzed in the same manner as for RBP-1. Using Equation 4, the helix content (maximum) in methanol was about 49%, approximately 3 times the value for RBP-1 in methanol. The percentage

in SDS was 100% at the maximum ellipticity displayed, somewhat higher than the highest value for RBP-1 in SDS (see **Appendix A**). Application of Equation 5 gave more reasonable values for the helix contents particularly of the peptides dissolved in SDS but in general the two methods were in close agreement. These values enable one to see clearly how the solvent may be a crucial factor in determining how much and what type of secondary structure a short peptide can attain. The percentages do not indicate which residues of the peptide sequence fold into the helical state. Other techniques which can provide more detailed conformational information, such as NMR, must be used to determine this. Analysis of the individual amino acids in the sequence, with respect to helix propensities, can be done to speculate on which segments of the sequence are likely to be helical (Padmanabhan et al., 1990).

4.2.3 HELIX CONTENT CALCULATED BY THE CCA PROGRAM

Another method was used to determine the percentage of secondary structural components found in RBP-1 in different solvents. The CCA method deconvoluted the experimental CD spectra into their individual components of pure secondary structure and assigned percentages to each component. Analyses were performed assuming 2, 3, 4, or 5 pure components to each spectrum. For a peptide the length of RBP-1, it does not seem likely that more than two different secondary structural types could exist in such a short span. Therefore, only two-component analysis results were considered plausible for

RBP-1. The CCA results for RBP-1 in the solvents at the two-component level showed some differences from the simple treatment of the data by equations 4 and 5. The CCA results are shown in Appendix B. From CCA, the helix content in methanol was much higher than that calculated by the simple equations. In ethanol and TFE, the helical percentages were lower and in ethanol the peptide was shown to have a higher helical content. In SDS, the CCA analysis of RBP-1 reported that the helix content was 100% at nearly all temperatures, despite the fact that the ellipticities clearly decreased as the temperature increased.

A problem in using CCA to analyze short peptides like RBP-1 and alamethicin is the fact that the CCA method is based upon larger proteins and thus may attempt to force the experimental data to contain more than 2 pure components. Our conclusion is that CCA was not useful in the analysis of secondary structure in the two peptides studied.

4.3 Solvent and Sequence Effects on Structure

4.3.1 SOLVENT EFFECTS ON STRUCTURE OBSERVED BY CD ANALYSIS

Examination of the CD spectra of RBP-1 and alamethicin in different solvents and comparison of the spectra of the two peptides shows that there are significant, measurable effects on their secondary structures depending on the solvent used.

The observed maximum ellipticity values, which correlate closely with the

helix content for RBP-1 in methanol, ethanol, TFE, and SDS, are significantly different even at similar low temperatures (see Table 4). The value of the maximum amount of ellipticity attained by RBP-1 increases on going from methanol to ethanol then to TFE and finally to SDS. The large differences in ellipticities suggest again that the different solvents possess different abilities to promote or stabilize the formation of helical secondary structure.

These results agree with the literature about the helicogenic strengths of organic alcohols. Since only the solvent was a differing factor among the temperature titrations, the reason for the variation in behaviour of the peptides in response to temperature must lie in the peptides' interactions with the solvent. The literature in this area suggests that simple alcohols like methanol and ethanol are only weakly helicogenic. This is supported by the comparatively low helicities induced in RBP-1 by these agents with respect to TFE and SDS. Methanol displays a lower helicogenicity than ethanol, as evidenced by the lower helical content of RBP-1 in methanol as opposed to ethanol. This can be rationalized using the chain-length dependence described in the literature. As methanol is the smallest alcohol, it may not interact via non-polar interactions as strongly with the peptide as would a longer chain alcohol. The helix formed by the peptide in methanol may be "loosely wound" and may form somewhat stronger solute-solvent hydrogen bonds, thus weakening the helix. Ethanol is one carbon longer than methanol, so perhaps this causes the solute-solvent non-polar interactions to be stronger than in

methanol. In this case, the hydrogen bonding interactions between the peptide and solvent might be weaker than in methanol, thus stabilizing intramolecular hydrogen bonds and helix fractions.

Halogenated alcohols are some of the strongest helix-promoting organic liquids known and TFE has the strongest helicogenic character of the organic solvents tested on RPB -1 as confirmed by the differences in ellipticities. A possible explanation for this are the differences in hydrogen bond acceptor abilities of the alcohols. TFE is a much weaker hydrogen bond acceptor than water (and non-halogenated alcohols). In aqueous solution, the amide protons are strongly attracted to the oxygens of the water molecules. When TFE is added to a peptide solution, or is the primary solvent, it lowers the solvent's competitiveness for the available amide protons of the peptide backbone in comparison to the carbonyl oxygens (see **Introduction**).Therefore, in a solvent like TFE, intramolecular hydrogen bonds between the amide protons and carbonyl oxygens of the peptide backbone are strongly favoured. This means that the helical conformation is favoured.

The ellipticity value at -5° C in TFE is significantly less negative than the value for SDS at 26.5° C. With all solvents, the ellipticity of the peptide at lower temperatures is greater than at elevated ones, yet in SDS at a much higher temperature the peptide still possesses the greatest ellipticity. This shows that SDS is possibly the helicogenic agent that we used for protein structural study. An explanation for this helicogenicity can be proposed that is quite similar to

that for the effect of TFE. SDS forms micelles above certain critical concentrations and the non-polar, oily hydrocarbon interior of the micelle excludes water completely. Thus, at the micelle/peptide interface, intramolecular hydrogen bond formation is essentially the only hydrogen bonding scheme available due to the absence of water. This promotes formation of a helical structure.

In water, RBP-1 shows essentially no helical character. Rather, it possesses an unordered structure. This may also be due in part to the effect of the solvent. Water is a very strong hydrogen bond acceptor, while the amide groups of the peptide backbone are strong proton donors. Possibly, the solvent molecules compete more successfully for the amide protons than the carbonyl oxygens of the backbone. Intermolecular hydrogen bonds may be predominant in aqueous solutions and the extended conformation of the peptide would be favoured.

4.3.2 SEQUENCE EFFECTS ON THE PEPTIDES' STRUCTURES

The CD titrations of the two peptides reveal definite sequence effects on the secondary structural contents. Both RBP-1 and alamethicin were studied in methanol and SDS by circular dichroism temperature titrations.
In these experiments, only the sequences of the peptides were important differences. It can be seen from the CD results that the structures of the two peptides are significantly different under similar conditions.

The probable explanation for this is the difference in amino acid content of the two peptides. Alamethicin contains eight Aib residues, whereas RBP-1 has alanines in place of the Aibs. In methanol, alamethicin possesses more than twice the ellipticity and therefore twice the helical content of RBP-1 in methanol. This indicates very clearly that the Aib residues play a prominent role in determining the formation of secondary structure in peptides. Aib has been shown to have a high helical propensity when compared with alanine and this is evident from comparison of the results of the methanol and SDS titrations of each peptide.

Differences in the maximum ellipticity values of RBP-1 and alamethicin in SDS are not as striking, but still are significant. RBP-1 melts at a slightly lower temperature than alamethicin.

These observations show that secondary structure attained by peptides is influenced strongly by amino acid content, as well as by solvent.
Alanine is reported to have the strongest helix propensity of the common amino acids, but the present results show that it is much less helix-promoting than the Aib residue.

In addition to amino acid content, the sequence of the amino acids in a peptide can have important effects on the structure. This is shown by the structure, or lack of structure of RBP-1 in water. In water, the peptide is unordered. This may be explained in part by the effect of water as the solvent as discussed in the previous section, but the sequence of the peptide likely

contributes to the lack of ordered structure as well. RBP-1 (and alamethicin, also) has a glycine residue at position 11 and a proline at position 14. Proline is also present at position 2. Both types of residue are well known to be disruptive to helices, glycine because of its flexibility and proline due to its ring structure (see **Introduction**). The presence of these two helix-breakers in approximately the middle of the peptide would strongly disrupt helix formation in the peptides. The proline near the beginning hinders formation of helical structure in this part of the sequence, as well. This sequence effect combines with the solvent effect present in aqueous solution to prevent secondary structure formation in water.

4.4 Curve Fitting the Temperature Titrations

4.41 RBP-1 FITTING RESULTS

Examination of the temperature tritration curves in Figure 10 shows that temperature induced transitions from the more helical to the less helical form that was more or less linear for RBP-1 in ethanol, TFE, and SDS. Such linearity suggests that the denaturation of the peptide in these solvents is a relatively non-cooperative process.

To quantify the cooperativity, the CD temperature titration results were fit to Equation 6 assuming a two state helix/coil transition. This fitting procedure determined values for the midpoints, T_m, of the helix/coil transitions of the two peptides in each solvent. The widths of the transitions, ΔT, in degrees Kelvin

were also determined where ΔT corresponds to the temperature over which 80% of the transition occurs. For RBP-1, the T_m values ranged from 128 K in methanol to 349 K in SDS (see Table 5, **Results**) and followed the same order as the calculated maximum helicities (Table 4). A rationale for this result can be made in terms of the helicogenicity of the solvents used. Methanol is the weakest helicogenic solvent, while SDS promotes secondary structure formation most strongly. Thus, the stronger helicogenicity of the solvent the higher the melting point of the helix.

Interestingly, the widths of the transitions range from 169 to 493 K. The widths of the transitions are a measure of their cooperativity; the wider transitions are less cooperative, the narrower transitions indicative of more highly cooperative folding. The narrowest transition, that observed in SDS, is about twice as wide as the transition observed in helical Ala-based peptides in water (Shalongo et al., 1994). Because the transitions appear to occur over such a wide temperature range it is not certain that a true helix/coil two state model is appropriate to all the data. One diagnostic of a 2-state transition is the identification of an isodichroic point at 202 nm in the superimposed CD spectra from a temperature titration (Scholz et al., 1991). Unfortunately, due to the noise in our spectra at low wavelengths, the absence or presence of isodichroic points is unclear (see Table 4). Nevertheless, we can conclude that solvents can have a dramatic effect on the cooperativity of the transitions. Due to the large temperature ranges over which the transitions occur, the temperature

ranges of the titrations performed would have to be much larger than those actually used in order to observe both the beginnings and ends of the transitions. Temperatures such as those that would be necessary to observe sigmoidal transitions are not practical considering the solvents and equipment used. The apparent sigmoidal transition seen in methanol with RBP-1 may be due experimental error but in any case is not presently explainable.

4.4.2 ALAMETHICIN FITTING RESULTS

For alamethicin in methanol, the midpoint of the helix/coil transition was determined to be 261 K. This is much higher than the value for RBP-1 in methanol (128), which reflects the much greater helix-promoting character of the Aib residues. Thus, the alamethicin helix formed is much stronger than the RBP-1 helix in methanol. The width of the transition is less than that of RBP-1, which may also indicate the helix-promoting qualities of the Aibs. In SDS, the midpoints and widths of the transitions of the two peptides are very similar, but indicate a slightly more stable helix in alamethicin than in RBP-1. Thus, the solvent has almost entirely overcome the poorer helical propensities of the Ala residues in RBP-1 compared to the Aibs in alamethicin.

4.5 NMR Determination of Alamethicin Chemical Shift Temperature Dependence

The CD spectrum of alamethicin in methanol suggests that the peptide is about 50% helical at the lowest temperature studied. One possibility is that residues 1-11 are helical and 12-20 are unfolded. Another possibility is that the middle 10 residues are α-helical whereas 5 residues at each end are unfolded i.e. the helix is "frayed" at the ends. To examine which parts of the molecule are helical and which are not we used ^{1}H NMR spectroscopy.

The temperature-dependence of the chemical shifts of the amide protons of residues in alamethicin were studied on the 500 MHz NMR spectrometer. The magnitude of the chemical shift changes indicate if the residue is possibly involved in a hydrogen bond. Such participation in an H-bond is indicative that the residue is a part of a secondary structure. The results of this determination can be seen in Figure 19 in the **Results**.

This figure suggests that the majority of residues in the peptide are involved in hydrogen bonding to a moderate to strong degree. The amide of residue 1 and the two prolines, which lack amide resonances, are the only residues which do not participate in hydrogen bonding. This suggests that the greater part of the alamethicin sequence is in some form of ordered secondary structure, probably a helical conformation. The weakened secondary structure in the middle of the molecule is probably indicative of flexibility in the molecule at Gly-11. The flexibility in this region is likely the reason why the average

helicity measured by CD is only about 50%. Thus, in contrast to many alanine-based peptides the ends of the molecule are more stably folded than the middle.

CHAPTER 5

CONCLUSIONS

There are a number of conclusions that may be drawn from the findings of this research project. The goal of the research was to assess the influences of the Aib residue on the secondary structure of short peptides. This information was to be obtained from a comparison of the characteristics of the Aib-containing peptide alamethicin and the synthetic peptide RBP-1 containing alanine in place of Aib. From the CD spectra and analyses of the CD temperature titrations, there are some interesting results which can be commented upon.

The contrast in the shapes of the CD spectra of the two peptides in SDS merits a comment. The intensities of the two minima at 222-4 nm and 208-10 nm appear to be reversed for alamethicin in comparison to RBP-1. The probable reason for this is the presence of Aib residues in alamethicin. These residues must stabilize some type of interaction between the helical structures in two neighboring alamethicin molecules.

The maximum ellipticity values and the determination of the helix content of each peptide further supports the structural influences of the Aib residue. In methanol solution, the maximum mean residue ellipticity attained by RBP-1 was -7297 $deg \cdot cm^2 \cdot dmol^{-1}$ whereas alamethicin has a maximum value of -17048 $deg \cdot cm^2 \cdot dmol^{-1}$ in the same solvent. This indicates that alamethicin has more than two times the degree of secondary structure in methanol than its non-Aib

containing analog.

In SDS, the differences between the effects on RBP-1 and alamethicin are not quite as striking but they are still definite. The maximum ellipticity values possessed by each peptide are still significantly different even after taking into account the difference in temperature range examined. The percentage helix calculated for each peptide is very high, with slightly higher values being ascribed to alamethicin in SDS.

These findings clearly suggest that α-aminoisobutyric acid has a much greater ability to promote or enhance helical structures in short peptides than Ala. This is entirely in agreement with the literature which gives Aib a very strong helix propensity. The results described suggest that Aib has roughly two and a half to three times the helix propensity of the alanine residue in organic solvent. From these results, it may be said with some confidence that Aib may be a useful residue in the field of protein engineering for assisting in the formation of helical segments in synthetic or modified natural proteins.

It is interesting to note that some of the findings of this research is in disagreement with some published results of a study involving a synthetic peptide of identical sequence. In 1989, analogs of alamethicin in which Aib residues were substituted with alanines (A1) or leucines (L1) were studied by Molle et al. by infrared and CD spectroscopy to study ionophore activity. This group states that the leucine analog was predominantly α-helical in the solvents used, while the alanine analog underwent a solvent-induced

transconformation to β-structure. In hexafluoro-2-propanol/methanol, the A1 peptide displayed α-helical character according to IR and CD studies. Changing the solvent to HF2P alone or methanol/water (1/1) induced a conformational change to a structure with as much β-structural character as α-helical character. These results are in conflict with my research findings which indicate that the alanine-containing analog is primarily α-helical in the three organic solvents used for CD study, and a random coil in water.

Future Research Avenues

Several possibilities for future research involving this peptide exist. Circular dichroism has been employed to deduce the probable secondary structure of RBP-1 in different solvents. These findings should be supported and augmented, particularly in a quantitative sense, by other techniques. Attempts to examine the peptide in solution by NMR could be resumed, using a larger range of solvents and conditions to solubilize the peptide. Other techniques such as X-ray crystallography could potentially be used to provide some detailed structural information.

The seeming insolubility of this peptide offers some intriguing research possibilities. Much more detailed work could be done to try to explain the relative insolubility of RBP-1 in the solvents tried where current information and established facts indicate that there should be no solublity problems. Additional solvents and conditions could be utilized to overcome or at least gauge the scope of this insolubility. Mixtures of solvents in different proportions could be used to try to dissolve the peptide. Conditions such as solvent pH may be examined to determine if there is any pH-dependence underlying the low solubility. (The peptide sequence suggests that there should be no significant effect of pH, however.)

The circular dichroism studies could be continued and extended by using different solvents or mixtures of the solvents previously used. The temperature titrations of the peptide conformation could be done in more detail with greater

temperature ranges used for some solvents than previously studied.

In order to make NMR study of the analog more feasible, a new peptide with more charged residues, but with still nearly the same sequence could be obtained. A slightly different peptide may prove to be more tractable and suitable solutions for NMR studies could be made.

Also, the study of alamethicin by CD could be taken further. CD temperature titrations in organic solvents other than methanol could be done to directly compare Aib-enhanced helicity with the helicity of RBP-1. A determination of the helicity (%) attained by the peptide requires more in depth analysis of the spectra for RBP-1 in each solvent over the temperature range considered. Performing a titration of alamethicin in water could be interesting, with respect to the results for the analog in water. Perhaps the Aib content of alamethicin would "force" the peptide to attain a much more helical structure in water than RBP-1 possesses.

Another avenues for future research might be to replace the protein CD basis spectra in the CCA program with the spectra of peptides of secondary structure known from NMR or X-ray diffraction. This might make the program more reliable for the analysis of small peptides than it currently is.

References

Adler, A. J., Greenfield, N. J. and Fasman, G. D. (1973) Methods in Enzymology **27**, 675-735.

Aléman, C. (1994) Biopolymers **34**, 841-847.

Anfinsen, C. B., Haber, E., Sela, M. and White, F.H. (1961) Proc. Natl. Acad. Sci. USA **47**, 1309-1314.

Arkawa, T. and Goddette, D. (1985) Archives of Biochemistry and Biophysics **240**, 21-32.

Bai, Y. and Englander, S. W. (1994) PROTEINS: Structure, Function, and Genetics **18**, 262-266.

Bairaktari, E., Mierke, D. F., Mammi, S. and Peggion, E. (1990) Biochemistry **29**, 10090-10096.

Basu, G., Bagchi, K. and Kuki, A. (1991). Biopolymers **31**, 1763-1774.

Beychok, S. (1966) Biochemistry **154**, 1288-1298.

Bierzynski, A., Kim, P. S. and Baldwin, R. L. (1982) Proc. Natl. Acad. Sci. USA **79**, 2470-2474.

Blaber, M., Zhang, X-j., and Matthews, B.W. (1993) Science **260**, 16371640.

Buck, M., Radford, S. E., and Dobson, C. M. (1993) Biochemistry **32**, 669-678.

Bundi, A. and Wuthrich, K. (1979) Biopolymers **18**, 285-297.

Cantor, C. R. and Schimmel, P. H. (1980) in Biophysical Chemistry Vol. III: The Behavior of Biological Macromolecules.

Carver, J. A. and Collins, J. G. (1990) Eur. J. Biochem.**25**, 645-650

Chakrabarrty, A., Schellman, J. A. and Baldwin, R. L. (1991) Nature **361**, 586-588.

Chou, P. Y. and Fasman, G. D. (1973) Biochemistry **13**, 211-222.

Chou, P. Y. and Fasman, G. D. (1978) Ann. Rev. Biochem. **47**, 251-276.

Dearborn D. G. and Wetlaufer, D. B. (1970) Biochem. Biophys. Res. Comm. **39**, 314-320.

Dyson, H. J. and Wright, P. E. (1991) Annu. Rev. Biophys. Biophs. Chem. **20**, 519-538.

Fasman, G. D., Hoving, H. and Timasheff, S. N. (1970) Biochemistry **9**, 3316-3324.

Fasman, G. D., Lindblow, C. and Bodenheimer, E. (1964) Biochemistry **3**, 155-166.

Fox, A. O. Jr. and Richards, F. M. (1982) Nature **300**, 325-330.

Greenfield, N. and Fasman, G. D. (1969) Biochemistry **10**, 4108-4115.

Gans, P. J., Lyu, P. C., Manning, M. C., Woody, R. W. and Kallenbach, N. R. (1991) Biopolymers **31**, 1605-1614.

Garel, J-R. and Baldwin, R. L. (1973) Proc. Natl. Acad. Sci. USA **70**, 3347-3351.

Gratzer, W. B. and Cowburn, D. A. (1969) Nature **222**, 426-431.

Hennessey, J. P. and Johnson Jr., W. C. (1981) Biochemistry 20, 1085-1094.

Hermans Jr., J., Anderson, A. G. and Yun, R. H. (1992) Biochemistry **31**, 5646-5653.

Holzwarth, G. and Doty, P. (1965) J. Amer. Chem. Soc. **87**, 218-220.

Igou, D. K., Lo, J-T., Clark, D. S., Mattia, W. L. and younathan, E. S. (1974) Biochem. Biophys. Res. Comm. **60**, 140-146.

Jackson, M. and Mantsch, H.H. (1992). Biochimica et Biophysica Acta **1118**, 139-143.

Johnson, W. C. Jr. (1988) Ann. Rev. Biophys. Biophys. Chem. **17**145-166.

Kabsch, W. and Sander, C. (1984) Proc. Natl. Acad. Sci. USA **81**, 1075-1078.

Karle, I. L., Flippen-Anderson, J. L., Uma, K., Balaram, H. and Balaram, P. (1987) Proc. Natl. Acad. Sci. USA **84**, 5087-5091.

Karle, I. L. and Balaram, P. (1990) Biochemistry **29**, 6747- 6756.

Kim, C. A. and Berg, J. M. (1993) Nature **362**, 267-270.

Kim, P. S. and Baldwin, R. L. (1984) Nature **307**, 329-334.

Lehrman, S.R., Tuls, J.L., and Lund, M. (1990). Biochemistry **29**, 5590-5596.

Lifson, S. and Roig, A. (1961) J. Chem. Phys. **34**, 1963-1974.

Llinas, M. and Klein, I. M. P. (1975) J. Am. Chem. Soc. **97**, 4731-4737.

Lustig, B. and Fink, A.L. (1992). Biochimica et Biophysica Acta **1119**, 205-210.

Lyu, P. C., Sherman, Chen, A. and Kallenbach, N. R. (1991) Proc. Natl. Acad. Sci. USA **88**, 5317-5320.

Madison, V. and Schellman, J. (1972) Biopolymers **11**, 1041-1076.

Marqusee, S., Robbins, V.H. and Baldwin, R.L. (1987). Proc. Natl. Acad. Sci. USA **84**, 8898-8902.

Marshall, G.R., Hodgkin, E.E., Langs, D.A., Smith, G.D., Zabrocki, J. and Leplawy, M.T. (1990). Proc. Natl. Acad. Sci. USA **87**, 487-491.

Marshall, G. R. and Bosshard, H. E. (1972) Circl. Res. **30/31**, 143-150.

Mayr, W., Oekonomopulos, R. and Jung, G. (1979) Biopolymers **18**, 425-450.

Merutka, G., Lipton, W., Shalongo, W., Park, S.-H. and Stellewagen, E. (1990). Biochemistry **29**, 7511-7515.

Merutka, G. and Stellewagen, E. (1989) Biochemistry **28**, 352-357.

Merutka, G. and Stellewagen, E. (1990). Biochemistry **29**, 894-898.

Miick, S.M., Martinez, G.V., Fiori, W.R., Todd, A.P. and Millhauser, G.L. (1992). Nature **359**, 653-655.

Minor, D. L. Jr. and Kim, P. S. (1994) Nature **371**, 264-267.

Molle, G., Duclohier, H., Dugast, J.-Y. and Spach, G. (1989). Biopolymers **28**, 273-83.

Myer, Y. P. (1985) Current Topics in Bioenergetics **14**, 149-187.

Nelson, J. and Kallenbach, N.R. (1989). Biochemistry **28**, 5256-5261.

Nelson, J. and Kallenbach, N. R. (1986) PROTEINS: Structure, Function, and Genetics **1**, 211-217.

Nozaki, Y. and Tanford, C. (1971). Journal of Biological Chemistry **7**, 2211-2217.

O'Neil, K.T. and DeGrado, W.F. (1990). Science **250**, 646-651.

Otada, K., Kitagawa, Y., Kimura, S. and Imanishi, Y. (1993). Biopolymers **33**, 1337-1345.

Padmanabhan, S., and Baldwin R. L. (1991) J. Mol. Biol. **219**, 135-137.

Padmanabhan, S., Marqusee, S., Ridgeway, T., Laue, T. M. and Baldwin, R. L. (1990) Nature **344**, 268-270.

Perczel, A. and Fasman, G. D. (1992) Protein Science **1** 378-395.

Perczel, A., Hollósi, M., Tusnády, G. and Fasman, G. D. (1991) Protein Engineering **4**, 669-679.

Perczel, A., Park, K. and Fasman, G. D. (1992) Analytical Biochemistry **203**, 83-93.

Rosenheck, K. and Doty, P. (1961) Biochemistry **47**, 17751785.

Sarkar P. K. and Doty, P. (1966) Biochemistry 55, 981-989.

Satake, I. and Yang, J. T. (1973) Biochem. Biophys. Res. Comm. **54**, 930-936.

Scheraga, H. A. (1974) Macromolecules **7**, 1-8.

Scheraga, H. A. (1985) Proc. Natl. Acad. Sci. USA **82**, 5585-5587.

Scholtz, J. M., Qian, H., York, E. J., Stewart, J. M. and Baldwin, R. L. (1991) Biopolymers **31**, 1463-1470.

Shalongo, W. Dugad, L. and Stellewagen, E. (1994) J. Am. Chem. Soc. **116**, 2500-2507.

Shoemaker, K.R., Kim, P.S., Brems, D.N., Marquesee, S., York, E.J., Chaiken, I.M., Stewart, J.M. and Baldwin, R.L. (1985). Proc. Natl. Acad. Sci. USA **82**, 2349-2353.

Singer, S.J. (1962). Advances in Protein Chemistry, pp 1-68.

Sönnischen, F. D., Van Eyk, J. E., Hodges, R. S. and Sykes, B. D. (1992) Biochemistry **31**, 8790-8798.

Sueki, M., Lee, S., Powers, S. P., Denton, J. B., Konishi, Y. and Scheraga, H. A. (1984) Macromolecules **17**, 148-155.

Tessari, M., Foffani, M. T. Mammi, S. and Peggion, E. (1993) Biopolymers **33**, 1877-1887.

Thomas, P. D. and Dill, K. A. (1993) Protein Science **2**, 2050-2065.

Tiffany, M. L. and Krimm, S. (1969) Biopolymers **8**, 347-359.

Toniolo, C. (1989) Biopolymers 28, 247-257,

Toniolo, C., Bonora, G. M., Bavoso, A., Benedetti, E., Di Blasio, B., Pavone, V. and Pedone, C. (1983) Biopolymers 23, 205-215.

Touati, A., Creuznet, C., Chobert, J. M., Dufour, E. and Haertlé, T. (1992) Journal of Protein Chemistry **11**, 613-621.

van Stokkum, I. H. M., Spoelder, H. J., Bloemendal, M., van Grondelle, R. and Groen, F. C. A. (1990) Analytical Biochemistry **191**, 110-118.

Wishart, D. S., Sykes, B. D. and Richards, F. M. (1991) J. Mol. Biol. **222**, 322-333.

Woody, R. W. and Tinoco, I. Jr. (1967) J. Chem. Phys. **46**, 4927-4925.

Woolley, G. A. and Wallace, B. A. (1993) Biochemistry **32**, 9819-9825.

Yamamoto, Y., Ohkubo, T., Kohara, A., Tanaka, T., Tanako, T. and Kikuchi, M. (1990) Biochemistry **29**, 8998-9006.

Yada, R.Y., Jackman, R.L. and Nakai, S. (1988). Int. J. Peptide Protein. Res. **31**, 98-108

Yang, J. T., Wu, C-S. and Martinez, H. (1986) Methods in Enzymology **11**, 208-269.

Yee, A.A. and O'Neil, J.D.J. (1992). Biochemistry **31**, 3135-3143.

Zhong, L. and Johnson, C. W. Jr. (1992) Proc. Natl. Acad. Sci. USA **89**, 4462-4465.

Zimm, B. H. and Bragg, J. K. (1959) J. Chem. Phys. **31**, 526-535.

Appendix A RBP-1 in Methanol

Temperature ℃	Θ_{222} (deg•cm^2•dmol^{-1})	f_H (%)[1]	f_H (%)[2]
-5	-7297	21.2	16.5
0	-7297	21.2	16.5
5	-7240	21.1	16.2
10	-7240	21.1	16.2
15	-5429	15.8	10.2
20	-5488	16.0	10.4
26	-5317	15.5	9.8
30	-5090	14.8	9.1
35	-5160	15.0	9.3
40	-5147	15.0	9.3
45	-5147	15.0	9.3
50	-5104	14.9	9.1
60	-4905	14.3	8.5

[1] - calculated from Eq. 5

[2] - calculated from Eq. 4

RBP-1 in Ethanol

Temperature ℃	Θ_{222} (deg•cm^2•dmol^{-1})	f_H (%)	f_H (%)
-2.5	-12542	36.5	33.4
0	-12236	35.6	32.7
4.5	-11319	32.9	29.6
13.5	-10911	31.8	28.3
20	-10299	30.0	26.3
25	-9789	38.5	24.6
30	-9483	27.6	23.6
34.5	-8871	25.8	21.6
38.5	-8667	25.2	20.9
44	-8565	24.9	20.5
50	-8056	23.4	18.9

RBP-1 in TFE

Temperature ℃	Θ_{222} (deg•cm^2•dmol^{-1})	f_H (%)	f_H (%)
-5	-23019	67.0	68.4
0	-21984	64.0	64.8
5	-21173	61.6	63.0
9	-20895	61.1	61.2
15	-19154	55.7	55.5
20	-18065	52.6	51.9
23	-17630	50.5	50.5
30	-15889	46.2	44.7
34	-15543	45.2	43.6
40	-15543	45.2	43.6
45	-14366	41.8	39.7
50	-14583	42.4	40.4
55	-14583	42.4	40.4
60	-13277	38.6	36.1
65	-13277	38.6	36.1

RBP-1 in SDS

RBP-1 in SDS

Temperature℃	Θ_{222} (deg•cm^2•dmol^{-1})	f_H (%)	f_H (%)
26.5	-28589	83.3	86.6
30	-27780	81.0	84.0
33.5	-26431	77.1	79.5
36	-25083	73.1	75.1
39	-24274	70.8	72.4
42.5	-23195	67.6	68.8
46	-22925	66.9	67.9
50.5	-22656	66.1	67.0
55.5	-20768	60.5	60.8
59	-20228	59.0	59.0
69	-20498	59.8	59.9

Alamethicin in Methanol

Temperature °C	Θ_{222} (deg•cm^2•dmol^{-1})	f_H (%)	f_H (%)
-3	-17048	49.7	49.1
2	-15698	45.7	44.1
7	-15360	44.8	43
12	-14853	43.3	39.9
17	-13672	39.9	37.4
26.5	-13672	39.9	37.4
32.5	-12828	37.4	34.9
37.5	-11815	34.4	32.1
42.5	-11815	34.4	31.6
47.5	-11815	34.4	30.4
52.5	-11478	33.5	27.9
57.5	-11815	34.4	27.9

Alamethicin in SDS

Temperature ℃	Θ_{222} (deg•cm^2•dmol^{-1})	f_H (%)	f_H (%)
11	-32946	95.9	100
16	-30246	88.0	92.0
24.5	-29165	84.9	88.5
31	-29706	86.5	90.3
37	-28625	83.3	86.7
40	-28085	81.7	85.8
47	-27005	78.6	81.4
51.5	-24845	72.3	74.3
66	-24305	70.7	72.5
77	-23225	67.6	68.9
81	-22684	66.0	67.1
86	-20524	59.7	60.0

Appendix B RBP-1 in Methanol

Temperature ℃	f_H (%)
-5	30.4
0	27.5
5	26.6
10	25.5
18	19.5
20	23.6
26	21.8
30	22.4
35	22.1
40	22.6
45	20.2
50	18.1
60	16.8

RBP-1 in Ethanol

Temperature ℃	f_H (%)
-2.5	56.0
0	55.8
4.5	54.7
13.5	50.9
20	47.2
25	45.7
30	44.0
34.5	40.9
38.5	40.3
44	39.3
50	37.9

RBP-1 in TFE

Temperature ℃	f_H (%)
-5	50.0
0	48.3
5	47.0
9	42.4
15	40.8
20	39.1
23	36.8
30	35.6
34	35.5
40	34.9
45	(27.6)*
50	33.5
55	31.5
60	31.2
65	36.1

* - truncated data set, not reliable

RBP-1 in SDS

Temperature ℃	f_H (%)
26.5	100.0
30	97.6
33.5	96.9
36	94.3
39	94.6
42.5	89.2
46	97.4
50.5	100
55.5	100
59	100
69	100

Alamethicin in methanol

Temperature ℃	f_H (%)
-3	86.0
2	77.8
7	74.5
12	71.8
17	68.4
26.5	66.2
32.5	63.0
37.5	62.5
42.5	59.8
47.5	58.2
52.5	56.5
57.5	56.7